Louisiana Transportation Research Center

Final Report 547

Performance and Analysis of Concrete Bridge Railing using Conventional and Composite Reinforcement Materials

by

Walid R. Alaywan, Ph.D., P.E.
LTRC

4101 Gourrier Avenue | Baton Rouge, Louisiana 70808
(225) 767-9131 | (225) 767-9108 fax | www.ltrc.lsu.edu

TECHNICAL REPORT STANDARD PAGE

1. Report No.	2. Government Accession No.	3. Recipient's Catalog No.
FHWA/LA.16/547		

4. Title and Subtitle	5. Report Date
Performance and Analysis of Concrete Bridge Railing using Conventional and Composite Reinforcement Materials	September 2018
	6. Performing Organization Code LTRC Project Number:09-2ST State Project Number:736-99-1619
7. Author(s) Walid R. Alaywan, Ph.D., P.E.	8. Performing Organization Report No.
9. Performing Organization Name and Address Louisiana Transportation Research Center Rouge, LA 70808	10. Work Unit No.
	11. Contract or Grant No.
12. Sponsoring Agency Name and Address Louisiana Department of Transportation and Development P.O. Box 94245 Baton Rouge, LA 70804-9245	13. Type of Report and Period Covered **Final Report** **May 2009 - March 2011**
	14. Sponsoring Agency Code

15. Supplementary Notes

Conducted in Cooperation with the U.S. Department of Transportation, Federal Highway Administration

16. Abstract

The guidelines proposed by the NCHRP Report 350 pertaining to the safety of roadway hardware devices necessitated the evaluation of those devices *[2]*. This study deals with the strength evaluation of precast concrete bridge railing that is a part of the roadway hardware devices.

Though many articles, reports, and publications were found regarding the testing of cast-in-place concrete barriers, similar publications pertaining to precast concrete bridge railing were almost non-existing and so testing a precast concrete barrier was the focus of this study. The study of the performance of a concrete barrier with composite reinforcement was not warranted since such barriers can be replaced if they get damaged and investing in composite reinforcement would not be a good decision.

The theoretical work was performed using the yield line theory to predict the strength of the precast barrier. Though the theory was developed for cast-in-place barriers where the lateral impact force would be transferred to the reinforcement in the deck, there was no developed equations for evaluating the strength of the precast or bolted section. The theory was tested in this study.

The experimental work consisted of casting, instrumenting, testing, and evaluating data collected afterwards.

Even though the reinforcement pattern remained unchanged along and across the faces of the barrier throughout, the section capacity of the barrier at the end region was smaller and thus, controlled the ultimate yield strength of the barrier. This is due to the end region being semi-continuous, unlike the intermediate region of the barrier. This led to different failure patterns.

The failure of the precast section was in torsion of the wall followed by concrete break out at some anchor locations. This result is due to the different mechanisms through which a cast-in-place barrier and a precast barrier transfers the applied load to the deck.

The measured resistive force at the intermediate section ranged from 40 kips (first appearance of cracks) to 79 kips (failure of the section) while the estimated value was 83 kips. Since the barrier collapsed while testing the intermediate region, testing of the end region could not be carried out. Since the transverse force causing failure of the end region is the controlling one and could not be verified, the estimated value of that resistive force (56 kips) could be used to conservatively imply that this barrier is TL-2 compliant. The use of this section should be limited to conditions that qualify for TL-2, i.e., work zones and most local and collectorroads as well as where a small number of heavy vehicles is expected and posted speeds are reduced. Speed limit in work zones is limited to 45 mph. However, by properly designing the section and the anchoring detail, the performance of this barrier may upgraded to comply with TL-3 requirements,or higher, after successful full-crash testing.

17. Key Words	18. Distribution Statement
Precast barriers, yield line theory, collapse, instrumentation,	**Unrestricted. This document is available through the National Technical Information Service, Springfield, VA 21161.**

19. Security Classif. (of this report)	20. Security Classif. (of this page)	21. No. of Pages	22. Price
	N/A	153	

Project Review Committee

Each research project will have an advisory committee appointed by the LTRC Director. The Project Review Committee is responsible for assisting the LTRC Administrator or Manager in the development of acceptable research problem statements, requests for proposals, review of research proposals, oversight of approved research projects, and implementation of findings.

LTRC appreciates the dedication of the following Project Review Committee Members in guiding this research study to fruition.

LTRC Project Manager

Walid Alaywan, Ph.D., P.E.
Sr. Structures research Engineer

Members

Paul Fossier, P.E.
Gill Gautreau, P.E.
Mike Boudreaux, P.E.
David Hodnett, P.E.
Art Aguirre, P.E.

Directorate Implementation Sponsor

Christopher P. Knotts, P.E.
DOTD Chief Engineer

Performance and Analysis of Concrete Bridge Railing using Conventional and Composite Reinforcement Materials

by
Walid R. Alaywan, Ph.D., P.E.

Louisiana Transportation Research Center
Baton Rouge, Louisiana 70808

LTRC Project No. 09-2ST
State Project No. 736-99-1619

conducted for

Louisiana Department of Transportation and Development
Louisiana Transportation Research Center

September 2018

ABSTRACT

The guidelines proposed by the NCHRP Report 350 pertaining to the safety of roadway hardware devices necessitated the evaluation of those devices *[2]*. This study deals with the strength evaluation of precast concrete bridge railing that is a part of the roadway hardware devices.

Though many articles, reports, and publications were found regarding the testing of cast-in-place concrete barriers, similar publications pertaining to precast concrete bridge railing were almost non-existing, and so testing a precast concrete barrier was the focus of this study. As such, the study of the performance of a concrete barrier with composite reinforcement was not warranted since such barriers can be replaced if they get damaged and investing in composite reinforcement would not be a good decision.

The theoretical work was performed using the yield line theory to predict the strength of the precast barrier. Though the theory was developed for cast-in-place barriers where the lateral impact force would be transferred to the reinforcement in the deck, there was no developed equations for evaluating the strength of the precast or bolted section.

The experimental work consisted of casting, instrumenting, testing, and evaluating data collected afterwards.

Even though the reinforcement pattern remained unchanged along and across the faces of the barrier throughout, the section capacity of the barrier at the end region was smaller and thus, controlled the ultimate yield strength of the barrier. This is due to the end region being semi-continuous, unlike the intermediate region of the barrier. This led to different failure patterns.

The failure of the precast section was in torsion of the wall followed by a concrete break out at some anchor locations. This result is due to the different mechanisms through which a cast-in-place barrier and a precast barrier transfers the applied load to the deck.

The measured resistive force at the intermediate section ranged from 40 kips (first appearance of cracks) to 79 kips (failure of the section), while the estimated value was 83 kips. Since the barrier collapsed while testing the intermediate region, testing of the end region could not be carried out. Since the transverse force causing failure of the end region is the controlling one and could not be verified, the estimated value of that resistive force (56 kips) could be used to conservatively imply that this barrier is TL-2 compliant. The use of this section should be limited to conditions that qualify for TL-2, i.e., work zones and most

local and collector roads as well as where a small number of heavy vehicles is expected and posted speeds are reduced. Speed limit in work zones is limited to 45 mph. However, by properly designing the section and the anchoring detail, the performance of this barrier may upgraded to comply with TL-3 requirements, or higher, after successful full-crash testing.

ACKNOWLEDGMENTS

Appreciation goes to Louisiana Department of Transportation and Development (DOTD) and the Louisiana Transportation Research Center (LTRC) for the funding of this research project.

Sincere gratitude and appreciation are expressed to Dr. Aziz Saber and Dr. Erez Allouche, from Louisiana Tech University, and their staff for availing themselves and the Trenchless Technology Center to conduct the experimental portion for this project.

Many thanks and appreciations are extended to Sims Regard and his people from Waskey Bridges, in Baton Rouge, for donating the material, the man power, the bridge railing to conduct this research.

I would like to extend my thanks to Dr. Roger Bligh form the Texas Transportation Institute (TTI) and Dr. Dean Sicking form Midwest Roadside Safety Facility, University of Nebraska-Lincoln (MwRSF) for the materials they provided me with and their discussions over the phone or at the AASHTO Conference in New Orleans, Louisiana.

My thanks go to Gill Gautreau, former bridge maintenance administrator, and Nick Fagerburg, bridge maintenance repair engineer, for the tremendous support they provided in working out the plans for transporting the barrier and the slab to Louisiana Tech University for testing.

Last, I would like to extend my appreciation to the Project Review Committee (PRC) for serving on this project by reviewing the proposal, the comments they provided, and the review of the draft final report.

IMPLEMENTATION STATEMENT

The use of precast concrete barrier offers distinct advantages over the conventional cast-in-place concrete barrier: (1) the ease of replacing damaged segments without the need to repair the deck areas to which they are bolted, (2) little disruption of traffic, and (3) relatively less expensive repair since the section can be cast at the plant. As such, this type of barrier is easier to replace than the conventional cast-in-place types.

Though the tested precast concrete barrier was found to be TL-2 compliant, by properly increasing the section capacity of the barrier, increasing its height, and improving the anchoring connection, this type of barrier will be able to withstand higher impact forces experienced under test levels 3 or higher and thus becoming a useful part of the accelerated bridge construction components. This can be done only after the redesigned railing system shows acceptable performance through full-scale crash tests for desired test levels [A.13.7.3.1] of AASHTO (1994) *LRFD Bridge Design Specifications.*

TABLE OF CONTENTS

LIST OF TABLES

LIST OF FIGURES

INTRODUCTION

Since the 1920s, the American Association of State Highway and Transportation Officials (AASHTO) has provided various specifications to address the design and details of bridge railings. Dramatic changes in bridge railing specifications have been needed to adapt to the changes in the auto industry and the wide variety of vehicles present on highways. In the 1960s, AASHTO defined the primary purpose of bridge railings as the ability to contain the average vehicle. The application of the 10-kip load was established for the design of such railings, and it remained AASHTO's primary criteria in AASHTO through the 1980s. Throughout the nation, multiple-fatality truck and school bus accidents involving bridge railings focused bridge engineers' attention on how closely the 10-kip load represented the real-life impact loads. The load indicator walls in the crash test sites suggested that the actual loads were in the range of 30 kips to 200 kips. In August 1986, the Federal Highway Administration (FHWA) required the full-scale crash testing of all bridge rails that are to be used on federal aid projects. At the same time, AASHTO requested the FHWA to assist them in the development of a new bridge rail specification.

In 1989, AASHTO adopted a guide specification for bridge railing. This specification was intended to be a basis for the design of prototype bridge railings that are to be crash tested. It was also intended to provide a basis for the design of one-of-a-kind bridge railing where the cost of crash test program may not be justified. The guide specification was based on a multiple performance level theory, which requires a different rail for a different situation.

In 1994, AASHTO published its first series of Load and Resistance Factor Design (LRFD) specifications, both in English and metric units *[1]*. The LRFD Railing Specification and the guide specification were very similar. Performance levels and the design loads have been extracted from the Guide specification and placed in the LRFD specifications, with the exception that the LRFD specifications offer step-by-step design criteria and analysis procedures for various bridge railings.

In 2007, AASHTO reached a consensus that, because of the dramatic change in the traffic vehicle and vehicle geometry, and the speed on the highways, the 1994 LRFD specification needed to be revised.

A report published by Texas Department of Transportation (Tx DOT) recommended new design forces from different performance levels of bridge barriers. The report assessed the safety of existing barriers and recommended changes to some that failed. Concrete barriers that were assessed in that study covered cast-in-place barriers but not precast barriers *[2]*. Therefore, those precast barriers should be assessed to ascertain their successful performance

under the new recommended lateral, longitudinal, and vertical forces that result from an errant vehicle that collides with the barrier.

OBJECTIVE

The principal objective of this study was to assess the structural adequacy and strength of a precast concrete bridge railing section used by DOTD for the current national cooperative highway's (NCHRP Report 350) guidelines and for the recommended changes in the Texas study.

SCOPE

The work was carried out through the execution of the following steps:

- Conducting a background review on bridge barriers that are used in Louisiana and elsewhere.
- Constructing a concrete bridge rail based on an existing section that is used for rapid construction.
- Evaluating the ultimate flexural capacity of a selected concrete bridge rail that is being used for bridge and roadway repairs and in rapid bridge construction activities.
- Investigating the ultimate section capacity of a constructed bridge barrier by subjecting it to a static lateral load.
- Collecting and analyzing load data from the performed tests.
- Comparing the predicated and the evaluated flexural capacities for the tested barrier.
- Limiting the literature search to the type “F” and “New Jersey” barriers.

METHODOLOGY

Literature Review

Previous Studies

For the last 50 years, the safety of the traveling public has been of utmost importance to the United States, demonstrated by its commitment in the funding of numerous studies pertaining to the testing of roadside appurtenances, or accessories. Accessories were placed on roadsides for the purpose of the protection of drivers and passengers by containing errant vehicles where drivers lost control.

Placing those roadside accessories necessitated developing unified guidelines to test them. Those guidelines have always been updated as needed, and their use was mandated by the Federal Government on all state highways.

In 1962, a one-page document titled "Proposed Full-Scale Testing Procedures for Guardrails" was disseminated under *Highway Research Circular 482 [3]*. This document included (1) four specifications on test article installation, (2) one test vehicle, (3) six test conditions, and (4) three evaluation criteria.

In 1970, *National Cooperative Highway Research Program (NCHRP) Report 86* "Tentative Service Performance Requirements for Bridge Rail Systems," was published *[4]*. In this 62-page document, four hazardous conditions were identified: (1) vehicle penetration of bridge or approach barrier rails, (2) snagging of a vehicle by a bridge or approach barrier rails, (3) vehicle collisions with the approach end of bridge or approach barrier rails, and (4) collisions in which a vehicle is redirected by a railing system. With those four hazardous conditions in mind, the report provided 10 service requirements to assist the designer in the design of a bridge barrier rail. By following those requirements, a safe and economical railing system may be achieved. The report was based on the current understanding of available information at that time.

In 1974, *NCHRP Report 149* "Bridge Rail Design–Factors, Trends, and Guidelines" was published *[5]*. In this 49-page document, the researchers collected and analyzed information on accidents regarding different factors namely, vehicle geometry, barrier configurations, and heights. The report examined the barrier strength and height requirements as well as outlining the barrier design process at that time. It recommended that full-scale crash tests and accident statistics were needed to assess the safety and the performance of a bridge rail design.

In 1974, *NCHRP Report 153*, "Recommended Procedures for Vehicle Crash Testing of Highway Appurtenances" was published. This 16-page document provided the first complete test matrix for evaluating safety features. Data collection methods, evaluation criteria, and limited guidance on reporting formats were included *[6]*.

In 1978, Transportation Research Circular 191, "Recommended Procedures for Vehicle Crash Testing of Highway Appurtenances" was published. The report provided a limited interim update on *NCHRP Report 153* to address minor changes requiring modified treatment of particular problem areas *[7]*.

In 1981, *NCHRP Report 230*, "Recommended Procedures for the Safety Performance Evaluation of Highway Features," was published. The report was an extensive revision and update to procedures practiced at that time. This 42-page document contained different service levels for evaluating longitudinal barriers that were designed to withstand the impact of vehicles ranging from small passenger cars to intercity buses *[8]*.

In 1993, *NCHRP Report 350*, "Recommended Procedures for the Safety Performance Evaluation of Highway Features" was published *[9]*. This 132-page document was a comprehensive update to crash test and evaluation procedures.

There were distinct differences between *NCHRP Report 350* and *NCHRP Report 230:*

- *NCHRP Report 350* provided a wider range of test procedures to permit safety performance evaluations for a wider range of barriers, terminals, crash cushions, breakaway support structures and utility poles, truck-mounted attenuators, and work zone traffic control devices.
- In *NCHRP Report 350,* a 4,409-lb., 3/4-ton pickup truck was set as the standard design test vehicle, thus replacing the 4,500-lb. passenger sedan that was used in *NCHRP Report 230.* This change was attributed to the growing population of light trucks in the vehicle fleet.
- *NCHRP Report 350* introduced other test vehicles such as an 18,000-lb. single-unit cargo truck and 80,000-lb. tractor-trailer vehicle to provide the basis for optional testing to meet higher performance levels. *NCHRP Report 230* lacked other test vehicles.
- *NCHRP Report 350* provided six basic test levels for the various classes of roadside safety features.

The Federal Highway Administration (FHWA) formally adopted the new performance evaluation guidelines for highway safety features set forth in *NCHRP Report 350* as a "Guide

or Reference" document in the Federal Register, Volume 58, Number 135, dated July 16, 1993, which added paragraph (a)(13) to 23 CFR 625.5. FHWA subsequently mandated that, starting in September 1998, only highway safety appurtenances that have successfully met the performance evaluation guidelines set forth in *NCHRP Report 350* may be used on new construction projects on the National Highway System (NHS).

In 1996, a discussion with the AASHTO Highway Subcommittee on Bridges and Structures Technical Committee (T-7) for Guardrail and Bridge Rail noted, among other issues, that no selection procedures for the use of a specific test level are included in *NCHRP Report* 350 *[10]*. And finally, to add to the conflicting guidance for selecting appropriate bridge railing, AASHTO issued its 1994 "LRFD (Load and Resistance Factor Design) Bridge Design Specifications" as an alternate to the long-standing "Standard Specifications for Highway Bridges." Section 13 of the new publication contains recommendations on railing designs and a crash test matrix that differs from *NCHRP Report* 350 and the AASHTO guide specifications.

FHWA's current position can be summarized as follows:

- All bridge railings installed on national highway system (NHS) projects let to contract after August 16, 1998, shall meet the acceptance criteria contained in *NCHRP Report 350* or an FHWA recognized successor to those criteria. The minimum acceptable bridge rail will be a TL-3 (MSL-2 until August 1998), unless an alternative is supported by a rational selection procedure. Acceptability under *NCHRP Report 350* and a rational selection procedure are defined below.

- Railings that have been found acceptable under the crash testing and acceptance criteria in *NCHRP Report 230*, the AASHTO Guide Specifications for Bridge Railings, or the AASHTO LRFD Bridge Design Specifications will be considered as meeting the requirements of *NCHRP Report 350* without further testing as indicated in Table 1.

Table 1
Railing level equivalency

Bridge Rail Testing Criteria	Acceptance Equivalencies					
NCHRP Report 350	TL-1	TL-2	TL-3	TL-4	TL-5	TL-6
NCHRP Report 230		MSL-1 MSL-2*		MSL-3		
AASHTO Guide Specifications		PL-1		PL-2	PL-3	
AASHTO LRFD Bridge Specifications		PL-1		PL-2	PL-3	

* This is the performance level usually cited when describing a barrier as tested under *NCHRP Report 230*. It is close to a TL-3 but adequate TL-3 performance cannot be assured without a pickup truck test.

- The FHWA strongly suggests that ASHTO adopt the test level definitions in *NCHRP Report 350*.

- The FHWA strongly recommends that all future testing of bridge railings be conducted in accordance with the recommendations in *NCHRP Report 350* or an FHWA-recognized successor to *NCHRP Report 350*

- The FHWA strongly encourages AASHTO to support the ongoing NCHRP efforts to develop railing level selection procedures and, after appropriate review, and adjustment, if needed, adopt railing level selection procedures.

- Until AASHTO adopts a new railing level selection procedure, FHWA will accept the procedures in the "Guide Specifications for Bridge Railings" or a rational, experience based, cost-beneficial, consistently applied procedure proposed by a state.

- Exceptions to the items in this position, which are expected to be rare, will be considered on their merits on a case-by-case basis.

The test levels defined in *NCHRP Report 350* are explained in Table 2.

Table 2
Bridge rail test levels

Bridge Rail Test Levels (Adapted from AASHTO LRFD Article 13.7.2 4th Edition)		
Name	**Abbreviation**	**Description**
Test Level One	**TL-1**	Generally acceptable for work zones with low posted speeds and very low volume, low speed local streets
Test Level Two	**TL-2 (Equivalent to PL-1)**	Generally acceptable for work zones and most local and collector roads with favorable site conditions as well as where a small number of heavy vehicles is expected and posted speeds are reduced
Test Level Three	**TL-3**	Generally acceptable for a wide range of high-speed arterial highway with very low mixtures of heavy vehicles and with favorable site conditions.
Test Level Four	**TL-4 (Equivalent to PL-2)**	Generally acceptable for the majority of appliations on high speed highways, freeways, expressways, and interstate highways with a mixture of trucks and heavy vehicles.
Test level Five	**TL-5 (Equivalent to PL-3)**	Generally acceptable for the same applications as TL-4 and where larger trucks make up a significant portion of the average daily traffic or when unfavorable site conditions justify a higher level of rail resistance.
Test Level Six	**TL-6**	Generally acceptable for applications where tanker type trucks or similar high center-of-gravity vehicles are anticipated, particular along with unfavorable site conditions.

Previous Experimental Work

The evaluation of the performance of roadside accessories or longitudinal barriers is based on their desired use on highways, traffic speed, and the mix of the traveling fleet as was reported in Table 2. For every condition, there is a test level (TL) as specified in *NCHRP Report 350*. Below is a summary description of TL2 to TL-6:

- ***NCHRP Report 350 Test Designation 6-10:*** A 1,806-lb. passenger car impacting the bridge rail at the critical impact point (CIP) of the length of need at a nominal speed and angle of 62 mph and 20 degrees. The test is intended to evaluate occupant risk and post-impact trajectory.

- ***NCHRP Report 350 Test Designation 6-11:*** A 4,409-lb. pickup truck impacting the bridge rail at the CIP of the length of need at a nominal speed and angle of 62 mph and 25 degrees. The test is intended to evaluate strength of the section in containing and redirecting the 4,409-lb.vehicle.

- ***NCHRP Report 350 Test Designation 6-12:*** A 72,000-lb tractor-tanker trailer impacting the bridge rail at the CIP of the length of need at a nominal speed and angle of 50 mph and 15 degrees. The test is intended to evaluate strength of the section in containing and redirecting the 72,000-lb. vehicle.

- ***NCHRP Report 350 Test Designation 5-10:*** A 1,806-lb. passenger car impacting the bridge rail at the CIP of the length of need at a nominal speed and angle of 62 mph and 20 degrees. The test is intended to evaluate occupant risk and post-impact trajectory.

- ***NCHRP Report 350 Test Designation 5-11:*** A 4,409-lb. pickup truck impacting the bridge rail at the CIP of the length of need at a nominal speed and angle of 62 mph and 25 degrees. The test is intended to evaluate strength of the section in containing and redirecting the 4,409-lb. vehicle.

- ***NCHRP Report 350 Test Designation 5-12:*** A 72,000-lb. tractor-trailer impacting the bridge rail at the CIP of the length of need at a nominal speed and angle of 50 mph and 15 degrees. The test is intended to evaluate strength of the section in containing and redirecting the 72,000-lb, vehicle.

- ***NCHRP Report 350 Test Designation 4-10:*** A 1,806-lb. passenger car impacting the bridge rail at the CIP of the length of need at a nominal speed and angle of 62.2 mph and 20 degrees. The test is intended to evaluate occupant risk and post-impact trajectory.

- ***NCHRP Report 350 Test Designation 4-11:*** A 4,409-lb. pickup truck impacting the bridge rail at the CIP of the length of need at a nominal speed and angle of 62.2 mph and 25 degrees. The test is intended to evaluate strength of the section in containing and redirecting the 4409-lb. vehicle.

- ***NCHRP Report 350 Test Designation 4-12:*** A 17,621-lb. single-unit truck impacting the bridge rail at the CIP of the length of need at a nominal speed and angle of 49.7 mph and 15 degrees. The test is intended to evaluate strength of the section in containing and redirecting the 17,621-lb. vehicle.

- ***NCHRP Report 350 Test Designation 3-10:*** A 1,806-lb. passenger car impacting the bridge rail at the CIP of the length of need at a nominal speed and angle of 62.2 mph and 20 degrees. The test is intended to evaluate occupant risk and post-impact trajectory.

- ***NCHRP Report 350 Test Designation 3-11:*** A 4,409-lb. pickup truck impacting the bridge rail at the CIP of the length of need at a nominal speed and angle of 62.2 mph and 25 degrees. The test is intended to evaluate strength of the section in containing and redirecting the 4,409-lb. vehicle.

- ***NCHRP Report 350 Test Designation 2-10:*** A 1,806-lb. passenger car impacting the bridge rail at the CIP of the length of need at a nominal speed and angle of 43 mph and 20 degrees. The test is intended to evaluate occupant risk and post-impact trajectory.

- ***NCHRP Report 350 Test Designation 2-11:*** A 4,409-lb. pickup truck impacting the bridge rail at the CIP of the length of need at a nominal speed and angle of 43 mph and 25 degrees. The test is intended to evaluate strength of the section in containing and redirecting the 4,409-lb. vehicle.

Table 3 summarizes bridge railing test levels and crash test criteria.

Table 3
Bridge railing test levels and crash test criteria

Bridge RailTest Levels (Adapted from AASHTO LRFD Article 13.7.2 4th Edition)							
Vehicle Characteristics	**Small Automobiles**		**Pick up Trucks**	**Single-Unit Van Truck**	**Van-Type Tractor-Trailer**		**Tractor-Tanker Trailer**
W (kips)	1.55	1.8	4.5	18.0	50.0	80.0	80.0
B (feet)	5.5	5.5	6.5	7.5	8.0	8.0	8.0
G (inches)	22	22	27	49	64	73	81
Crash Angle, θ	20°	20°	25°	15°	15°	15°	15°
Test Level	**Test Speeds (mph)**						
TL-1	30		30	30	N/A	N/A	N/A
TL-2	45		45	45	N/A	N/A	N/A
TL-3	60		60	60	N/A	N/A	N/A
TL-4	60		60	60	N/A	N/A	N/A
TL-5	60		60	60	N/A	50	N/A
TL-6	60		60	60	N/A	N/A	50

where,

W = weight of vehicle corresponding to the required test level, (kips)
G = height of vehicle center of gravity above bridge deck, (in.)
B = out-to-out wheel spacing on an axle, (ft.)
θ = crash abgle, (degrees)

For a barrier to qualify for a certain test level, it must be able to sustain the impact forces shown in Table 4.

Table 4
Design forces for traffic railing

Design Forces and Designations	Railing Test levels					
	TL-1	TL-2	TL-3	TL-4	TL-5	TL-6
F_t Transverse (kips)	13.5	27-0	54.0	54.0	124.0	175.0
F_L Longitudinal (kips)	4.5	9.0	18.0	18.0	41.0	58.0
F_v Vertical (kips) Down	4.5	4.5	4.5	18.0	80.0	80.0
L_t and L_L (ft.)	4.0	4.0	4.0	3.5	8.0	8.0
L_v (ft.)	18.0	18.0	18.0	18.0	40.0	40.0
H_e (min) (in.)	18.0	20.0	24.0	32.0	42.0	56.0
Minimum H Height of Rail (in.)	27.0	27.0	27.0	32.0	42.0	90.0

Louisiana Practice

Louisiana's primary bridge rail in recent history has been the New Jersey safety shape made of reinforced concrete and in special cases, steel plates. This particular shape has been successfully crash-tested for performance level (PL-2). The most recently developed safety shape is referred to as the F-Shape. This shape, although not much different from the Jersey shape, has proven to gain a slight advantage over the Jersey shape in redirecting the 18000-lb. vehicle. This explain the reason Louisiana has opted to gradually eliminate the use of the New Jersey shape and adopt the F-Shape for use on new projects. Another advantage in the adoption of the F-Shape is being the only safety shape with a 3 ft. 6 in. height that has been crash tested for performance level. On the following pages are two F-Shape barriers (Figure 1 and Figure 2) used by DOTD.

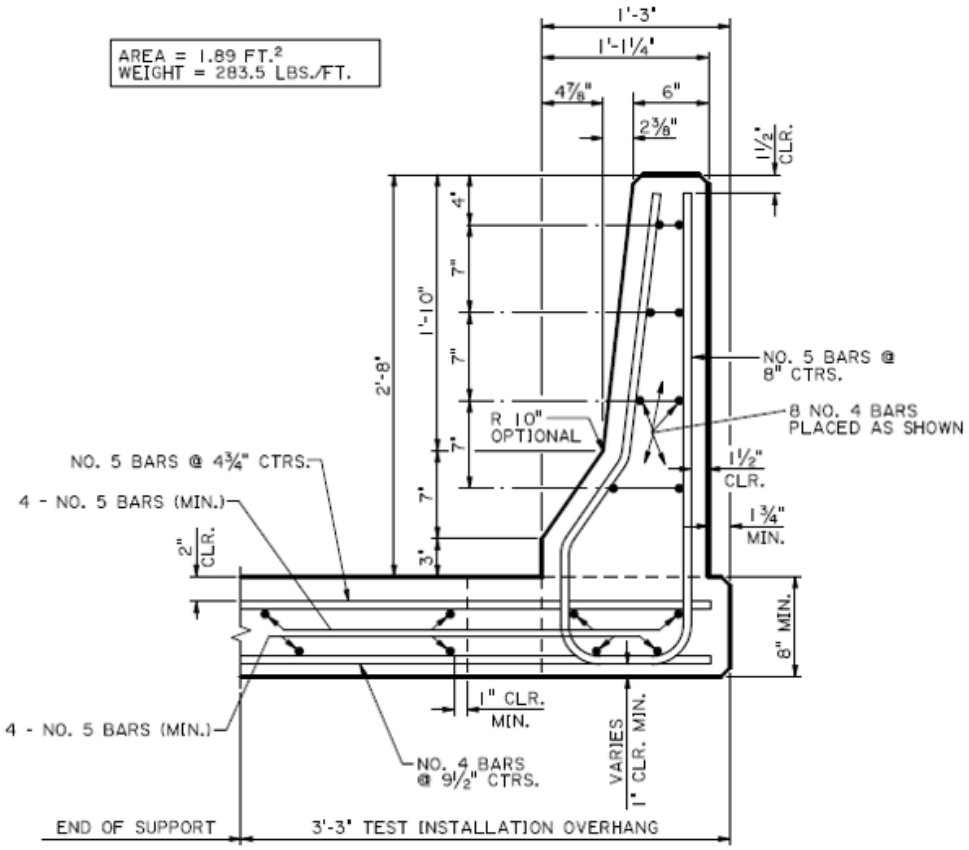

Figure 1
F-Shape (PL-2)

NOTES:

1. The above details are from FHWA-Rd-93-058 (June 1997) and have been modified. See Page 5(4) for design requirements.
2. Concrete to be Class AA, and exposed faces to receive Class 2A special surface finish in accordance with section 805.13(B) of the Louisiana Standard Specifications, 2000 Edition.
3. Reinforcing steel to be Grade 60.
4. The reinforcement used in 10 in. min. deck is based on crash test criteria using 40 ksi reinforced steel. See Note 16, Page 5 (46).
5. Details shown are for girder span bridges.

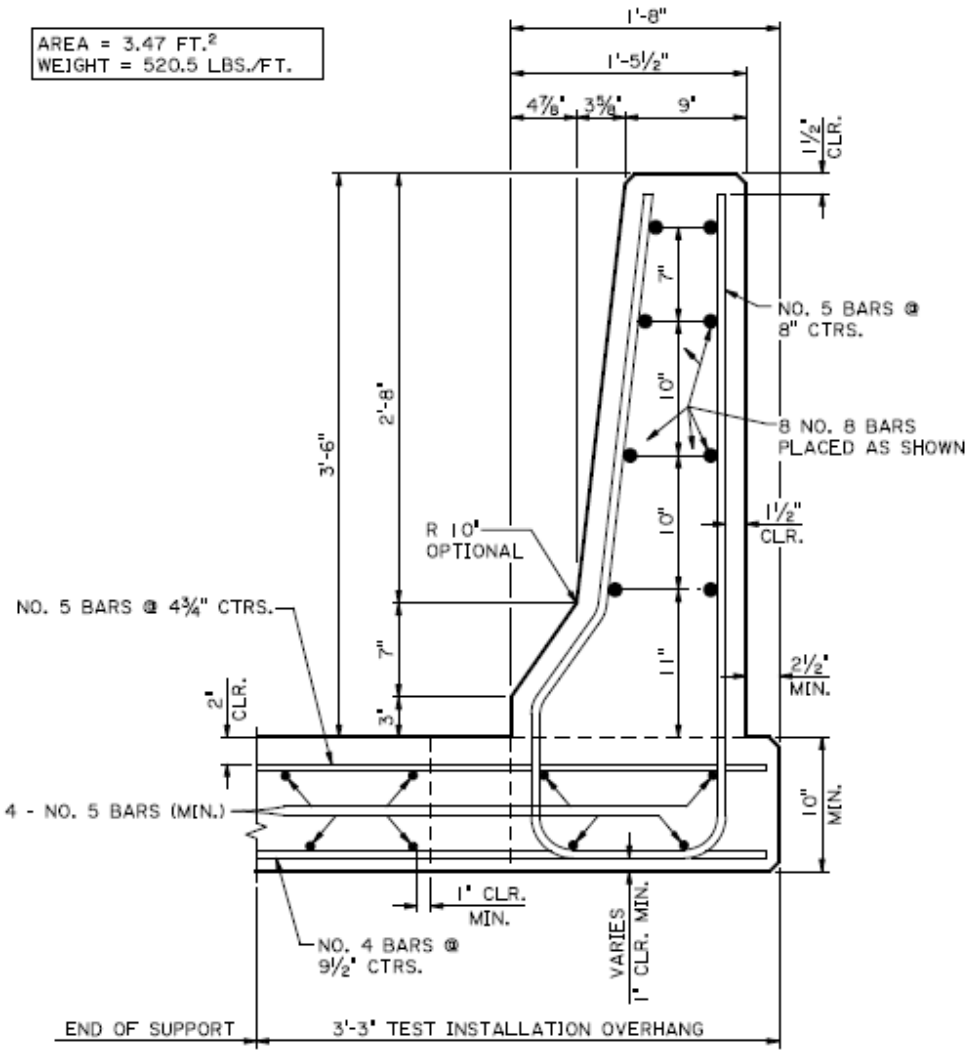

Figure 2
F-Shape (PL-3)

NOTES:

1. The above details are from FHWA-RD-93-058 (June 1997) and have been modified. See page 5(4) for design requirements.
2. Concrete to be Class AA, and exposed faces to receive class 2a special surface finish in accordance with section 805.13(b) of the Louisiana Standard Specifications, 2000 edition.
3. Reinforcing steel to be grade 60.
4. The reinforcement used in 10" min. deck is based on crash test criteria using 40 ksi reinforced steel. See note 16, page 5 (46).
5. Details shown are for girder span bridges.
6. PL-1, Pl-2, and PL-3 are defined on page 5(3) of DOTD Bridge Design Manual (4th English Edition).

Bridge Railing

Another type of F-shape barriers used on off-system bridges is bolted to the bridge deck, as seen in Figure 3.

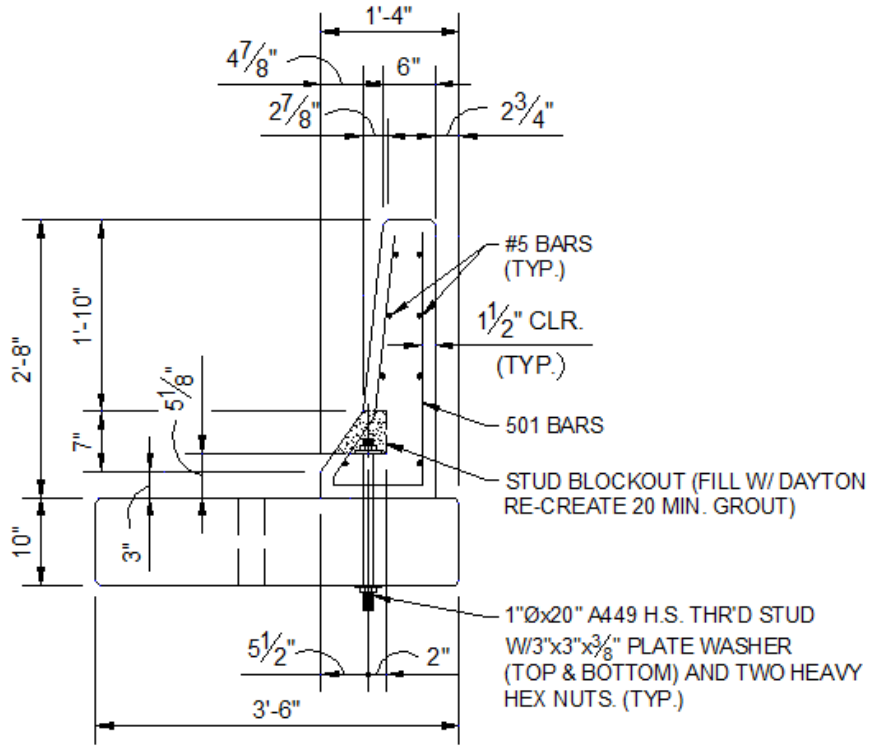

Figure 3
Bolted precast concrete bridge barrier used on Louisiana off-system bridges

Numerous experimental works have been performed by different agencies on different type of barriers to assess their performance for their intended uses. The Texas Transportation Institute (TTI) and the Midwest Roadside Safety Facility (MWRSF) have been leaders in bridge railing testing.

Years of testing longitudinal barriers have been reported in numerous publications. Ultimately, a bridge should contain and redirect errant vehicles with minimal damage to the bridge structure. A number of different types of concrete safety-shaped bridge rails are used by most states. Over the years, a number of different reinforcement schemes have been used and most have withstood the rigors of the highway environment. Obviously, reinforcement schemes may vary significantly and still achieve the objective to contain and redirect errant design vehicles.

Crash tests performed in the U.S. are evaluated in accordance with the criteria presented in *NCHRP Report 350*. As stated in *NCHRP Report 350*, "Safety performance of a highway

appurtenance cannot be measured be measured directly, but can be judged on the basis of three factors: structural adequacy, occupant risk, and vehicle trajectory after collision" *[9]*.

Buth et al. published a study titled "NCHRP Report 350 Test 3-11 of The Texas Type T411 Bridge Rail." In this study, the Texas Type 411 bridge rail, a concrete beam-and-posts system, which was crash tested and approved under *NCHRP Report 230* guidelines, was reevaluated after the adoption of the *NCHRP Report 350 [11]*. The purpose of the reevaluation was to check the performance of this rail under TL3 requirements. The test vehicle was a 2,000-kg pickup truck. The vehicle travelled at 100 km/hr. and impacted the bridge rail at an angle of 25 degrees. According to the specifications set for NCHRP Report 350 test designation 3-11, the Texas type T411 bridge rail met all requirements except occupant risk. Significant occupant compartment deformation occurred on the center and right side of the vehicle. This deformation was judged to have potential to cause serious injury. It was recommended that this bridge rail not be used on high-speed facilities where a TL-3 rail is needed. The FHWA has designated this bridge rail as being acceptable for TL-2 of *NCHRP Report 350*. This would indicate that continued used of the Texas Type T411 Bridge Rail, is acceptable on low-speed roadways (see Figure 4).

Figure 4
Texas Type T411 bridge rail section

Bligh et al. published a study titled "Design and Evaluation of the TxDOT F411 and T77 Aesthetic Bridge Rails." The objective of the study was to develop two crashworthy bridge rails: T77 and F411 *[12]*. The F411 bridge rail, see Figure 5, was evaluated through a full-scale crash test in accordance with *NCHRP Report 350* test 3-11. The rail performed successfully. The T77 bridge rail, see Figure 6, successfully met the evaluation criteria of

NCHRP Report 350 for Test 3-10 but not Test 3-11. The vehicle experienced snagging at the rail splice, causing excessive compartment deformation. It was recommended that additional crash testing on splice and/or rail modification be performed before T77 bridge rail was to be used.

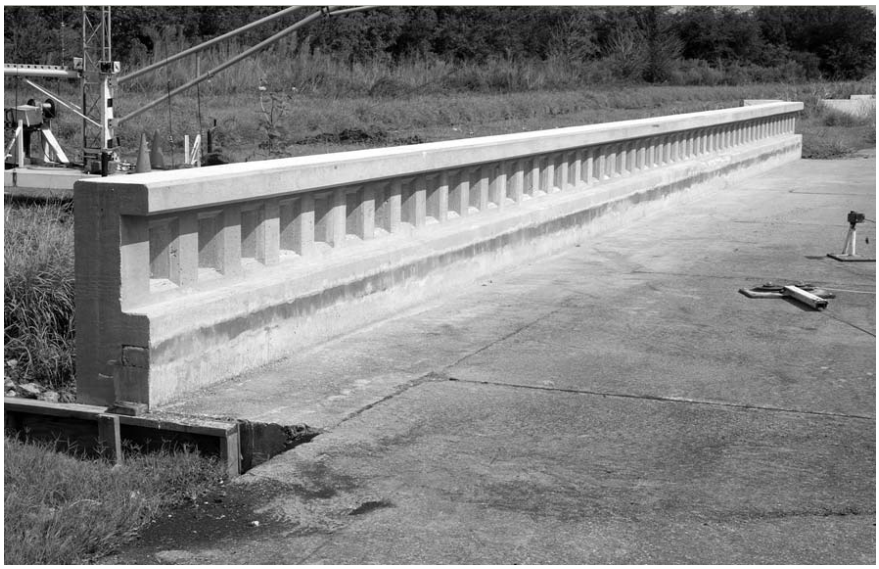

Figure 5
Texas Type F411 bridge rail section

Figure 6
Texas T77 bridge rail

Bullard, Jr. et al. published a study titled "Crash Testing and Evaluation of The Modified T77 Bridge Rail." The report mentioned that a previous study was performed to develop two crashworthy bridge rails: T77 and F411. The F411 bridge rail was evaluated through a full-

scale crash test in accordance with *NCHRP Report 350* test 3-11. The rail performed successfully. However, under the same evaluation, the T77 bridge rail failed to perform acceptably with the pickup truck. This failure led to the study reported herein with the objective of modifying the T77, see Figure 7, to perform acceptably. After modification, the T77 bridge rail performed successfully under NCHRP Report 350 test 3-11*[13]*.

Figure 7
Modified T77 bridge rail before test

Alberson et al. published a study titled "TL-4 Crash Testing of the F411 Bridge Rail." In this study, the F411 (Figure 8) bridge rail that successfully complied with *NCHRP Report 350* TL-3 crash test requirements was tested. The TxDOT F411 bridge rail performed acceptably for *NCHRP Report 350* test 4-12 and was able to contain an impacting 18,000 lb. single-unit truck *[14]*.

Figure 8
Texas Type F411 bridge rail section

Alberson et al. published a study titled "Testing and Evaluation of the Florida Jersey Safety Shaped Bridge Rail." The bridge rail performed satisfactorily under *NCHRP Report 350* TL-3 for containment and stability, and non-overturning. The rail, see Figure 9 below, also rail performed satisfactorily under *NCHRP Report 350* TL-4, thus, meeting containment and stability requirements *[15]*.

Figure 9
Florida Jersey safety shaped bridge railing

Sicking et al. published a study titled, "TL-5 Development of 42- and 51-in. Tall, Single-Faced, F-Shape Concrete Barriers." They studied the dynamic lateral vehicular loads that common barrier systems are subjected to *[16]*. They performed two linear regression

analyses for a number of crash tests and estimated the lateral peak load versus impact severity. This analytical investigation resulted in a peak lateral design load ranging between 153 and 155 kips and 243 to 248 kips for the AASHTO PL-3 and NCHRP 350 TL-5 impact conditions, respectively. Researchers then determined the re-directive capacities of four existing barrier designs using the standard yield-line analytical procedures. It was determined that the standard yield-line analytical procedures likely underestimate the re-directive capacity of solid, reinforced concrete parapets, since other factors likely contribute to the re-directive capacity of reinforced and non-reinforced concrete barrier systems. Since a "modified" yield-line analysis procedure is currently unavailable, the standard yield-line analysis procedure was used but in combination with a scaled-down design impact load. The new barrier systems were developed using a peak design impact load ranging between 211 kips and 224 kips or based on an average design impact load of approximately 217 kips. Two single-faced, F-Shape concrete barrier systems were designed to meet the TL-5 impact safety standards using the existing yield-line analysis procedures and for 42-in. and the 51-in. top-mounting heights. Attachment options were provided for anchoring the barriers to generic reinforced concrete slabs and a median foundation. The barrier and foundation systems were based on a conservative design approach where full-scale vehicle crash testing would not be required. Three research projects were recommended that would advance the state-of-the art for concrete barrier designs and provide new, more economical and innovative barrier and anchorage support systems. Figures 10 to 16 show different bridge rail tested in the study.

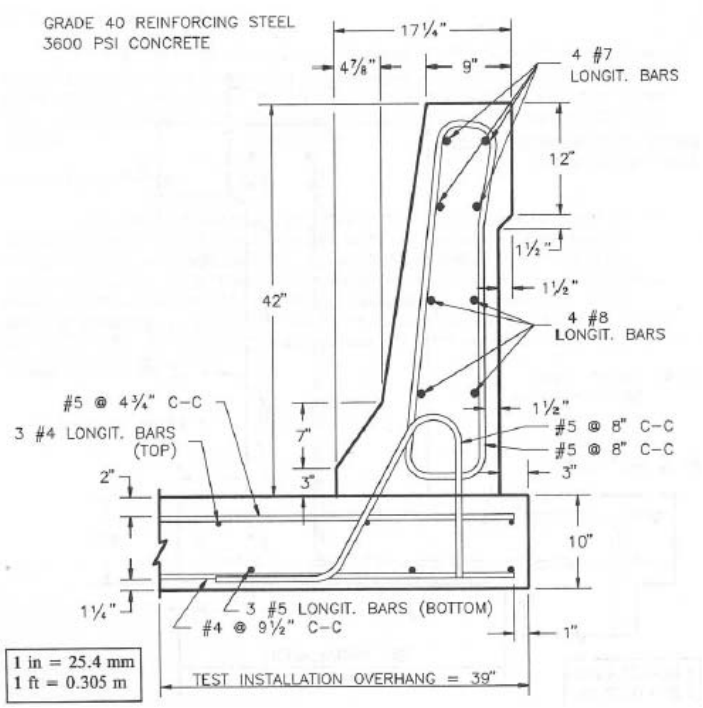

Figure 10
F-Shape bridge rail (PL-3 impact condition)

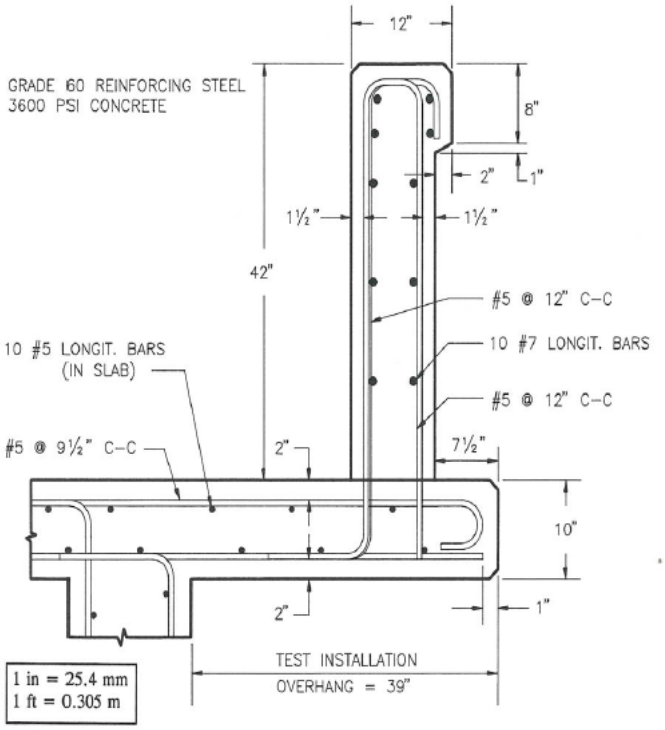

Figure 11
Vertical bridge rail (TL-5 impact condition)

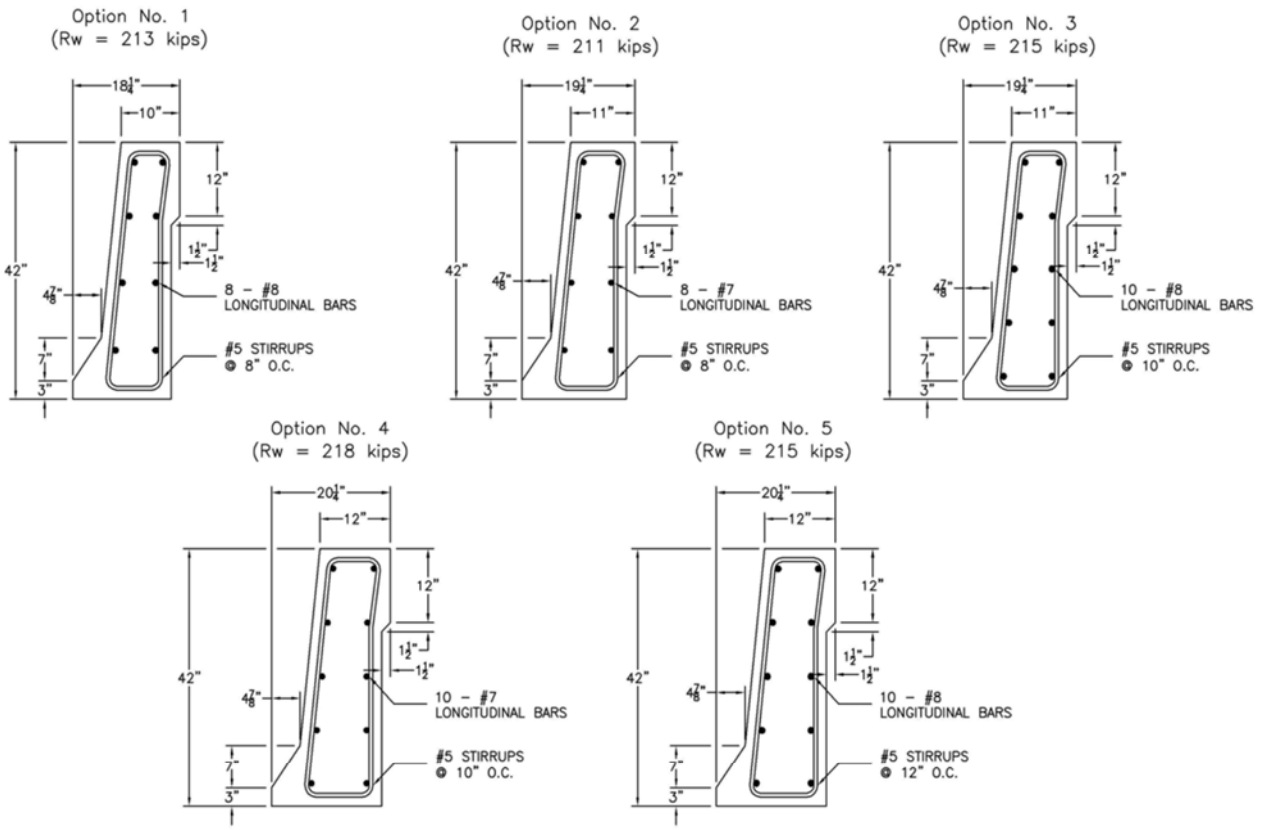

Notes: (1) Barrier capacity based on the development of the barrier's cantilevered bending capacity at the base and with the assumption that an equivalent size and spacing of steel bars, to that used for the vertical reinforcement, is included.
(2) Typical foundation and steel reinforcement details are included in subsequent details.
(3) Use Grade 60 reinforcing steel bars.
(4) Use a minimum 28–day concrete compressive strength of 4500 psi.
(5) Use 1½" clear cover.
(6) No. 5 stirrups shown with general looped configuration. Alternative configurations are permissible and to be determined by the individual State Departments of Transportation.
(7) 1 in. = 25.4 mm

Figure 12
Cross-sectional details and steel reinforcement for 42-in. tall concrete barrier

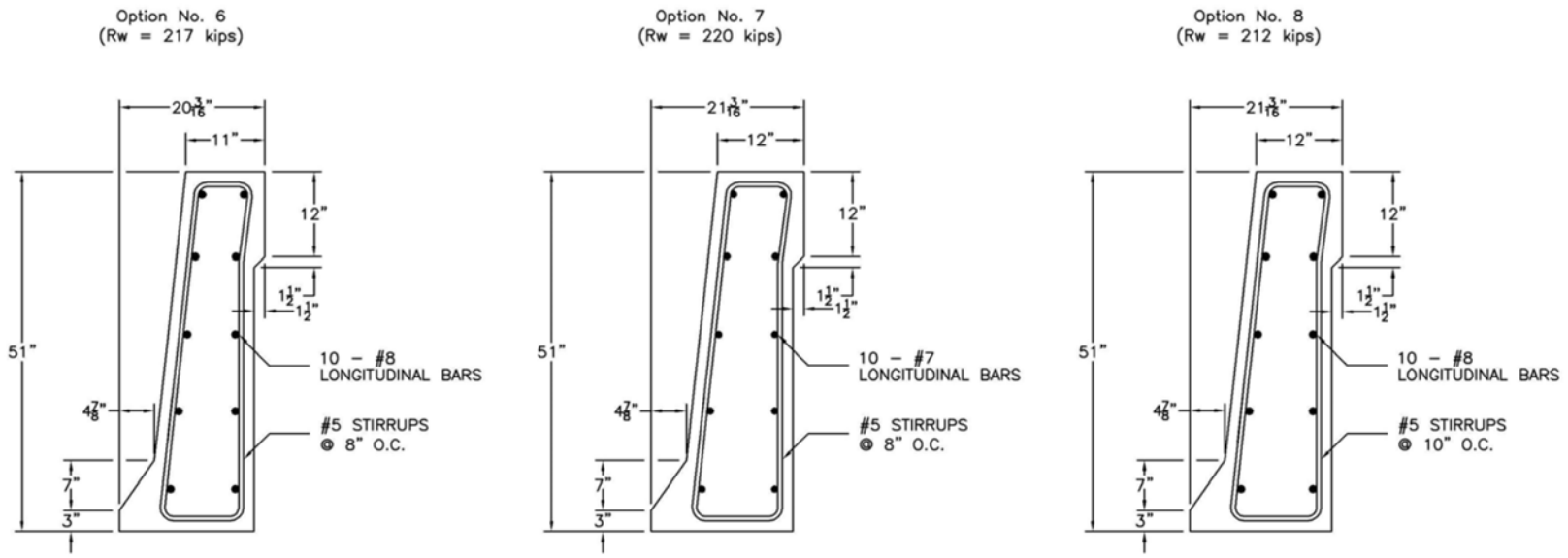

Notes:
(1) Barrier capacity based on the development of the barrier's cantilevered bending capacity at the base and with the assumption that an equivalent size and spacing of steel bars, to that used for the vertical reinforcement, is included.
(2) Typical foundation and steel reinforcement details are included in subsequent details.
(3) Use Grade 60 reinforcing steel bars.
(4) Use a minimum 28–day concrete compressive strength of 4500 psi.
(5) Use 1½" clear cover.
(6) No. 5 stirrups shown with general looped configuration. Alternative configurations are permissible and to be determined by the individual State Departments of Transportation.
(7) 1 in. = 25.4 mm

Figure 13
Cross-sectional details and steel reinforcement for 51-in. tall concrete barrier

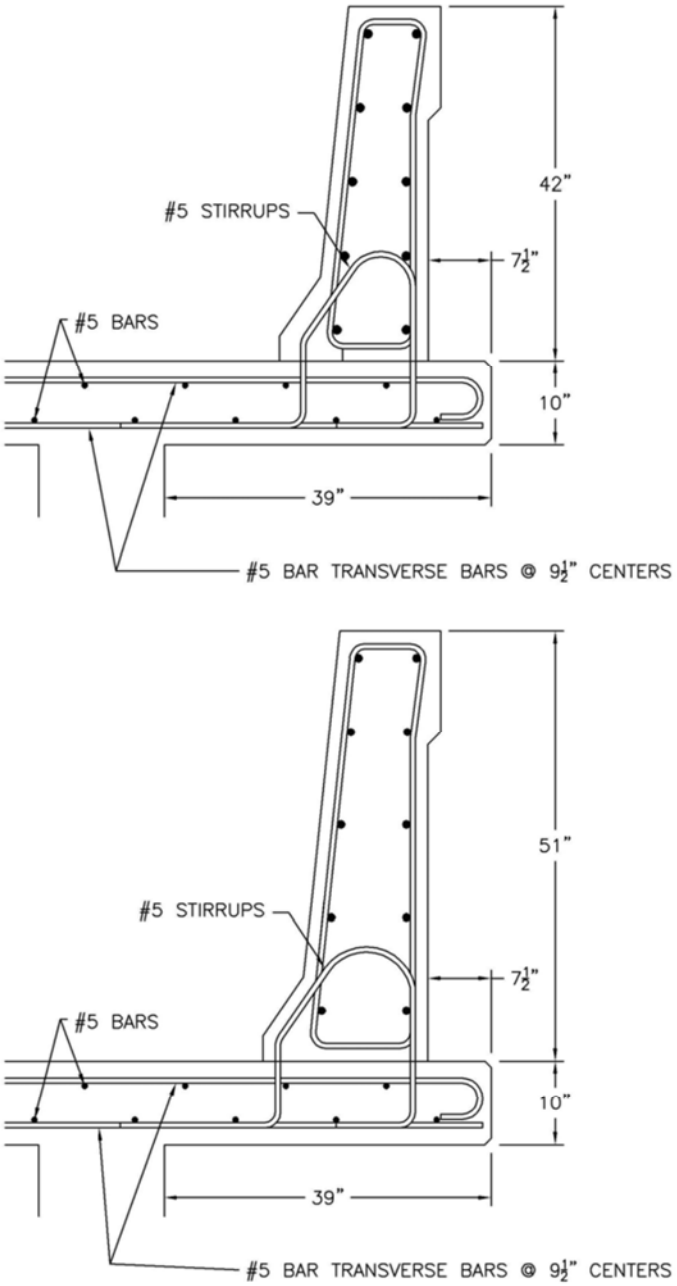

Notes: (1) No. 5 stirrups, used to attach the barrier to the deck, follow same spacing of barrier loop stirrups.
(2) Use Grade 60 reinforcing steel bars.
(3) Use a minimum 28–day concrete compressive strength of 4500 psi.
(4) 1 in. = 25.4 mm

Figure 14
Barrier attachment using a 10-in. thick, reinforced concrete bridge deck

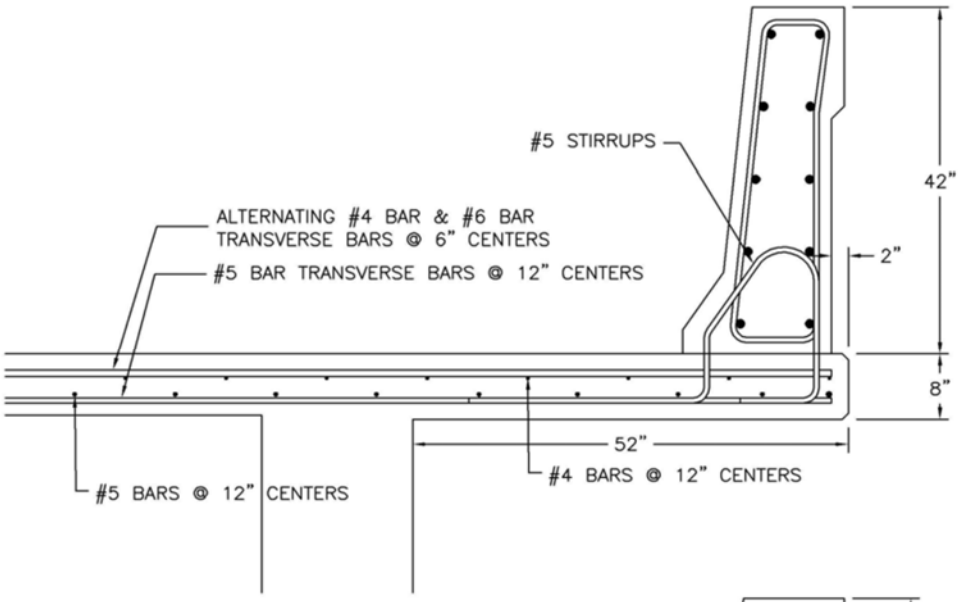

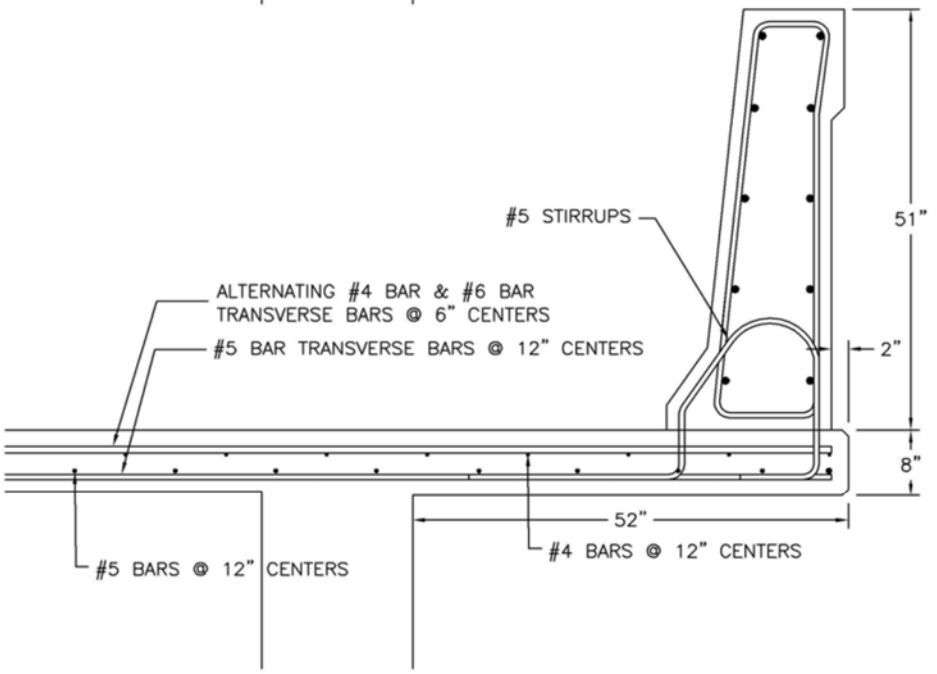

Notes: (1) No. 5 stirrups, used to attach the barrier to the deck, follow same spacing of barrier loop stirrups.
(2) Use Grade 60 reinforcing steel bars.
(3) Use a minimum 28–day concrete compressive strength of 4500 psi.
(4) 1 in. = 25.4 mm

Figure 15
Barrier attachment using an 8-in. thick, reinforced concrete bridge deck

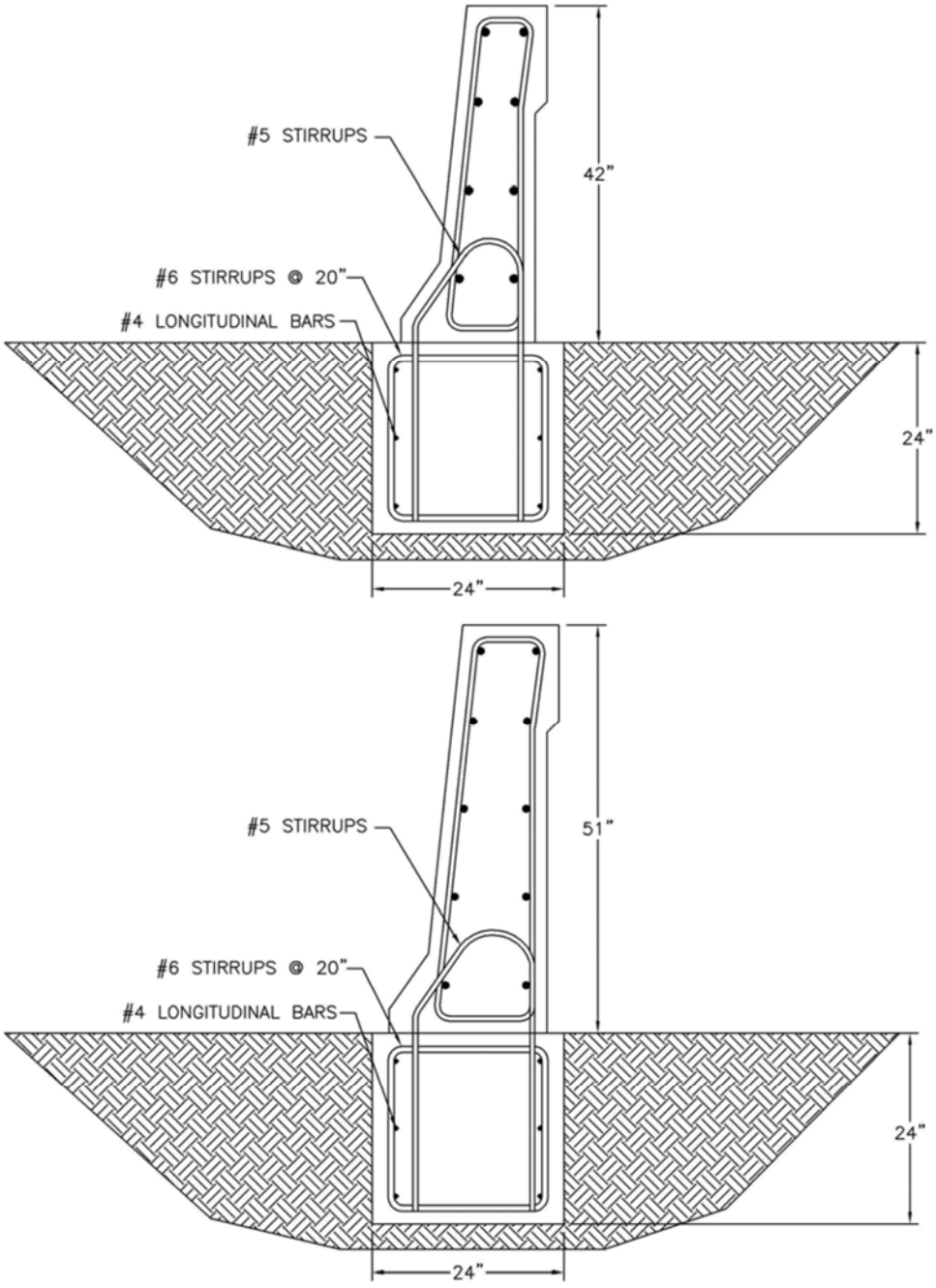

Notes: (1) No. 5 stirrups, used to attach the barrier to the deck, follow same spacing of barrier loop stirrups.
(2) Use Grade 60 reinforcing steel bars.
(3) Use a minimum 28–day concrete compressive strength of 4500 psi.
(4) 1 in. = 25.4 mm

Figure 16
Barrier attachment using a 24-in. square, reinforced concrete footing

Sicking et al. published a study titled, "Performance Evaluation of The Permanent New Jersey Safety Shape Barrier-Update to *NCHRP Report 350* Test No. 3-10 (2214NJ-1)." This study was performed based on the proposed changes to *NCHRP Report 350* guidelines, NCHRP Project 22-14(2). The researchers decided it was appropriate to evaluate the safety of permanent shape barrier systems prior to finalizing the new crash testing procedures and guidelines *[17]*. A permanent New Jersey safety Shape barrier was selected for evaluation. One full-scale vehicle crash test was performed on the longitudinal barrier system in accordance with the test Level 3 (TL-3) requirements presented in the *Update to NCHRP Report No. 350*. For the permanent barrier-testing program, an 1100C small car vehicle was used. The permanent safety shape barrier demonstrated an acceptable safety performance when impacted by the small car, thus meeting proposed TL-3 requirements presented in the Update to *NCHRP Report 350*.

In the same year, Sicking et al., published a study titled, "Performance Evaluation of The Permanent New Jersey Safety Shape Barrier-Update to NCHRP Report 350 Test No. 4-10 (2214NJ-2)." This study was performed based on the proposed changes to the *NCHRP Report No. 350* guidelines, NCHRP Project 22-14(2) *[18]*. The researchers decided it was appropriate to evaluate the safety permanent shape barrier systems prior to finalizing the new crash testing procedures and guidelines. A permanent New Jersey safety shape barrier was selected for evaluation. One full-scale vehicle crash test was performed on the longitudinal barrier system in accordance with the test level 4 (TL-4) requirements presented in *NCHRP Report 350*. For the permanent barrier-testing program, a 10000S single unit truck was used. The permanent safety shape barrier demonstrated an unacceptable safety performance when impacted by the single unit truck, thus failing to meet the proposed TL-4 requirements presented in the *Update to NCHRP Report 350*. The cross section of the NJ barrier used for both tests, TL-3 and TL-4, is shown in Figure 17.

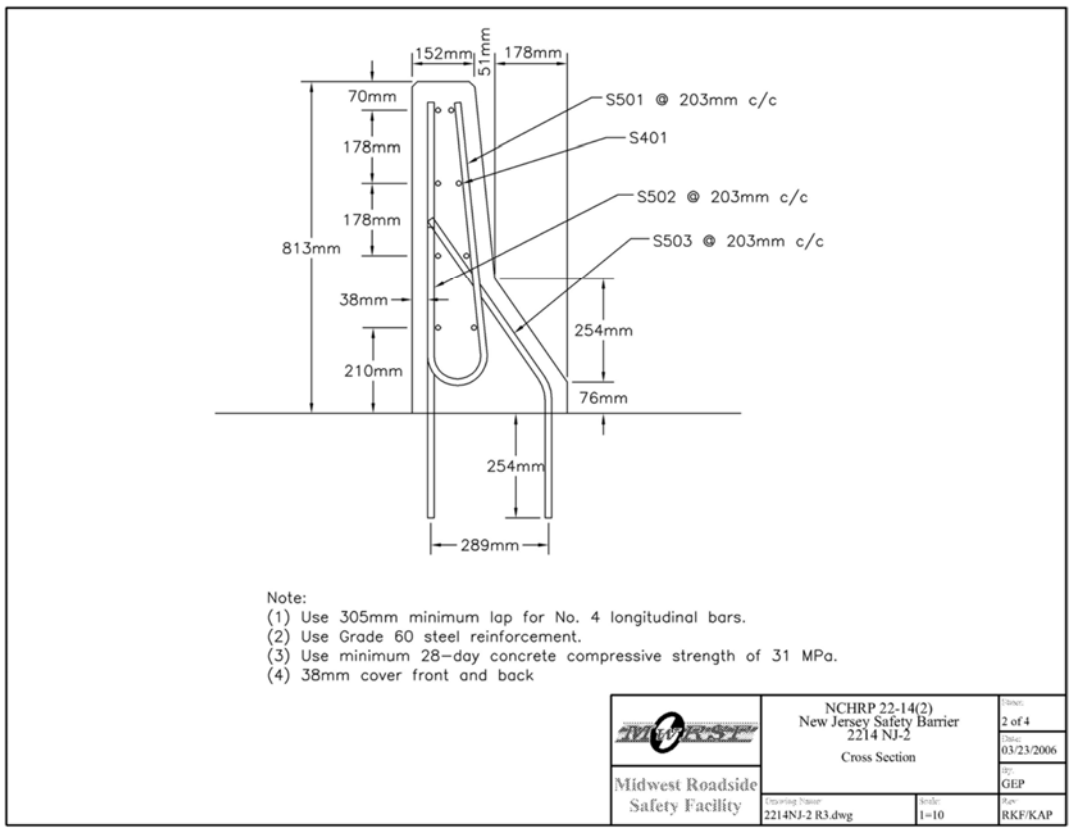

Figure 17
A permanent New Jersey safety shape barrier cross section

Bligh et al. published a study titled "Initial Assessment of Compliance of Texas Roadside Safety Hardware with Proposed Update to NCHRP Report 350." Based on the NCHRP Report 350 Update that was published under NCHRP Project 22-14(2), the researchers performed an initial assessment of the Texas roadside safety hardware to check for their compliance with the Update. During the study, the researchers derived relationships that used a measured lateral impact force resulting from vehicular barrier collision to estimate the impact force associated with a collision involving a different vehicle and/or impact conditions *[2]*.

The F-Shape and New Jersey-Shape Concrete Barriers

The 32-in. F-Shape was originally designed to meet performance level two of the proposed 1987 version of the *Guide Specifications for Bridge Railings*. The required strength test from that proposed version was 5,400-lb. pickup vehicle traveling at 65 mph and impacting at 20 degrees. The design force used for this test condition was 56 kips of line load uniformly distributed over 42 in. at 29 in. above the deck surface. The rail was eventually tested to performance level two requirements of the 1989 *Guide Specifications for Bridge Railings* which requires strength test conditions of 18,000 lb. 50 mph | 15 degrees).

A cross section of the rail design is shown in Figure 18. The total height of the F-Shape is 32 in. It has a lower 3-in. high vertical section, a middle 7-in. high inclined surface of 55 degrees, and an upper 22-in. high inclined surface of 84 degrees. It has a bottom width of 14.7 in. and a top width of 7.5 in. The slope at the bottom of the rail serves to limit the done to vehicles impacting at low angles by causing the front tire to ride up on the rail and redirect itself back to the pavement. A thickened portion of at the top of the rail serves to increase the longitudinal distribution of the force within the F-Shape and allow more strength of F-Shape and deck to resist the collision force.

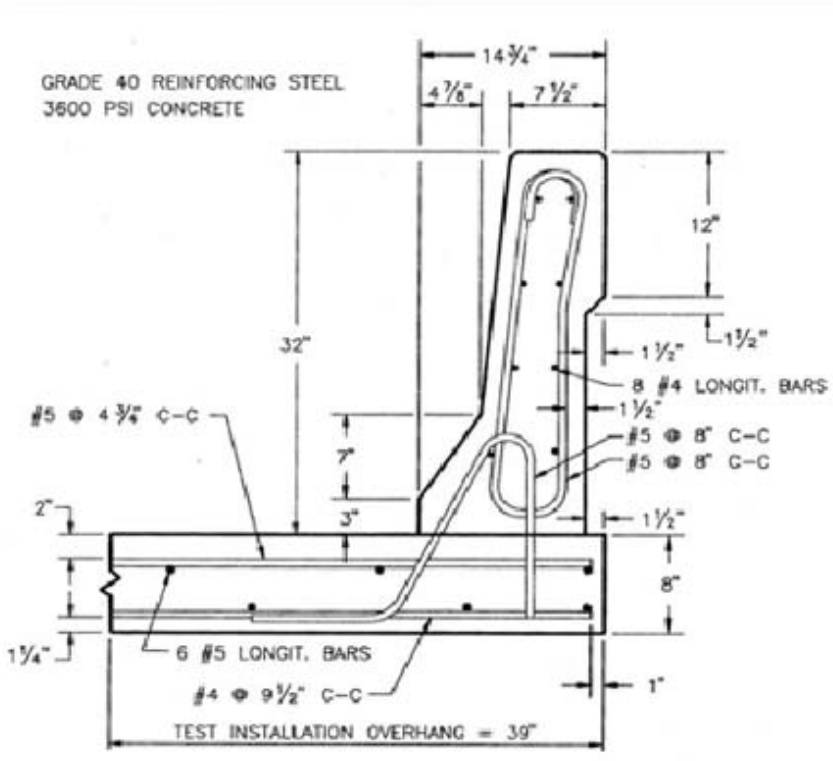

Figure 18
A 32-in. F-Shape concrete barrier

Eight # 4 longitudinal bars were used in the F-Shape. The vertical steel was # 5 stirrups at 8-in. spacing. Specified concrete strength was 3,600 psi at 28 days and specified steel yield was 40,000 psi. The cantilevered deck was supported on a foundation so that the deck overhang was 39 in.

The strength of the rail was computed using yield line analysis procedures. The analysis predicts the length of failure mechanism to be 8.3 ft. and the total ultimate capacity to be 59 kips. The analysis also shows that the yield lines are confined to the F-Shape rather than extending to the bridge deck.

The 32-in. New Jersey safety shape, shown in Figure 19, was designed to meet performance level two of the 1989 *Guide Specifications for Bridge Railings*. The design force used for this test condition was 56 kips of line load uniformly distributed over 42 in. located at least 29 in. above the deck surface.

The total height of the safety shape is 32 in. The thickness of the unit is 15 in. at the base and varies along the height, tapering to a minimum of 6 in. at the top. The slope at the bottom of the rail serves to minimize the damage done to vehicles impacting at low angles by causing the front tire to ride up on the parapet and to be redirected with limited contact between the body of the vehicle and the parapet.

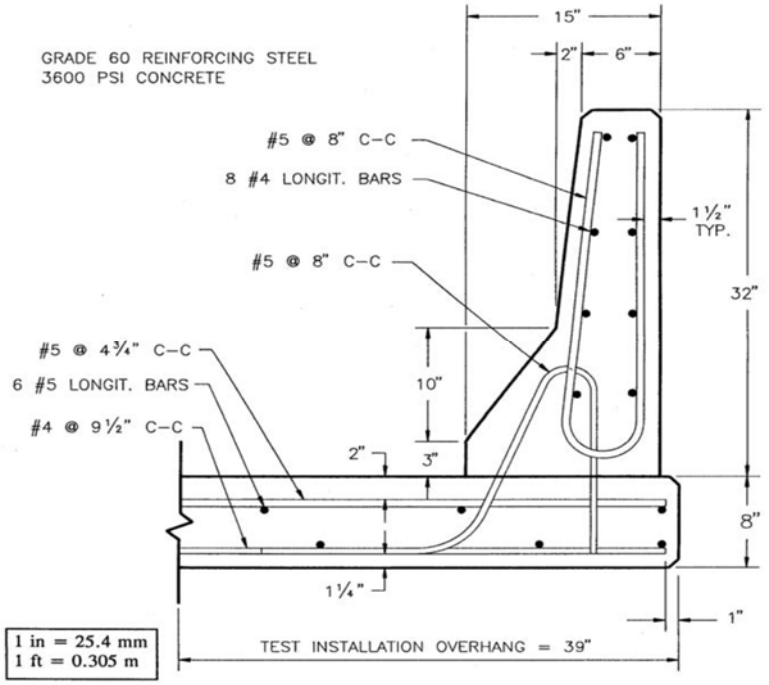

Figure 19
A 32-in. New Jersey concrete barrier

Eight # 4 longitudinal bars were used in the safety shape. The vertical steel was # 5 stirrups at 8-in. spacing. Specified concrete strength was 3,600 psi at 28 days and specified steel yield was 60,000 psi. The cantilevered deck was supported on a foundation so that the deck overhang was 39 in.

The strength of the rail was computed using yield line analysis procedures. The analysis predicts the length of failure mechanism to be 8.1 ft. and the total ultimate capacity to be 74 kips. The analysis also shows that the yield lines are confined to the F-Shape rather than extending to the bridge deck.

Alberson et al. published a study titled "NCHRP Report 350 Compliance Test of the 1.07-m Vertical Wall Bridge Railing." In the study, a crash test was performed on this 42-in. barrier section with an 80,000-lb. truck under *NCHRP Report 350* TL-5 conditions *[19]*. The purpose of the test was to see if the section would perform satisfactorily in containing and redirecting the impacting vehicle while at the same time not allowing it to overturn. The section contained and redirected the impacting vehicle, and the vehicle did not roll. No sign of structural damage to the bridge railing, rail connection, or the bridge deck was detected.

Theoretical Work

Before the development of the ultimate load analysis, structural engineers designed reinforced concrete slabs using the elastic plate theory. Not until the early 1960s was the yield line theory developed and presented by Danish engineer K.W. Johansen. Later, in the United States, bridge design engineers relied on the American Association of State Highway and Transportation Officials' (AASHTO) Bridge Design Manual for the design of bridge railings. In the AASHTO manual, the yield line analysis theory was clearly stated *[20]*.

In this theory, the strength of a slab is assumed to be governed by flexure alone; other effects such as shear and deflection are considered separately. The steel reinforcement is assumed to have fully yielded along the yield lines at collapse and the bending and twisting moments uniformly distributed along the yield lines.

There are two approaches to the calculation of the ultimate load-carrying capacity of a reinforced concrete slab involving yield line theory. One is an energy method that uses the principal of virtual work, and the other, an equilibrium method, studies the equilibrium of various parts of the slab form and by the yield lines. The work here is limited to the analysis performed by using the principle of virtual work that is used in the calculation of collapse loads of beams and frames.

Barker and Puckett defined the yield line method a procedure in which the slab is assumed to behave in-elastically and exhibits adequate ductility to sustain the applied load until the slab reaches a plastic collapse mechanism *[21]*. This assumption is very realistic since the reinforcement proportioning required by AASHTO gives under-reinforced or ductile systems. The slab is assumed to collapse at a certain ultimate load through a system of plastic

hinges called yield lines. The yield lines form a pattern in the slab creating the mechanism. Two methods are available for determining the ultimate load by the yield line method: the equilibrium approach and the energy approach. The energy approach is described here because it is, perhaps, the simplest to implement. The energy approach is an upper-bound approach, which means that the ultimate load established with the method is either equal to or greater than the actual load (i.e., non-conservative). If the exact mechanism or yield-line pattern is used in the energy approach, then the solution is theoretically exact. Practically, the yield pattern can be reasonably estimated and the solution is reasonable for design. Patterns may be selected by trial, or a systematic approach may be used. Frequently, the yield line pattern can be determined in terms of a few (sometimes one) characteristic dimensions. These dimensions may be used in a general manner to establish the ultimate load, and then, the load is minimized with respect to the characteristic dimensions to obtaining the lowest value.

Fundamental Assumptions

In applying the yield line theory to ultimate load analysis of reinforced concrete slabs, the following fundamental assumptions are made *[22]*:

1. The steel reinforcement is fully yielded along the yield lines at failure.

2. The slab deforms plastically at failure and is separated into segments by the yield lines.

3. The bending and twisting moments, m_α and m_t, (Figure 20), are uniformly distributed along the yield line and they are the maximum values provided by the moment strengths in two orthogonal directions (for two-way slabs).

4. The elastic deformations are negligible compared with the plastic deformations; thus, the slab parts rotate as plane segments in the collapse conditions.

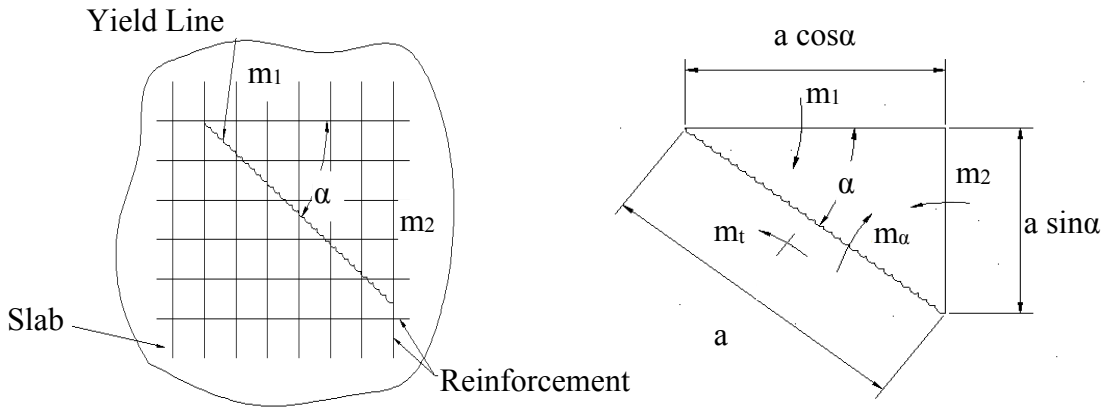

Figure 20
Bending and twisting moment on a yield line

Ghali and Neville stated the following fundamental assumptions of the yield line theory *[23]*:

1. In the mechanism, the bending moment per unit length along all yield lines is constant and equal to the moment capacity of the section.

2. The slab parts (area between yield lines) rotate as rigid bodies along the supported edges.

3. The elastic deformations are considered small relative to the deformation occurring in the yield lines.

4. The yield lines on the sides of two adjacent slab parts pass through the point of intersection of their axes of rotation.

Hirsh analyzed the lateral load carrying capacity of a uniform thick, solid concrete barrier *[24]*. He developed expressions for the strength of the barrier based on the formation of yield lines at the limit state. The assumed yield line pattern caused by the vehicle collision that produce a force F_t that is distributed over a length L_t, as shown in Figure 21. Hirsh et al. equated the external virtual work due to the applied loads to the internal virtual work done by the resisting moments along the yield lines. The analysis indicated that the applied load determined by this method was either equal to or greater than the actual load, that is; the solution was not conservative. Considering those, Hirsh et al. minimized the load for a particular yield line pattern.

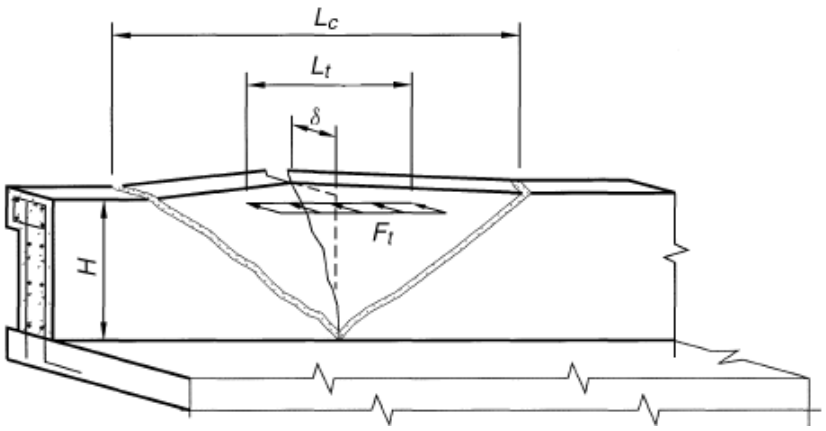

Figure 21
Loading and yield line pattern for concrete barrier [24]

External Virtual Work by Applied Loads

The original and deformed positions of the top of the wall are shown in Figure 22. These positions were proposed by Calloway *[25]*. The shaded area represents the integral of the deformations through which the uniformly distributed load W_t (= F_t /L_t) acts. For a virtual displacement δ, the displacement x is

$$x = \delta \left(\frac{L_c - L_t}{L_c}\right) \tag{1}$$

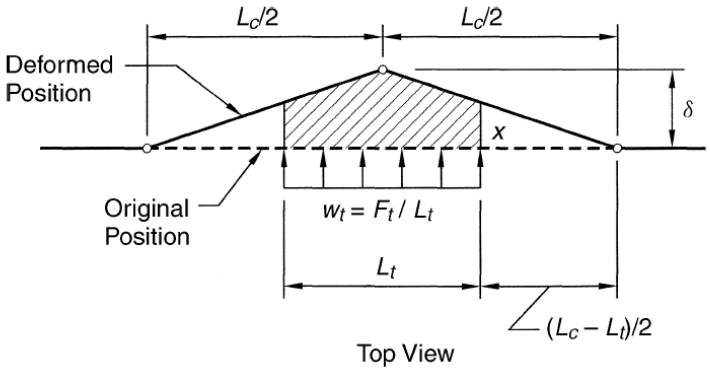

Figure 22
External virtual work by distributed load [25]

The area of the shaded region is given as:

$$\text{Area} = \left(\frac{\delta + x}{2}\right) * L_t = \frac{\delta}{2}\left(1 + \frac{L_c - L_t}{L_c}\right) * L_t \tag{2}$$

$$\text{Area} = \delta \frac{L_t}{L_c}\left(L_c - \frac{L_t}{2}\right) \tag{3}$$

The external virtual work, W, done by W_t (= F_t /L_t) is equal to

$$W = W_t(\text{area}) = \frac{F_t}{L_t}\delta\frac{L_t}{L_c}\left(L_c - \frac{L_t}{2}\right) \tag{4}$$

$$W = F_t \frac{\delta}{L_c}\left(L_c - \frac{L_t}{2}\right) \tag{5}$$

Internal Virtual Work along Yield Lines

The internal virtual work along the yield lines is the sum of the products of the yield moments and the rotations through which they act. The segments of the wall are assumed rigid so that all of the rotation is concentrated at the yield lines. At the top of the wall in Figure 23, the rotation θ of the wall segments for small deformations is

$$\theta \approx \tan\theta = \frac{2\delta}{L_c} \tag{6}$$

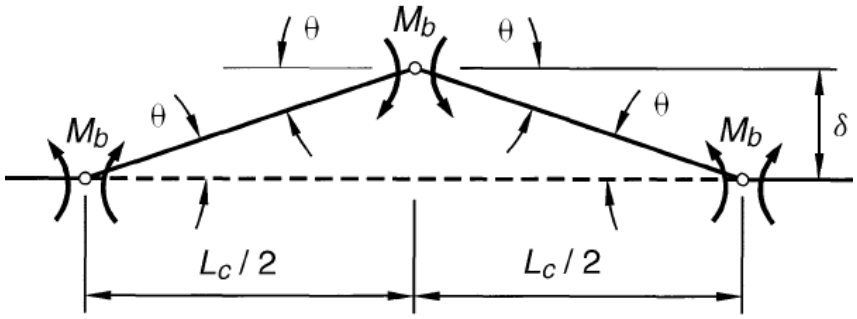

Figure 23
Plastic hinge mechanism for top beam [25]

The barrier can be analyzed by separating it into a beam at the top and a wall of uniform thickness below. At the limit state, the top beam will develop plastic moments M_b equal to its nominal strength M_n. Assuming that the negative and positive plastic moment strengths are equal, the internal virtual work U_b done by the top beam is

$$U_b = 4M_b\,\theta = \frac{8M_b\delta}{L_c} \tag{7}$$

The wall portion of the barrier will generally be reinforced with steel in both the horizontal and vertical directions. The horizontal reinforcement in the wall develops moment resistance, M_w, about a vertical axis. The vertical reinforcement in the wall develops a cantilever moment resistance, M_c, per unit length about a horizontal axis. These two components of moment will combine to develop a moment resistance M_α about the inclined

yield line as shown in Figure 24 and Figure 25. When determining the internal virtual work along inclined yield lines, it is simpler to use the projections of moment on and rotation about the vertical and horizontal axes.

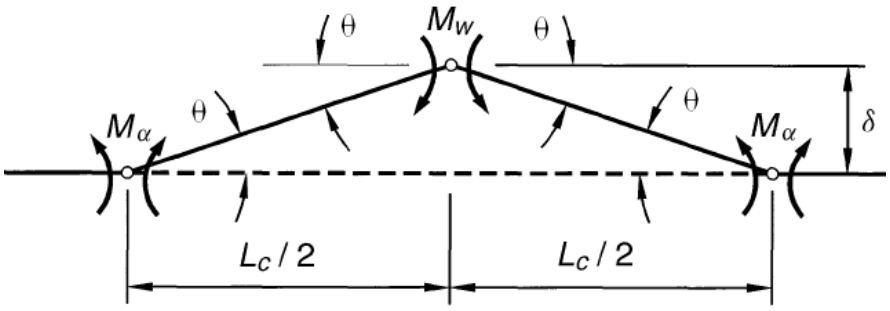

Figure 24
Internal virtual work by barrier wall (top view) [25]

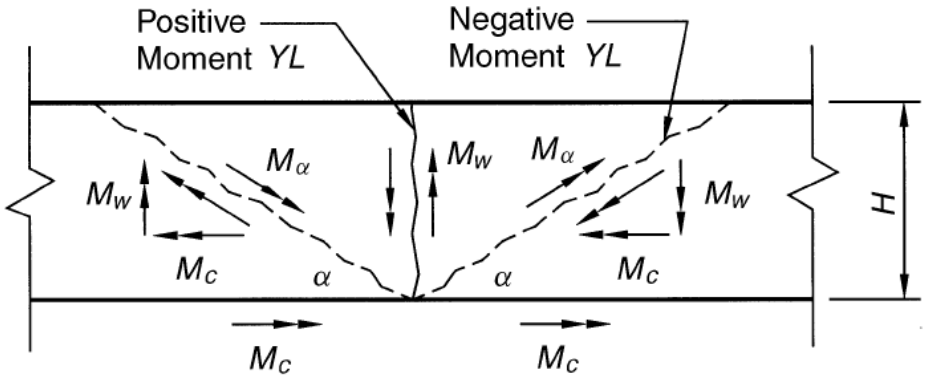

Figure 25
Internal virtual work by barrier wall (front view) *[25]*

Assuming that the positive and negative bending resistances, M_w, about the vertical axis are equal, and using θ as the projection on the horizontal plane of the rotation about the inclined yield line, the internal virtual work, U_w, done by the wall moment, M_w, is then

$$U_w = 4M_w\,\theta = \frac{8M_w\delta}{L_c} \tag{8}$$

The projection on the vertical plane of the rotation about the inclined yield line is δ/H, and the work done by the wall moment, M_w, is then

$$U_c = \frac{M_c L_c \delta}{H} \tag{9}$$

Nominal Railing Resistance Transverse Load, R_w

Equating the external virtual work, W, to the internal virtual work, U

$$W = U_b + U_w + U_c \tag{10}$$

Substituting equations,

$$\frac{F_t}{L_c}\left(L_c - \frac{L_t}{2}\right)\delta = \frac{8M_b\delta}{L_c} + \frac{8M_w\delta}{L_c} + \frac{M_c L_c \delta}{H} \tag{11}$$

Solving for the transverse force, F_t:

$$F_t = \frac{8M_b}{\left(L_c - \frac{L_t}{2}\right)} + \frac{8M_w}{\left(L_c - \frac{L_t}{2}\right)} + \frac{M_c L_c^2}{H\left(L_c - \frac{L_t}{2}\right)} \tag{12}$$

This expression depends on the critical length L_c that determines the inclination of α of the negative moment yield lines in the wall. The value for L_c that minimizes F_t can be determined by differentiating the above equation with respect to L_c and setting the result equal to zero, that is,

$$\frac{\partial F_t}{\partial L_c} = 0 \tag{13}$$

This minimization results in a quadratic equation that can be solved explicitly to give

$$L_c = \frac{L_t}{2} + \sqrt{\left(\frac{L_t}{2}\right)^2 + \frac{8H(M_b + M_w)}{M_c}} \tag{14}$$

When this value of L_c is used, then the minimum value for F_t results, and the result is denoted as R_w, that is,

$$M_{in}\, F_i = R_w \tag{15}$$

Where R_w is the nominal railing resistance to transverse load. By rearranging F_t equation, R_w is

$$R_w = \frac{2}{2L_c - L_t}\left(8M_b + 8M_w + \frac{M_c {L_c}^2}{H}\right) \tag{16}$$

Shear Design

Hirsch (1978) published a study titled "Analytical Evaluation of Texas Bridge Rails to Contain Buses and Trucks." In the appendix, they evaluated the section moment and shear capacity of the section based on basic reinforced concrete design and analysis principles *[24]*. It is noted that concrete barrier have to be designed separately for shear since the yield line theory is based on flexure only, i.e., moment and not shear.

Experimental And Computational Work

Material Characteristics

Structural Concrete. The *2006 Louisiana Standard Specification of Bridges and Roads Manual* states that "Structural concrete shall comply with section 901 of the Manual" *[26]*. Classes of concrete furnished for use on Louisiana's bridges and roadways shall be as shown in Table 5.

In Part IX, the Manual also provides a master proportion table for Portland cement concrete as shown in Table 6.

Table 5
Classes and uses of concrete

Concrete Class	Use
A or A(M)	Concrete exposed to sea water, and all other concrete except as listed herein
AA or AA(M)	Cast-in-place bridge superstructure
D	Pier footings
F	Dam and flood control structures
P or P(M)	Precast bridge members
P(X)	Precast-prestressed bridge girders
R	Non reinforced sections
S	Underwater sections

Table 6
Master proportion table for Portland cement concrete

	Average Compressive Strength, psi (MPa) at 28 days	Grade of Coarse Aggregate	Min. Cement, lb./yd^3 (kg/m^3)of Concrete [9,14]	Maximum Water/Cement ratio, lb/lb (kg/kg) [1,9]	Total Air Content (percent by volume) [4]	Slump Range [10], inches (mm)		
						Non-Vibrated	Vibrated	Slip Form Paving [2]
Structural Class [11]								
AA(M)	4400 (30.4)	A,P	560 (332)	0.44	5±1	2-5 (50-125)	2-4 (50-100)	N.A.
AA	4200 (29.0)	A,P	560 (332)	0.44	5±1	2-5 (50-125)	2-4 (50-100)	N.A.
A(M)	4400 (30.4)	A,P	510 (302)	0.53	5±2	2-5 (50-125)	2-4 (50-100)	N.A.
A	3800 (26.2)	A,F[8], P	510 (302)	0.53	5±2	2-5 (50-125)	2-4 (50-100)	1-2.5 (25-65)
D	3300 (22.8)	A,B,D P	420 (249)	0.58	5±2	2-5 (50-125)	1-3 (25-75)	N.A.
F	3400 (23.5)[5]	A, P	460 (273)	0.44	5±1	2-5 (50-125)	2-4 (50-100)	N.A.
P(X)	7500 (51.7)[5]	A,F[8], P	700 (415)	0.40	5±2	N.A.	2-10 (50-250)	N.A.
P(M)	6000 (41.4)[5]	A,F[8], P	600 (356)	0.44	5±2	N.A.	2-6 (50-150)	N.A.
p	5000 (34.5)[5]	A,F[8], P	560 (332)	0.44	5±2	N.A.	2-6 (50-150)[7]	N.A.
S	3800 (26.2)	A,P	650 (385)	0.53	5±2	6-8 (150-200)	N.A.	N.A.
Minor Structures Class [11]								
M	3000 (20.7)	A,B, P	470 (279)	0.56	5±2	2-5 (50-125)	2-4 (50-100)	1-2.5 (25-65)
R	1800 (12.4)	A,B,D,P	370 (219)	0.70	5±2	2-5 (50-125)	2-4 (50-100)	N.A.
Y	3000 (20.7)	Y	560 (332)	-[3]	6-9	N.A.	1-3 (25-75)	N.A.
Pavement Type [11]								
B	4000 (27.6)[6]	N/A[13]	475 (282)	0.53	5±2	N.A.	2-4 (50-100)	1-2.5 (25-65)
D	4000 (27.6)[6]	N/A[13]	450 (267)	0.53	5±2	N.A.	2-4 (50-100)	1-2.5 (25-65)
E	4000 (27.6)[6]	A, F[12],P	600 (356)	0.40	5±2	N.A.	2-4 (50-100)	1-2.5 (25-65)

N.A. – Not Applicable

[1]Except for Class AA, AA(M), or F-concrete , the maximum volume of water, gal, (L), shall be reduced 5 percent when a water-reducing admixture is used, and 10 percent when an air-entraining admixture, or air-entraining and water-reducing admixtures, is used. When the coarse aggregate portion of the mix is 100 percent crushed aggregate, the water may be increased by 5 percent provided the maximum water listed in Table 901-3 is not exceeded.

[2]Also slump range for other concrete placed by extrusion methods.

[3]Refer to Subsection 901.08(c).

[4]Total air content ranges when air-entrainment is allowed or specified. Air content shall be designed at midrange. See Subsection 901.08 (b)

[5]Values shown represent the minimum compressive strengths allowed.

[6]Average compressive strength for Pavement Type concrete shall be 3600 psi (25.0 MPa) when air-entrainment is used.

[7]No more than a 2 inch (50 mm) slump differential for any design pour.

[8] Grade F coarse aggregate shall be used only when specified or permitted. This minimum cement content shall be increased when this aggregate is used.

[9]For mixes including partial replacement of cement with fly ash or ground granulated blast furnace slag, the minimum cement and maximum water contents shown apply to the total cement and fly ash or ground granulated blast furnace slag content of the mix. Additional cement may be required to achieve minimum compressive strength.

[10]When a slump range is specified in other sections, that range shall govern.

[11]See Subsection 901.08(a) for allowable types of cement.

[12]For use in partial depth patching.

[13]Aggregate grading shall comply with the requirements of Subsection 1003.02(c).

[14]The minimum cement factors may be waived in writing by the District Laboratory Engineer in accordance with Subsection 901.06(a).

In order to comply with the requirement strength for the concrete mix used in casting the slab and the concrete barrier, a 7-day and a 28-day test was performed on concrete cylinder based on the requirement of ASTM C 39, "Compressive Strength of Cylindrical Concrete Specimens." An average 7-day test was 4,935 psi, while an average 28-day test was 7,638 psi for Waskey's lab cores while those values for LTRC lab cores were 5,309 psi and 6,624 psi, respectively. Table 7 shows a tabulation of compressive strength data.

Table 7
Detailed compressive strength data

Testing Source	Comp. Concrete Strength f'c, (psi)	Avg. Comp. Concrete Strength f'c, (psi)
Waskey, 7-day test	4,840 5,030	4,935
LTRC, 7-day test	5,103 5,486 5,338	5309
Waskey, 28-day test	7,600 7,675	7638
LTRC, 28-day test	6,524 6,471 6,879	6624

LTRC average 28-day compressive stress will be used since LTRC followed the ASTM C39 standards that included placing the concrete in a 95% humidity chamber. Therefore, an average compressive stress, f'_c, of 6,624 psi was used in the analytical computations. Figure 26 and Figure 27 show the concrete cylinders made at the plant and the testing of one cylinder.

Figure 26
Concrete cylinders made at the plant

Figure 27
Determination of the compressive strength, f'_c, of a concrete cylinder

The modulus of elasticity of concrete, E_c, was evaluated in compliance with ASTM C 469, "Static Modulus of Elasticity and Poisson's Ratio of Concrete in Compression." The test was performed at LTRC, and the modulus of elasticity was found to be equal to 5,750 and 6,000 ksi for a 7-day and 28-day test, respectively. Figures 28 through 42 show the different stages that took place at the plant from preparation of the forms to the casting of the F-Shape concrete barrier.

Figure 28
Slab reinforcement is placed in the casting bed

Figure 29
PVC Pipe blockings used for anchoring the slab to the strong floor

Figure 30
A close view for a blocking for anchoring the slab to the strong floor

Figure 31
Barrier slab formed and reinforcement placed

Figure 32
Placement of the reinforcement for concrete barrier

Figure 33
Concrete barrier's form and reinforcement

Figure 34
Placement of the special form to create the shear key base

Figure 35
Pouring of concrete in the formed slab frame

Figure 36
Working of the placed concrete

Figure 37
Removing of the block-out form

Figure 38
Shear key formed in base of slab

Figure 39
Placing and vibrating the concrete in barrier wall

Figure 40
Barrier wall poured

Figure 41
Bottom of concrete barrier

Figure 42
F-Shape concrete barrier after the forms were removed

After the barrier-slab system was cured at the plant in Baton Rouge, it was transported to the Trenchless Technology Center at Louisiana Tech University. The slab was first anchored to the strong floor at the center. The vertical wall was then connected to the slab via strong anchor rods. The shear key bases were filled with non-shrink epoxy grout. Figures 43 through 48 show how the precast concrete barrier was anchored to the strong floor.

Figure 43
Black squares are heavy steel plates to protect threaded sleeves of anchor rods

Figure 44
Typical bolt used to anchor slab to strong floor

Figure 45
A typical detail to connect the barrier to the slab

Figure 46
Anchoring the slab to the strong floor

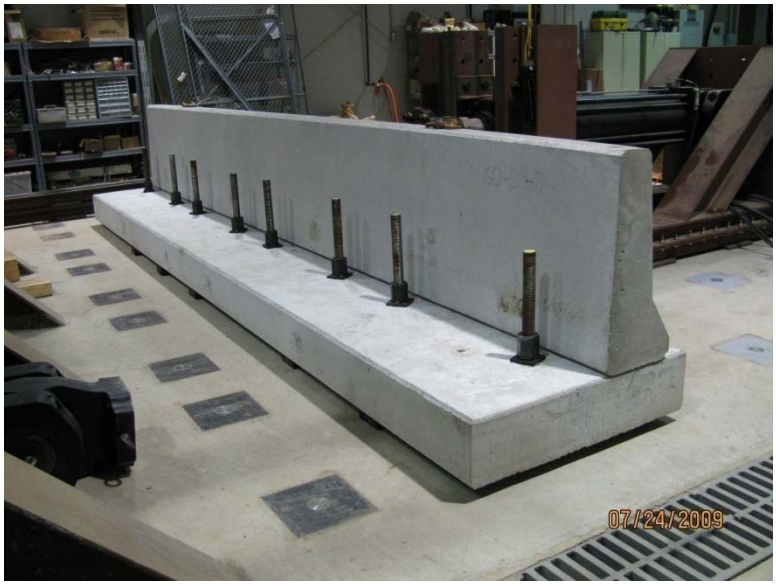

Figure 47
Rear view of slab-barrier system after it was connected at the center

Figure 48
Front view of slab-barrier system after it was connected at the center

Serviceability – Deflection

One of the benefits of using precast bridge rail in lieu of cast-in-place members is the ease of connection to the bridge deck. Though all bridge railings are designed with flexure due to bending moment, in mind, deflection of bridge railing is considered negligible since concrete bridge railing are classified as rigid sections (i.e., unyielding).

Cast-in-place railings transfer all lateral flexural forces they are subjected to, in the form of shearing forces across a cold joint, which in turn is transferred to the deck through additional tensile force on the deck reinforcement and a moment at the fixed end of the overhang.

Precast concrete barrier behave somewhat differently from cast-in-place concrete barriers. To a certain depth from the top surface of the barrier, the section can provide a resisting moment to the transverse force. The yielding moment depends on the development length of the reinforcing bars after which the additional overturning moment will be resistant in tension through the anchor bolts.

Cast-in-place railings transfer all transverse forces they are subjected to, moments and shear forces to the contact region between the rail and the deck. This shear force is, in turn, transferred to the deck through additional tensile force on the deck reinforcement. Precast bridge railings through their bolted connections can be viewed as easier to replace than cast-in-place railings.

Precast bridge railings through their bolted connections can be viewed as easier to replace than cast-in-place railings. Figure 49 shows how the lateral impact force is transmitted from the barrier to the deck.

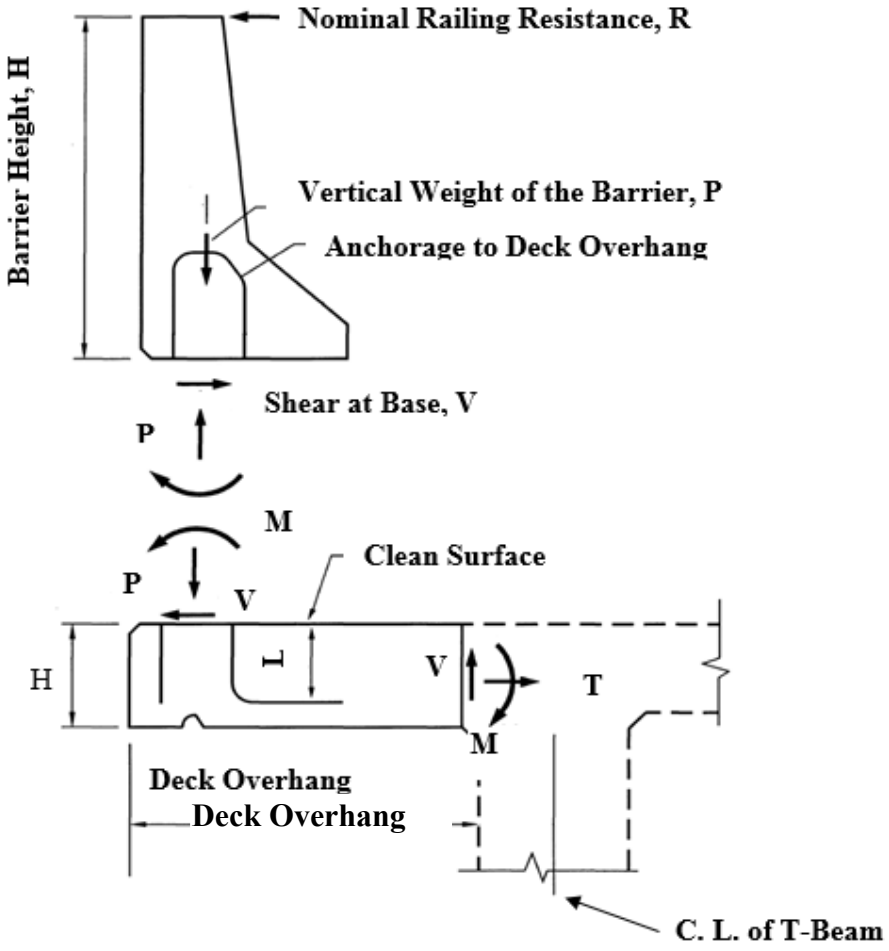

Figure 49
Force transfer between barrier and deck

Replacing a cast-in-place rail is more costly, time consuming, and requires lane closure for deck rehabilitation. Compared to that, precast bridge railings are easier to replace due to the ease of re-bolting a new precast bridge rail section to the existing deck. In essence, precast bridge railings may be viewed as sacrificial flexural members when compared to cast-in-place bridge railings.

Description of the Tested F-Shape Section

A cross section of the rail design is shown in Figure 50. The total height of the safety shape is 32 in. The thickness of the unit is 13.25 in. at its base and varies along the height, tapering to a minimum of 6 in. at the top. The slope at the bottom of the rail serves to minimize the damage done to vehicles impacting at low angles by causing the front tire to ride up on the parapet and to be redirected with limited contact between the body of the vehicle and the parapet.

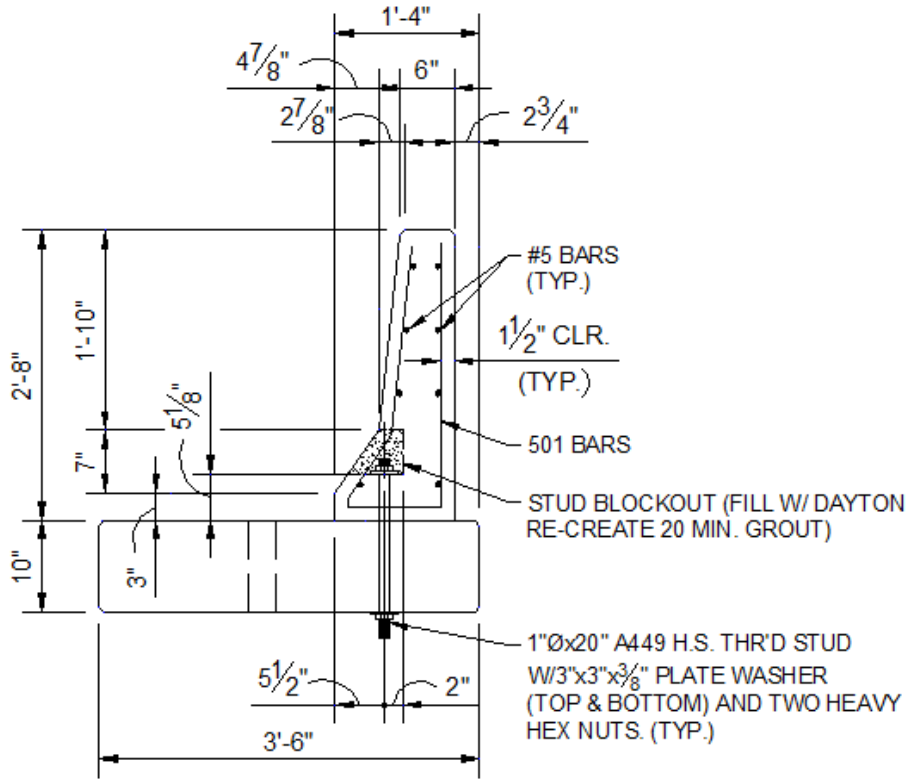

Figure 50
F-Shape section tested in the lab

Eight #5 longitudinal bars were used in the safety shape. The vertical steel was #5 stirrups at 8-in. spacing. The specified concrete strength was 6,500 psi at 28 days and the specified steel yield was 60,000 psi. The cantilevered deck was supported on a foundation so that the deck overhang was 42 in.

The strength of the rail was computed using yield line analysis procedures *[19]*. The analysis predicts the length of failure mechanism to be 5.81ft. and the total ultimate capacity to be 83 and 56 kips for interior region and end region, respectively. The analysis also shows that the yield lines are confined to the F-Shape rather than extending to the bridge deck.

Instrumentation Plans

The barrier was instrumented at points representing the virtual intersection points of the vertical and longitudinal reinforcing steel bars. The sloping face and the vertical face of the barrier were instrumented. Figure 51, Figure 52, and Figure 53 show the process of instrumentation of the barrier wall.

Figure 51
Marking up the barrier to place the strain gauges

Figure 52
Barrier rear face after instrumentation

Figure 53
Strain gauge wires being connected to the data logger

Distribution of Strain Gauges on the Sloping Side of the Barrier

Every location of a strain gauge is defined by a row and a column, letter and number, respectively. Every strain gauge designation contains either a letter "H" or a letter "V." This designation defines whether the stain gauge is horizontal or vertical. For example, the strain gauge "A3H" means a horizontal gauge placed at the intersection of row A and column 3, while AB3V means a vertical gauge placed between rows A and B and in the direction of column 3. Table 8 shows the distribution of horizontal and vertical strain gauges on the sloping face of the barrier.

Table 8
Strain gauges on sloping face of barrier

Row	Gauge Number
A	AB3V, AB5V, AB12V, AB13V
B	BC3V, BC13V, B3H, B5H, B12H, B13H
C	None

On this face of the barrier, eight strain gauges were placed in the horizontal direction of the longitudinal bars and six stain gauges were placed in the vertical direction along the vertical stirrups. Of the fourteen placed strain gauges, only four horizontal and four vertical strain gauges were considered active during the testing. This was due to the fact that the data logger used during the testing could only accommodate 20 strain gauges. All gauges were each 2 in. long, seven on tensile side and seven on compressive side, were attached to the concrete surface in order to record strain on the outermost fiber of the GPC barrier

Distribution of Strain Gauges on the Vertical Side of the Barrier

Every location of a strain gauge is defined by a row and a column, letter and number, respectively. Every strain gauge designation contains either a letter "H" or a letter "V." This designation defines whether the stain gauge is horizontal or vertical. For example, the strain gauge "A3H" means a horizontal gauge placed at the intersection of row A and column 3. Table 9 and Table 10 show the distribution of horizontal and vertical strain gauges on the vertical face of the barrier.

Table 9
Horizontal strain gauges on vertical face of barrier

Row	Horizontal Strain Gauges
A	A1H, A4H, A6H, A10H, A12H, A14H, A15H
B	B4H, B6H, B10H

Table 10
Vertical strain gauges on vertical face of barrier

Row	Vertical Strain Gauges
A	A8V
B	B8V
C	C8V

Ten strain gauges were placed in the horizontal direction in the direction of the longitudinal bars, and three stain gauges were placed in the vertical direction along the vertical stirrups. All strain gauges were placed externally and on the vertical face of the barrier.

Of the thirteen strain gauges, only nine horizontal and three vertical strain gauges were considered active during the testing. Table 11 shows the channel number assigned to each strain gauge. This result was because the data logger used during the testing could only accommodate 20 strain gauges.

Table 11
Channel assigned numbers and designated strain gauges

Channel Number	Strain Gauge
101	A8V
102	A6H
103	A10H
104	A4H
105	A12H
106	A1H
107	A15H
108	B8V
109	B6H
110	B10H
111	B4H
112	C8V
113	AB3V*
114	B3H
115	AB5V*
116	B5H*
117	AB12V*
118	B12H*
119	AB13V*
120	B13H*

* Denotes on sloping face of barrier

Hydraulic Ram

An MTS, closed-loop servo, Series 201 Hydraulic Actuator linear hydraulic actuator was used to apply the transverse load on the concrete barrier. The actuator has a compressive capacity of 330 kips and a tensile capacity of 215 kips. Figure 54 shows the hydraulic ram used in transverse load application. The hydraulic ram is bolted to the strong floor of the lab and equipped with shear plates to resist the reaction of the barrier when the load is applied. Additional information regarding this system is available in Appendix C.

Figure 54
Hydraulic ram used in transverse load application

Figure 55 shows a close-up of the ram head. The head was mounted with a 6 in. x 6 in. by 42-in. steel beam. The purpose of the beam is to spread the concentrated load applied by the ram over a length of 42 in., which is approximately the diameter of a tire when making contact with the barrier.

Figure 55
View of the ram head (before modification)

Figures 56 to 59 show a side view of the hydraulic ram that is controlled by a computer, which in turn controls the incremental load that it would be applied. This process is performed through the hydraulic hoses that run between the ram itself and the ram controlling unit.

Figure 56
View of the ram with the metal box bolted to its head

Figure 57
Close view of the hydraulic ram

Figure 58
Ram in slight contact with the sloping face of barrier

Since the tested F-Shape concrete barrier has a sloping face, it was necessary to fit the front of the ramming head with a certain "wedge." This fitting was done to make sure that the line of action of the applied force is exactly normal to the sloping face of the barrier.

Strain gauges were connected to a 20-channel data logger that was controlled by a laptop. Figure 59 shows the laptop and the data logger.

The median barrier was tested in a 'Load Control' fashion. Loading was applied in 2-kip increments. The barrier was thoroughly checked for cracking following each load increment. Cracks were marked and designated with sequential labels. The hydraulic ram was equipment with an LDVT sensor to measure the horizontal deflection at load increments. Load increments and measured barrier deflection were collected by the hydraulic ram control station.

Figure 59
Laptop and data logger used in the test

Test Procedure

After the concrete barrier has been properly anchored and instrumented, the hydraulic ram was extended to the sloping face. The bolted box that was attached to the ram head was lined up with the top edge of the barrier. In this way, a maximum bending moment with the respect to the base of the barrier could be achieved. After the box was in contact with the barrier face, the force indicator zeroed out.

Field Testing of the Bolted Concrete Barrier

After the rail was instrumented, the test was performed on the section. The field testing of the bolted concrete barrier was performed by lining up the 42-in. mounted element of the ram against the top face of the sloping side of the barrier. Figure 60 and Figure 61 show the mounted element on the ram along which a uniform load will be applied.

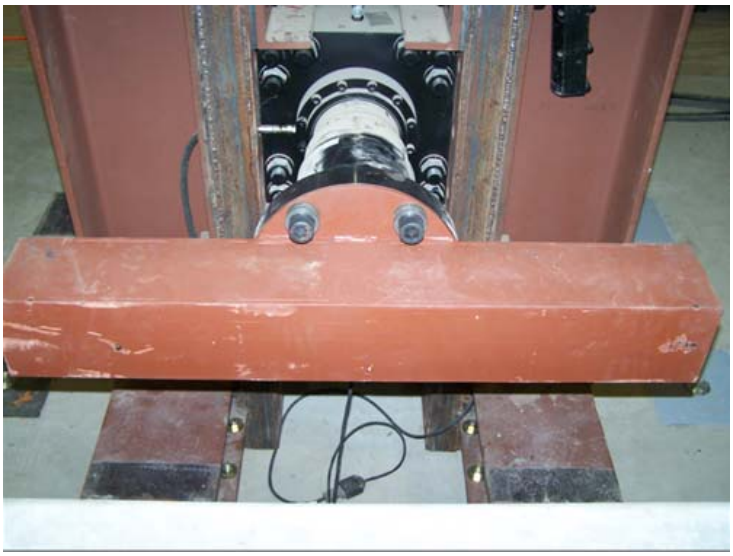

Figure 60
Mounted element of the ram

Figure 61
Lining of the hydraulic ram head against sloping face of barrier

The tip of the ram was applied against the sloping face of the barrier. The top of the head is about 4 in. below the top surface of the barrier at approximately the location of the top horizontal #5 bar.

The static (quasi-static) load was applied at 2000-lb. intervals, after which it was sustained without any increments for a small duration of time to allow for checking and marking of any developing cracks.

Figure 62 shows the process of checking and marking the cracks developing during the test.

Figure 62
Checking and marking cracks

Figure 63 shows the growth pattern of diagonal cracks on the vertical face of the barrier.

Figure 63
Diagonal cracks developing on vertical face of barrier

Figure 64 shows the diagonal cracks developed during the test on the sloping (inside) face of the barrier.

Figure 64
Diagonal cracks developing on sloping face of barrier

At around 40 kips of applied load; diagonal cracks started developing at different locations of the barrier's faces. Some cracks were intermittent and some were running from the location of bolted anchor and to the top of the barrier as shown in Figure 65.

Figure 65
Cracks developing at top face of barrier slab

As testing progressed, cracks continued developing on the inside face of the barrier as shown in Figure 66.

Figure 66
Continued diagonal crack propagation

Diagonal cracks kept propagating from the bottom of the inside face of the barrier toward the top as shown in Figure 67.

Figure 67
Diagonal cracks through barrier anchor supports

The purpose of the barrier is to successfully contain the impact of a load and transfer the load to the deck through the deck reinforcement. Under no situation should the crack propagate from the barrier to the deck. This occurrence will lead to structural problems and costly repair in the form of materials, labor, and traffic delay.

Cracks in the slab of this tested rail started developing around an applied lateral load of 40,000 lb. At this point, the test could have been stopped, but it would be questionable if this barrier could be TL-3 compliant (resisting a 54-kip lateral load). However, when the test continued, the cracks in the slab did not propagate nor did new ones form.

Testing continued at the same load intervals and more cracks developed and were marked. When the applied lateral load reached a value of 64 kips, it was deemed unsafe to stop, mark the cracks, and resume the testing. Audible cracking noises could be heard inside the end of the barrier. It was decided to continue the testing and the data collection without any stoppage. A loud cracking noise was heard, and part of the barrier could be seen tilting back only to be supported by the long strong floor anchors as seen in Figure 68, which shows cracks propagation around and through the barrier anchor bolt, which holds it to the slab.

Figure 68
Frontal view of vertical face yield failure

Figures 69 to 80 show the failure the barrier experienced.

Figure 69
Close up failure at the top 11 in. of barrier (vertical face)

Figure 70
Close-up failure at bottom of barrier (vertical face)

Figure 71
Hydraulic ram cracking top of barrier

Figure 72
Cracked region of barrier (sloping face)

Figure 73
Cracked region of barrier (sloping face)

Figure 74
Close-up of cracked region of barrier (sloping face)

Figure 75
Failure of barrier at one of its ends (sloping face)

Figure 76
Close-up failure of barrier at one of its ends (sloping face)

Figure 77
Torsional failure of barrier from vertical face

Figure 78
Torsional failure of barrier

Figure 79
Breakout failure of barrier

Figure 80
Close-up of breakout (notice intact anchor bolt)

After the torsional failure that the rail underwent, another mode of failure occurred. The barrier broke out at several anchored supports and proceeded to fall backwards. The anchor bolts remained intact and the concrete around it was crushed.

Analysis of Collected Data

In reinforced concrete design practice, it is assumed that the concrete will crush at a strain of 0.003 and that Grade 60 steel yield at 0.00207 (f_y / E_s = 60 ksi/29,000 ksi).

In this study, collected data obtained from different strain gauges show how the impact of the load at any location was transferred to other locations via the longitudinal and vertical bars interconnected at equally spaced distances. Those nodes did not experience the impact of the load on the member all at one in the form of equal strain readouts. Those nodes shared in the load distribution from its point of application to other locations of the barrier. Thus the fluctuation in strain readouts that instrumented gauges gave at different location of the barrier. The reinforcement nodes distributed the acting load in different directions and to all places. This has been manifested by the readout obtained at the edge of the barrier when the load was applied in the intermediate region of the barrier.

Furthermore, the reinforcing cages acted like a "buddy" system in sharing or redistributing strains. It was observed that when the strain was increasing at a certain node, some of that strain was redirected to neighboring nodes thus causing the strain in the first node to drop. As the strain increased in the adjacent node, similar concept of strain redistribution to other adjacent nodes including the original could be observed in the charts.

In the analysis of data, local maximum stains and global maximum strains were observed. The local maximum strain is the maximum stain that was collected by a certain gauge at a certain node at a certain applied load. This means that strain may or may not have reached a maximum value. The global maximum strain is the maximum strain that the whole barrier have experienced at any gauge under the applied force. That maximum strain represent the maximum that the barrier, as a whole, has experienced.

Following is a discussion of the strain response behavior for one gauge for collected data in Figure 81.

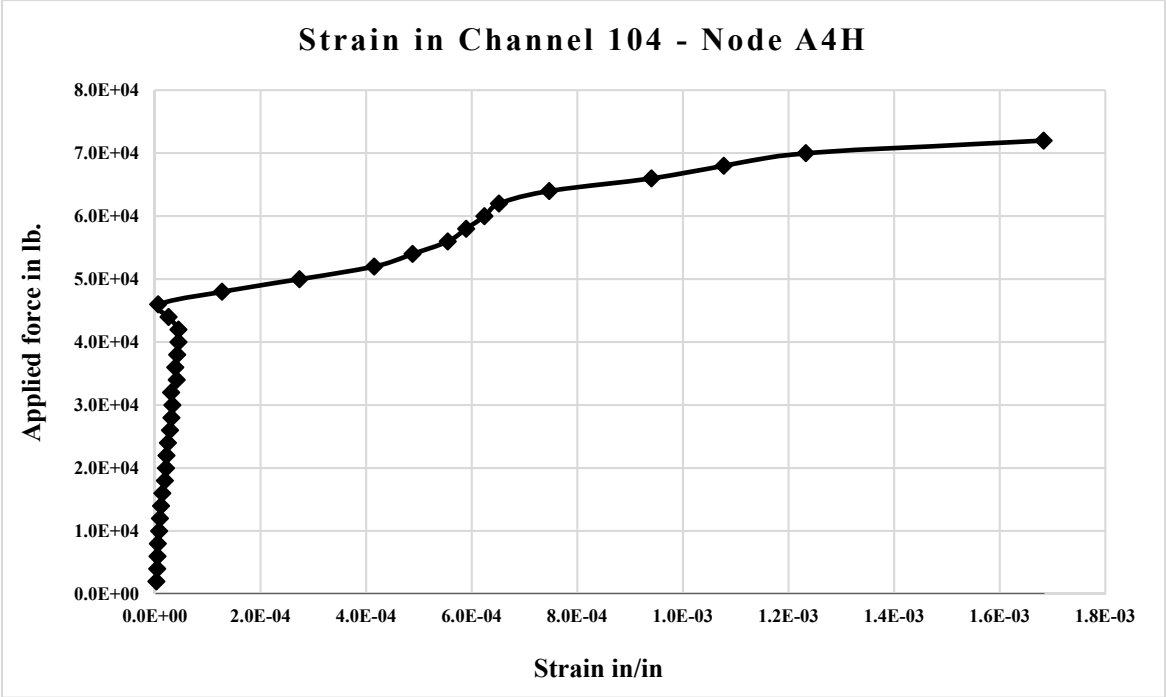

Figure 81
A plot of force vs. strain at node A4H (vertical face of barrier)

Figure 81 represents the relationship between applied lateral force and induced strain at node A4H, which is placed at a location 4 in. below the top surface of the vertical side of the concrete barrier. From this figure, the following are observed:

A strain value of 0.00168 corresponds to a maximum acting force of 72,000 lb. This strain value is much smaller than the concrete ultimate strain of 0.003 and steel yield strain of 0.00207.

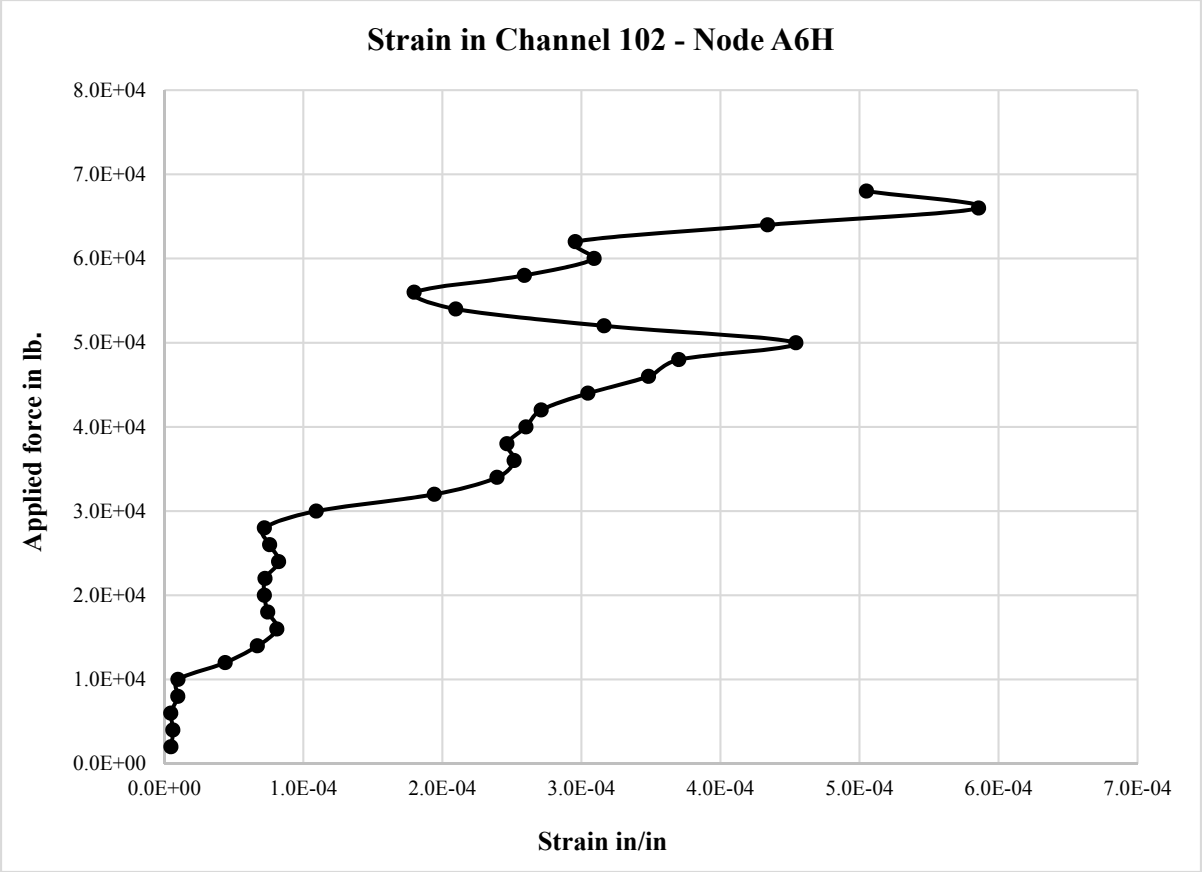

Figure 82
A plot of force vs. strain at node A6H (vertical face of barrier)

Figure 82 represents the relationship between applied lateral force and induced strain at node A6H that was placed at a location 4 in. below the top surface of the vertical side of the concrete barrier. It is at this location where the maximum M_w would occur because of the load application. This moment will be resisted by the top # 5 top longitudinal bar.

A strain value of 0.000505 corresponds to a maximum acting force of 68,000 lb. This strain value is much smaller than the concrete ultimate strain of 0.003 and steel yield strain of 0.00207.

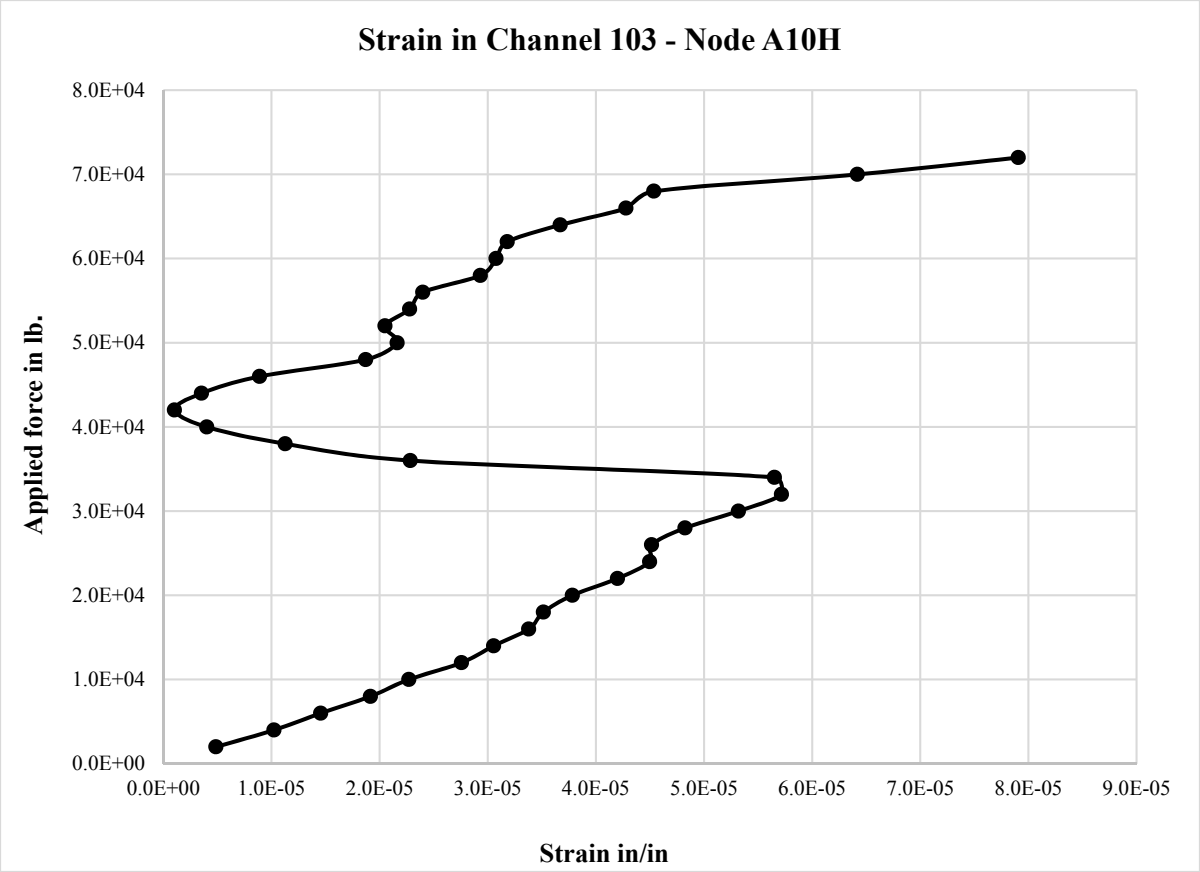

Figure 83
A plot of force vs. strain at node A10H (vertical face of barrier)

Figure 83 represents the relationship between applied lateral force and induced strain at node A10H that was placed at a location 4 in. below the top surface of the vertical side of the concrete barrier.

A strain value of 0.000079 corresponds to a maximum acting force of 72,000 lb. This strain value is much smaller than the concrete ultimate strain of 0.003 and steel yield strain of 0.00207.

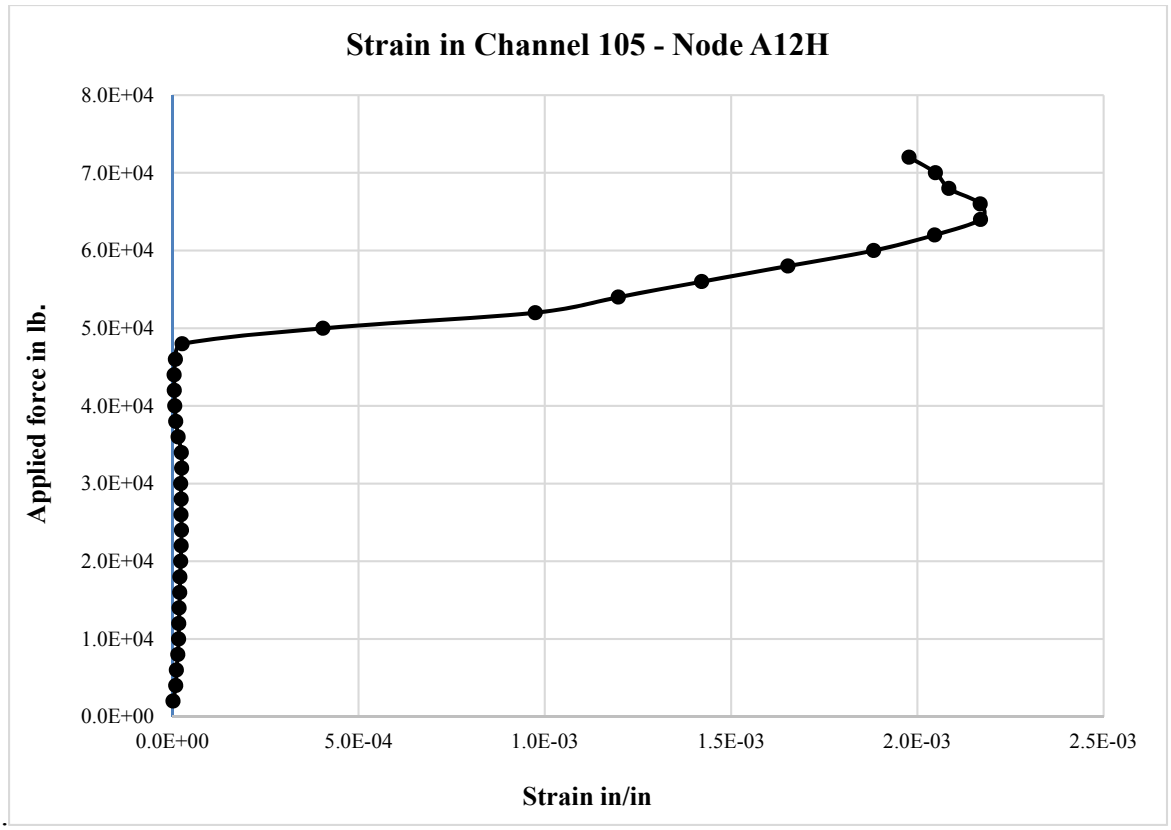

Figure 84
A plot of force vs. strain at node A12H (vertical face of barrier)

Figure 84 represents the relationship between applied lateral force and induced strain at node A12H that is placed at a location 4 in. below the top surface of the vertical side of the concrete barrier. It is at this location where the maximum M_w would occur because of the load application. This moment will be resisted by the # 5 top longitudinal bar.

The strain shown is 0.00198 with a corresponding maximum acting force of 72,000 lb. This maximum strain value is much smaller than the concrete ultimate strain of 0.003 and steel yield strain of 0.00207.

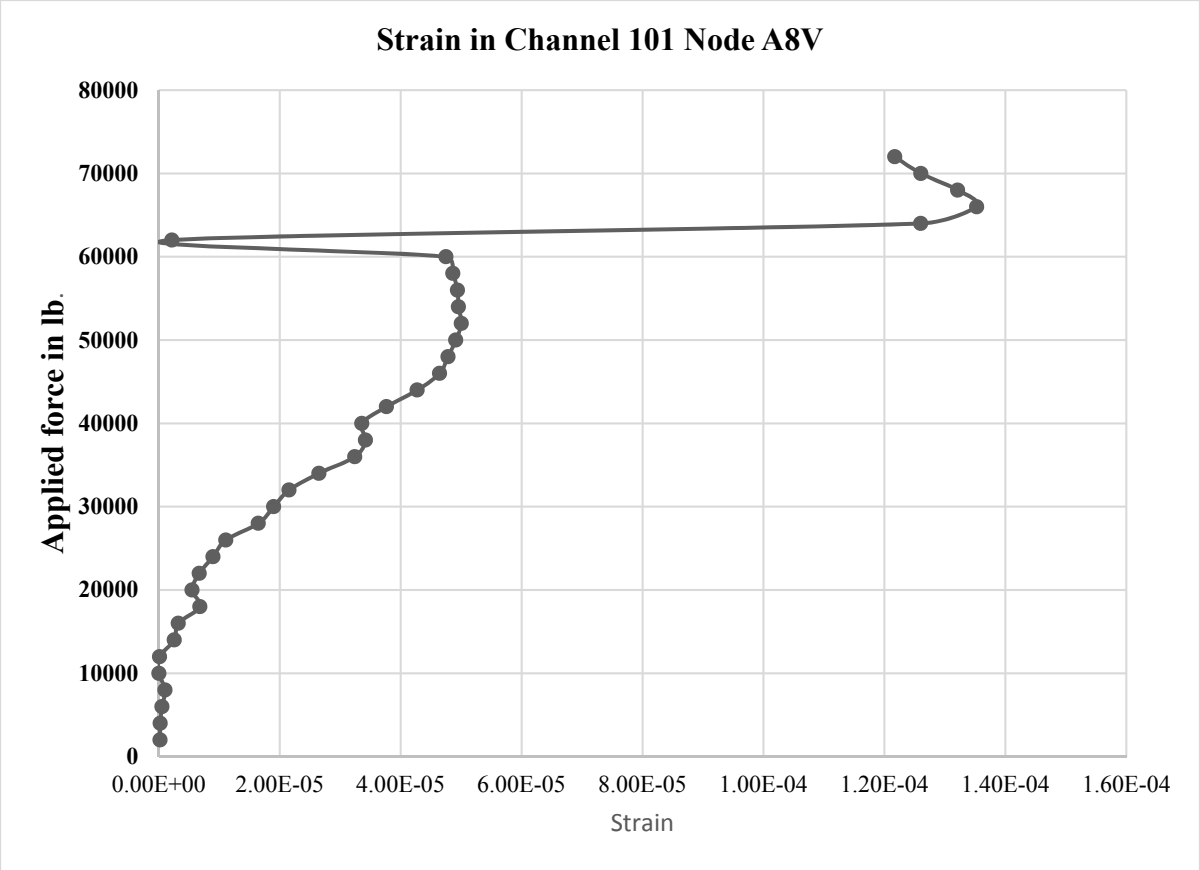

Figure 85
A plot of force vs. strain at node A8V (vertical face of barrier)

Figure 85 represents the relationship between applied lateral force and induced strain at node A8V that was placed at a location 4 in. below the top surface of the vertical side of the concrete barrier.

The strain shown is 0.00012 with a corresponding maximum acting force of 72,000 lb. This maximum strain value is much smaller than the concrete ultimate strain of 0.003 and steel yield strain of 0.00207.

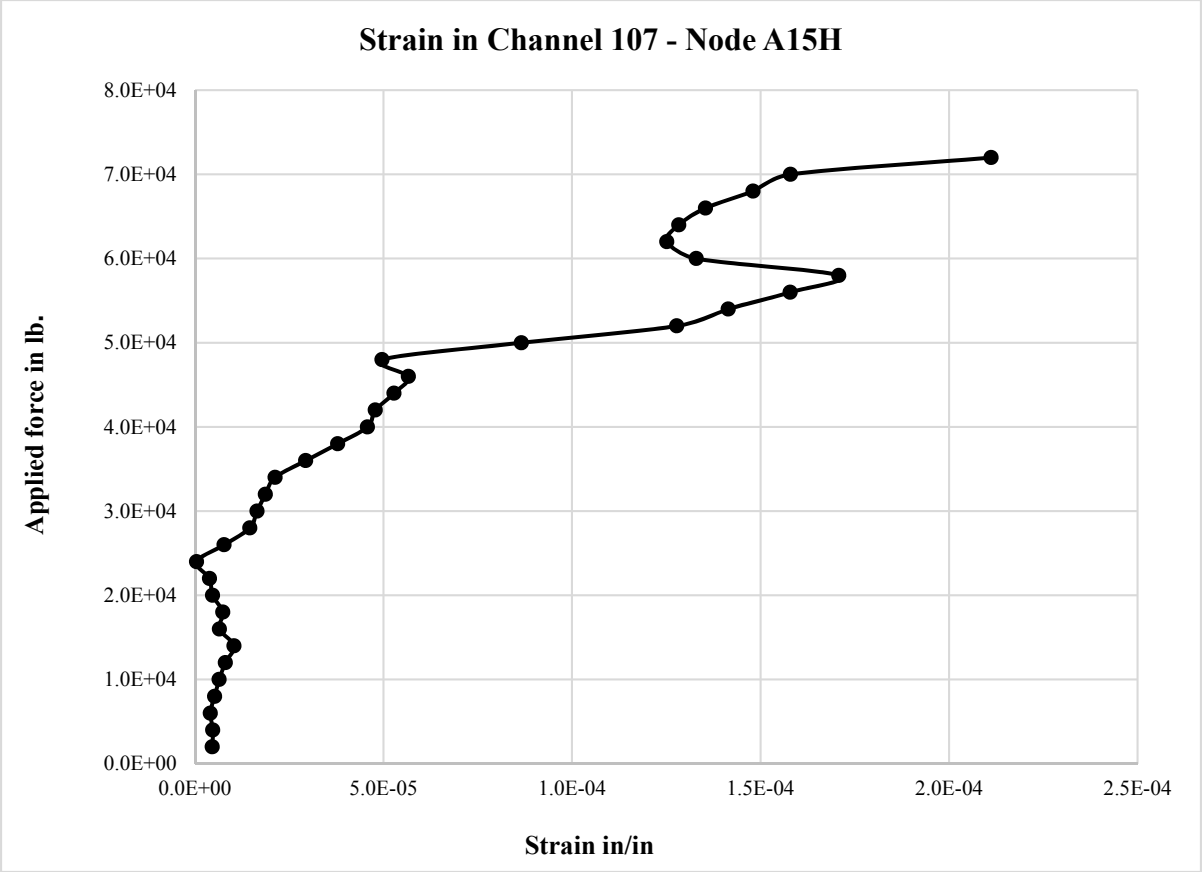

Figure 86
A plot of force vs. strain at node A15H (vertical face of barrier)

Figure 86 represents the relationship between applied lateral force and induced strain at node A15H that was placed at a location 4 in. below the top surface of the vertical side of the concrete barrier. It is at this location where the maximum M_w would occur because of the load application. This moment will be resisted by the top #5 longitudinal bar.

The strain shown is 0.000211 with a corresponding maximum acting force of 72,000 lb. This maximum strain value is much smaller than the concrete ultimate strain of 0.003 and steel yield strain of 0.00207.

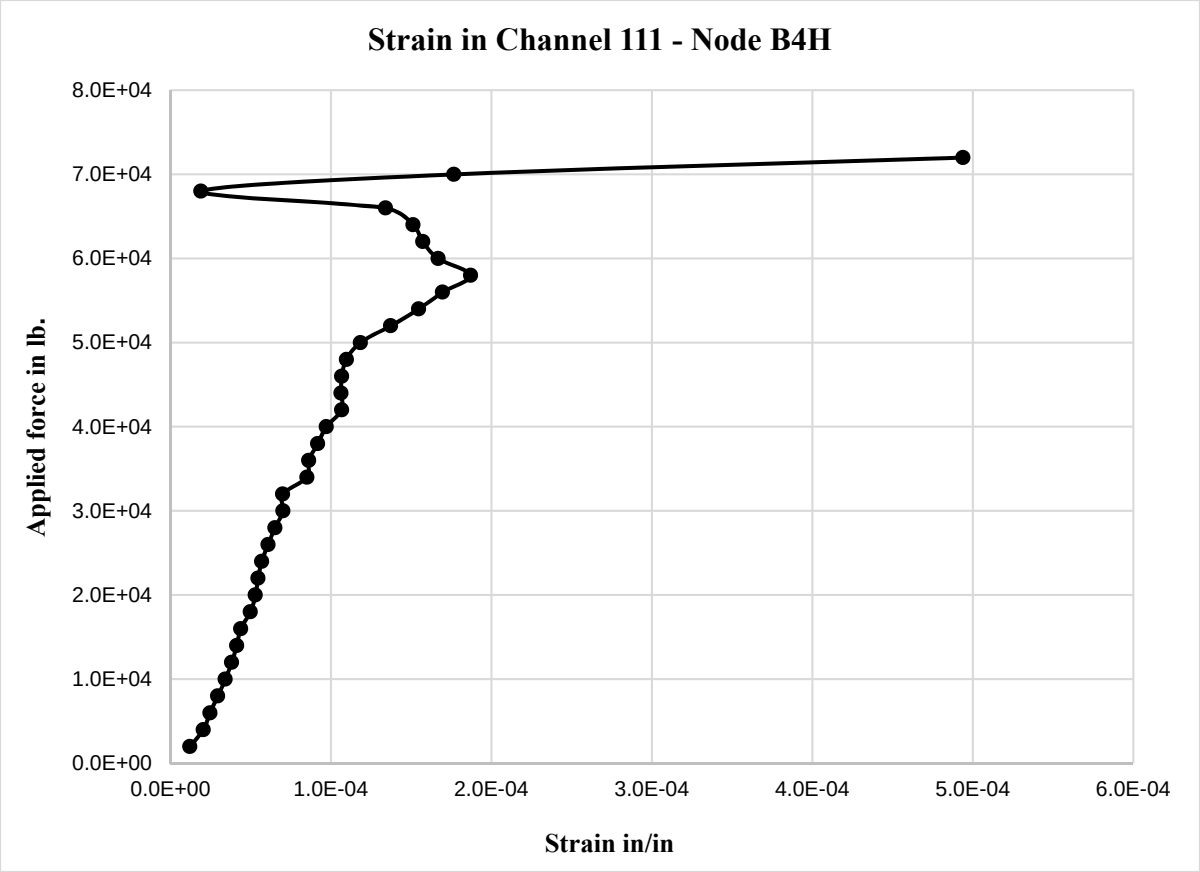

Figure 87
A plot of force vs. strain at node B4H (vertical face of barrier)

Figure 87 represents the relationship between applied lateral force and induced strain at node B4H that was placed at a location 11 in. below the top surface of the vertical side of the concrete barrier.

The strain shown is 0.00049 with a corresponding maximum acting force of 72,000 lb. This maximum strain value is much smaller than the concrete ultimate strain of 0.003 and steel yield strain of 0.00207.

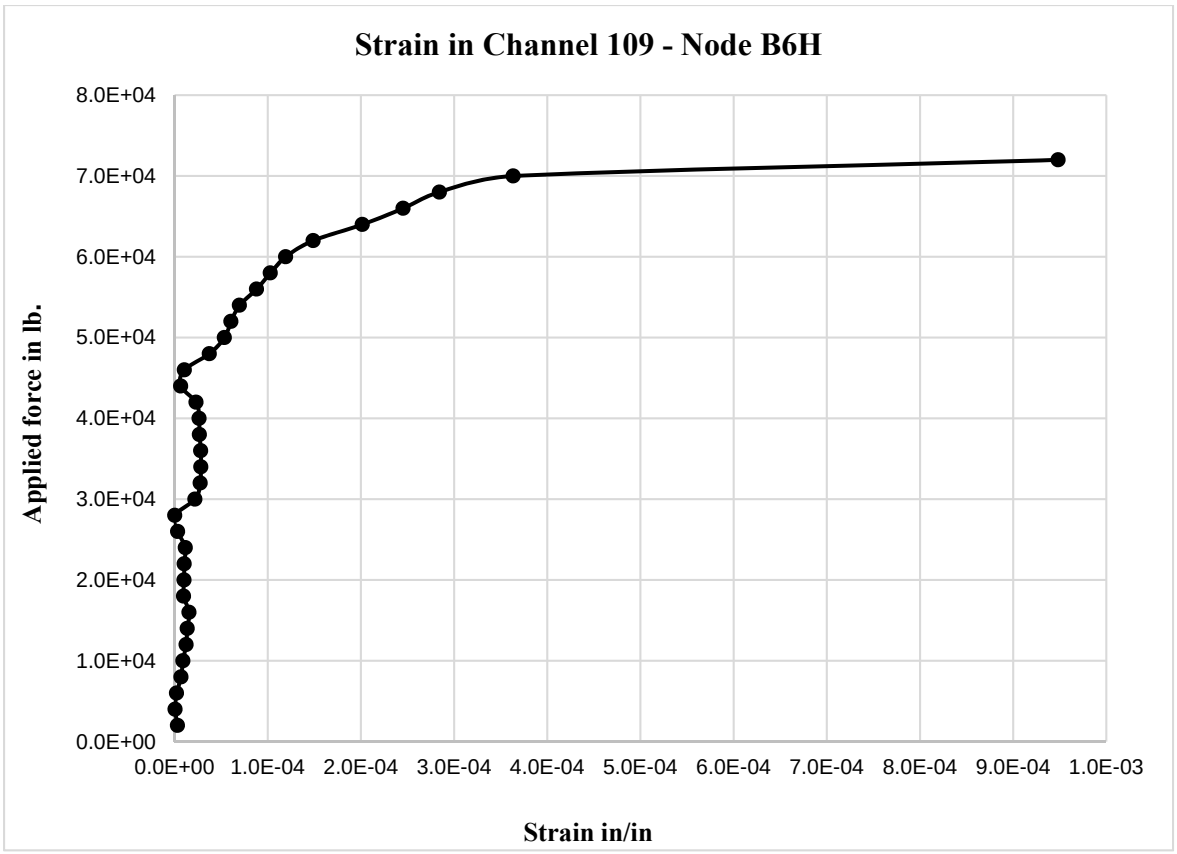

Figure 88
A plot of force vs. strain at node B6H (vertical face of barrier)

Figure 88 represents the relationship between applied lateral force and induced strain at node B6H that was placed at a location 11 in. below the top surface of the vertical side of the concrete barrier.

The strain shown is 0.00095 with a corresponding maximum acting force of 72,000 lb. This maximum strain value is much smaller than the concrete ultimate strain of 0.003 and steel yield strain of 0.00207.

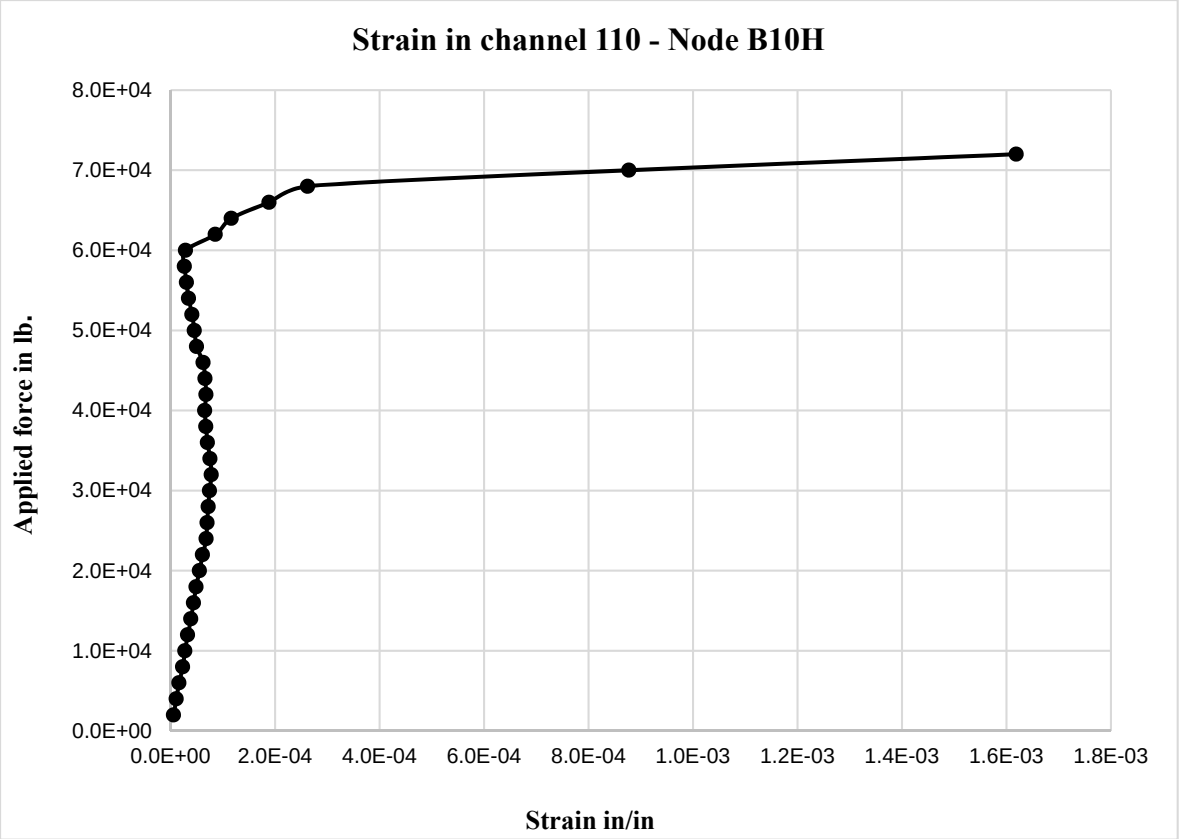

Figure 89
A plot of force vs. strain at node B10H (vertical face of barrier)

Figure 89 represents the relationship between applied lateral force and induced strain at node B10H that was placed at a location 11 in. below the top surface of the vertical side of the concrete barrier. It is at this location where the maximum M_w would occur because of the load application. This moment will be resisted by the top #5 longitudinal bar.

The strain shown is 0.0016 with a corresponding maximum acting force of 72,000 lb. This maximum strain value is much smaller than the concrete ultimate strain of 0.003 and steel yield strain of 0.00207.

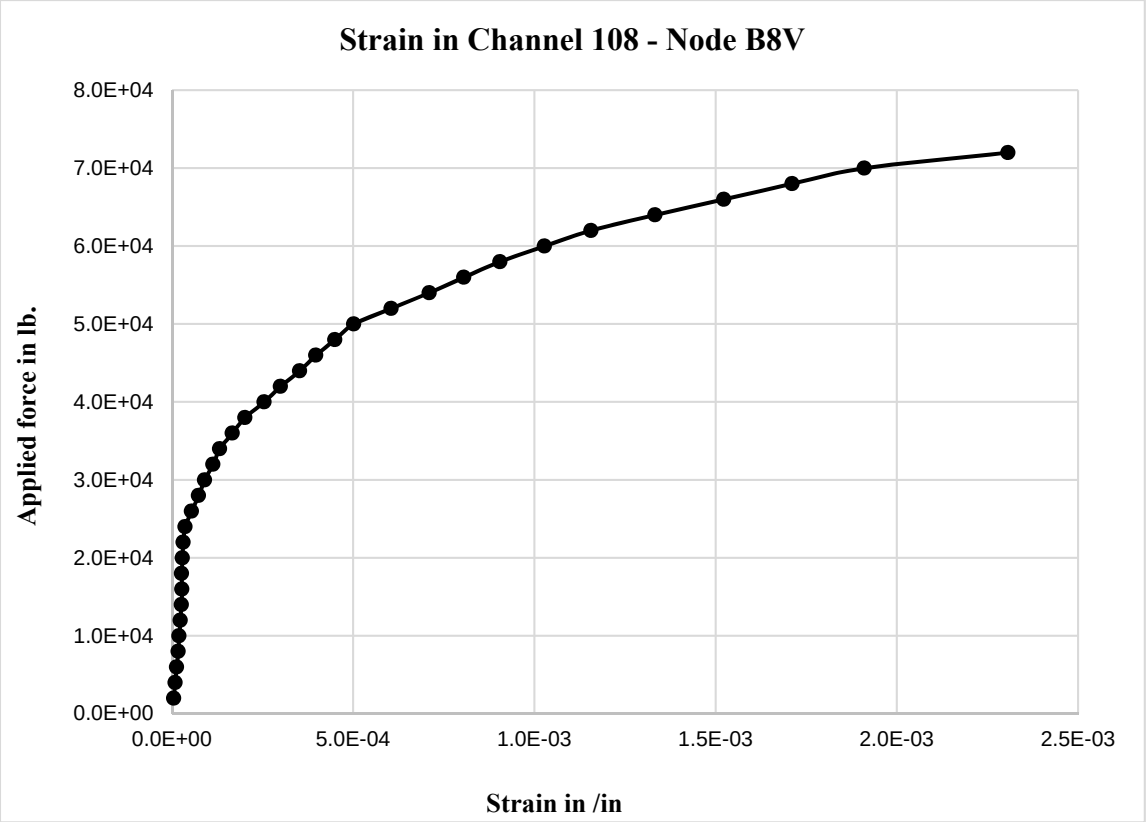

Figure 90
A plot of force vs. strain at node B8V (vertical face of barrier)

Figure 90 represents the relationship between applied lateral force and induced strain at node B8V that was placed at a location 11 in. below the top surface of the vertical side of the concrete barrier.

The strain shown is 0.0023 with a corresponding maximum acting force of 72,000 lb. This maximum strain value is much smaller than the concrete ultimate strain of 0.003 and little higher than the steel yield strain of 0.00207.

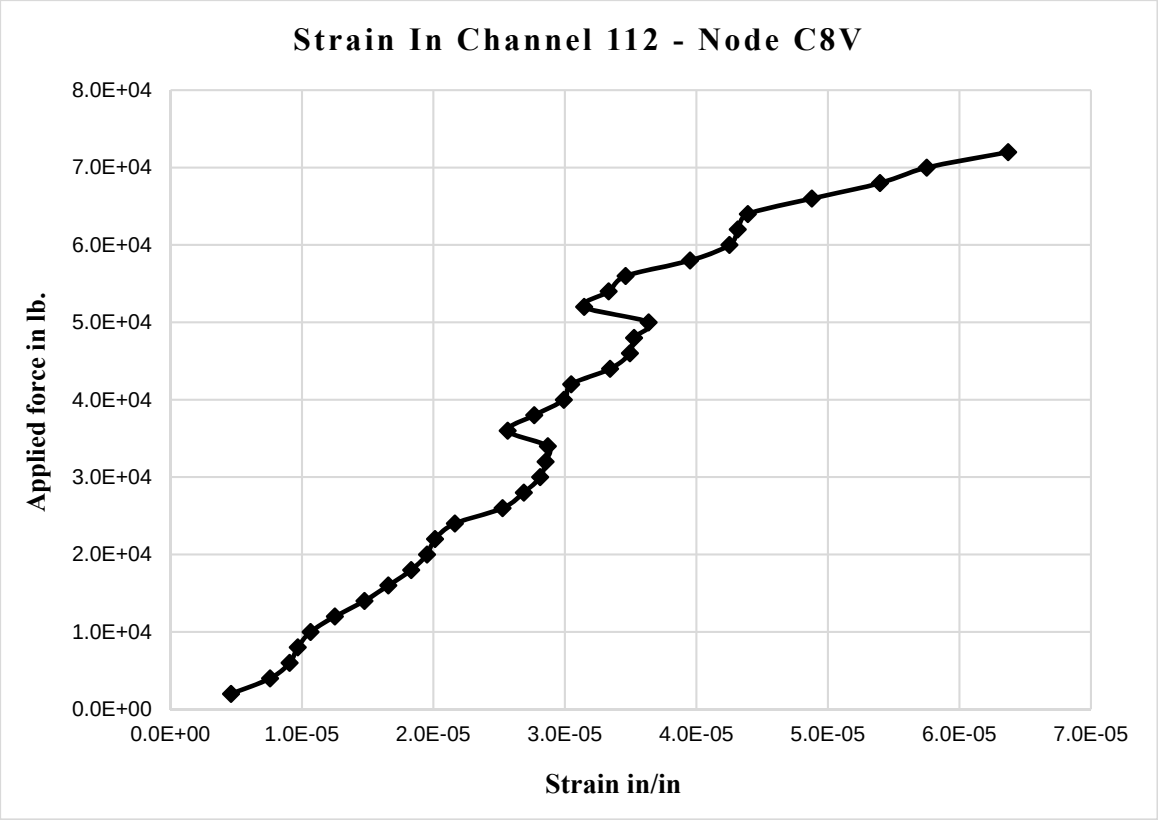

Figure 91
A plot of force vs. strain at node C8V (vertical face of barrier)

Figure 91 represents the relationship between applied lateral force and induced strain at node C8V that was placed at a location 18 in. below the top surface of the vertical side of the concrete barrier. The maximum strain attained was 0.00003 when the applied lateral force reached 34,000 lb.

The strain shown is 0.00006 with a corresponding maximum acting force of 72,000 lb. This maximum strain value is much smaller than the concrete ultimate strain of 0.003 and steel yield strain of 0.00207.

Strength Evaluation of the Bolted Section

Calculation for Bending Moment Resistance about Horizontal Axis

The Type F-barrier does not have a uniform thickness. Consequently, the "d" dimension of the vertical reinforcement varies with the vertical location in the rail. Averaged "d" dimensions are used to compute M_c separately for the top and bottom sections. Then, a weighted average of the two sections is taken to determine M_c for the entire rail section. Since the vertical bars were not anchored in the bridge deck, they will not be fully developed at a section below 23 in. (development length for #5, 60-ksi bars and 6.6-ksi compressive strength concrete) from the tip of the bar located at the top of the railing. There will be two blocks: one 23 in. deep, (vertical bars are 100% developed) and the other is 9 in. deep (vertical bars are 9/23 or 39% developed).

Determination of M_c

The Type F barrier does not have a uniform thickness. Consequently, the "d" dimension of the vertical reinforcement varies with the vertical location in the rail. Averaged "d" dimensions are used to compute Mc separately for the top and bottom sections. Then a weighted average of the two sections is taken to determine M_c for the entire rail section. The calculation of "d" dimension of the vertical reinforcement is presented in Table 12.

Table 12
Average of barrier width

Location	d (in.)	Average, d (in)
Top of Block 1	6.43-1.5 - (5/16) = 4.62	5.59
Bottom of Block 1	8.37- 1.5 - (5/16) = 6.56	
Top of Block 2	6.56	8.66
Bottom of Block 2	12.56 -1.5 - (5/16) = 10.75	

Bending Moment Resistance about Horizontal Axis for Interior Region, M_c

The internal flexural lever arm is dependent on the amount of reinforcement in the section. The maximum spacing of vertical reinforcement in interior region is 8 inches. A 12 in.-wide strip will be used to evaluate the interior rail region.

The development length for the # 5 bars used in this barrier is 11 in., based on a yield stress of steel and a compressive strength of concrete of 60,000 and 6,620 psi, respectively. From the available section, it seems there is enough development length at the interface between

the top and bottom part, i.e., at 10 inches above the base of the barrier. The value of M_c will be computed for both section and the lower value will be used as M_c

For the top portion, $A_s = 0.465$ in^2, $f_y = 60$ ksi, $f'_c = 6.62$ ksi, and $\varphi = 1.0$ (for Extreme Event Limit State),

For top portion of the table, $d_{avg} = 5.59$ in. and for bottom portion of the table, $d_{avg} = 8.66$ in.

The moment capacity of any concrete section is given by:

$$\varphi M_n = \varphi A_s f_y \left(d - \frac{a}{2}\right) \quad (17$$

$$a = \frac{0.465\ (60)}{0.85\ (6.62)(\ 12)} = 0.41 \text{ in.} \quad (18)$$

$$M_{c1} = 1.0(0.465)(60)\left(5.59 - \frac{0.41}{2}\right)\left(\frac{1}{12}\right) = 12.52 \frac{\text{kip.ft}}{\text{ft}} \quad (19a)$$

$$M_{c2} = 1.0(0.465)(60)\left(8.66 - \frac{0.41}{2}\right)\left(\frac{1}{12}\right) = 19.65 \frac{\text{kip.ft}}{\text{ft}} \quad (19b)$$

The strength at the base is greater than the strength at 10 inches above the base. Therefore, the value for bending moment resistance about horizontal axis for interior region 10 in. above the base will be considered in the analysis, $M_c = M_{c1} = 12.52$ ft.-k/ft.

Bending Moment Resistance about Vertical Axis for Interior Region, M_w

Capacities φM_n for a typical interior region are listed in Table 13. The lever arm dimension bars is found by subtracting half the depth of the flexural compression block,

$\varphi M_n = \varphi A_s f_y (d - a/2)$

$A_s = 0.31$ in^2, $A_{stotal} = 3(0.31)$ in^2, $f_y = 60$ ksi, $f'_c = 6.62$ ksi, and $\varphi = 1.0$ (for Extreme Event Limit State),

$$a = c\,\beta_1 = \frac{A_{s\,\text{total}} \cdot f_y}{0.85 \cdot f'c \cdot b} = \frac{3(0.31)(60)}{0.85(6.62)(32)} = 0.31 \text{ in.} \quad (20)$$

Table 13
Computation of M_w at interior region for inside face

Bar Layer from top to bottom 11 in. above base	h (in.)	d (in.)	Lever Arm (d-a/2), (in.)	φM_{ni} (in-k)
1	6.43	4.00	3.85	71.62
2	7.19	4.50	4.35	80.91
3	7.94	5.50	5.35	99.51
			Totals	**252.04**

"h" and "d" are total and effective width and of section considered, respectively.

Now the moment per unit foot due to inside and outside tension yield line is calculated as:

$$M_w = \left[\frac{\varphi M_{ni}}{H}\right] = \left[\frac{\frac{(252.04)}{12}}{1.75}\right] = 12.00\,\frac{\text{kip. ft}}{\text{ft}} \tag{21}$$

For the interior rail regions, there is one outside tension yield line and two inside tension yield line. Compute the average M_w:

Critical Length of Wall Failure for Interior Section

Equation (14) is used to calculate the critical length of wall failure for interior section (L_{ci}).

$$L_{ci} = \frac{L_t}{2} + \sqrt{\left(\frac{L_t}{2}\right)^2 + \frac{8H(M_b + M_w)}{M_c}} \tag{22}$$

H: Effective height of wall, ft.,

L_{ci}: Critical length of wall failure at interior section

M_b: Ultimate moment capacity of beam at top of wall, ft-k,

M_w: Ultimate moment capacity of wall per foot of wall height, ft-k/ft,

M_c: Ultimate moment capacity of wall cantilever up from bridge deck per foot length of wall, ft-k/ft.,

L_t: Length of distributed impact load, ft.,

M_b = 0 ft.-k, M_w = 12.0 ft.-k/ft., M_c = 12.52 ft.-k/ft., and l_t = 42 in. (3.5 ft.),

$$L_{ci} = \frac{3.5}{2} + \sqrt{\left(\frac{3.5}{2}\right)^2 + \frac{8(1.75)(0 + 12.0)}{12.52}} \quad (23)$$

Lci = 5.81 ft.

Capacity Checking of Interior Region

$$R_{wi} = \left(\frac{2}{2L_{ci} - L_t}\right)\left((8M_{bint} + 8M_{wint}) + \frac{(M_{cint})(L_{ci}^2)}{H}\right) \quad (24)$$

$$R_{wi} = \left(\frac{2}{2(5.81) - 3.5}\right)\left((0 + 8(12.0) + \frac{(12.52)(5.81^2)}{1.75}\right)$$

For M_c = 12.52 ft.-k/ft., M_w = 12.0 ft.-k/ft. and L_{ci} = 5.81ft.

R_{wi} = 83 kips > 54 kips OK

Bending Moment Resistance about Vertical Axis for End Region

At end regions not all of the horizontal bars will be fully developed by the time they intersect with the anticipated yield line. Assume L_{ce} dimension is at least 4.0 ft. With the yield stress of steel and compressive strength of concrete being 60 ksi and 6.62 ksi, respectively, the #5 bars have a development length of 11 in (see computation on next page). Figure 92 shows the reinforcement in the end region of the rail in relation to the assumed yield line.

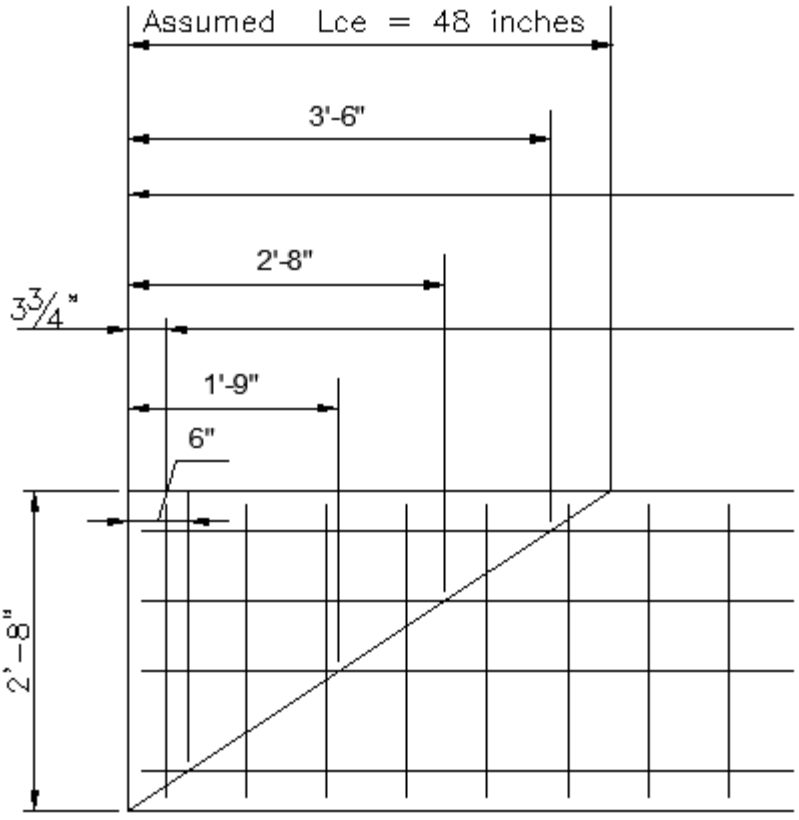

Figure 92
Estimation of the length of the yield line failure for end region

Computation of Development Length. The computation of the developed length is based on Equation 12-1 of Section 12.2.3 of the American Concrete Institute (ACI).

$$\boldsymbol{l_d = \frac{3}{40}\left(\frac{f_y}{\lambda\sqrt{f'_c}}\right)\left[\frac{\psi_t\psi_e\psi_s}{\left(\frac{c_b + k_{tr}}{d_b}\right)}\right]d_b} \tag{25}$$

in which, the term $\left(\frac{c_b+k_{tr}}{d_b}\right)$ shall not be taken greater than 2.5 and where

$\boldsymbol{l_d}$ = development length (in.)

f_y = specified yield strength of non-prestressed reinforcement (psi)

$\boldsymbol{f'_c}$ = specified compressive strength of concrete (psi); the value $\sqrt{\boldsymbol{f'_c}}$ shall not exceed 100 psi (ACI Code, Section 12.1.2).

d_b = nominal diameter of bar or wire (in.) = 0.625 for # 5 bar.

In this research, a value of 1 will be applied to $\boldsymbol{\lambda}$, $\boldsymbol{\psi_t}$ and $\boldsymbol{\psi_e}$, and a value of 0.8 for $\boldsymbol{\psi_s}$.

$\boldsymbol{k_{tr}}$ will be assumed equal to 0 and $\frac{\boldsymbol{c_b}}{\boldsymbol{d_b}}$ equal to 2.5.

$\boldsymbol{l_d}$ will be equal to 11 inches.

End Region Elevation of Railing

Similar to the interior region, the lever arm is found by subtracting off one-half the depth of the flexural compression block. The detailed calculation for M_w at the end region is presented in Table 14. Extreme event limit state is

$$\varphi M_n = \varphi\ A_s\ f_y\ (d - a/2) \tag{26}$$

$A_s = 0.31$ in^2, $A_{stotal} = 0.93$ in^2, $f_y = 60$ ksi, $f'_c = 6.62$ ksi, and $\varphi = 1.0$ (for Extreme Event Limit State),

$$a = \frac{A_{stotal}\ .\ f_y}{0.85(f'c)(b)} = \frac{0.93(60)}{0.85(6.62)(32)} 0.31 \text{ in.}$$

Table 14
Computation of M_w at end region for interior region

Bar Layer from top to bottom 11 inches above base	h (in)	d (in)	Lever Arm (d-a/2), (in)	φM_{ni} (in-k)
1	6.43	4.00	3.85	71.62
2	7.19	4.50	4.35	80.91
3	7.94	5.50	5.35	99.51
			Totals	**252.04**

M_w is found by averaging the capacity of rail over the height of the rail,

$$M_{wend} = \left[\frac{\varphi M_n}{H}\right] = \left[\frac{\left(\frac{252.04}{12}\right)}{1.75}\right] = 12.0 \frac{\text{kip. ft}}{\text{ft}} \tag{28}$$

Bending Moment Resistance about Horizontal Axis for End Region

The end region has similar reinforcement as the intermediate region. Therefore, similar work will be repeated for M_c = 12.52k-ft./ft.

Critical Length of Wall Failure for End Region

Critical length for wall failure for end region (L_{ce}) can be found from a similar equation that we have already used for interior regions.

$$L_{ce} = \frac{L_t}{2} + \sqrt{\left(\frac{L_t}{2}\right)^2 + \frac{H(M_b + M_w)}{M_c}} \tag{29}$$

M_b = 0.0 ft.-k M_w = 12.0 ft.-k/ft., M_c= 12.52 ft.-k/ft.

L_t= 42 in. (3.5 ft.), and L_{ce}= 4 ft. (assumed)

$$L_{ce} = \frac{3.5}{2} + \sqrt{\left(\frac{3.5}{2}\right)^2 + \frac{(1.75)(0 + 12.0)}{12.52}}$$

L_{ce} = 3.93 ft. (close to assumed L_{ce})

Capacity Checking of End Region

M_b = 0.0 ft.-k M_w = 12.0 ft-k/ft., M_c = 12.52 ft.-k/ft., L_t = 3.5 ft.

$$R_{we} = \left(\frac{2}{2L_{ce} - L_t}\right)\left(\left(M_{b_{end}} + M_{w_{end}}\right) + \frac{\left(M_{c_{end}}\right)\left(L_{c_e}{}^2\right)}{H}\right) \tag{30}$$

$$R_{we} = \left(\frac{2}{2(3.93) - 3.5}\right)\left((0 + 12.0) + \frac{(12.52)(3.93^2)}{1.75}\right)$$

For M_c = 12.52 ft-k/ft. and L_{ce} = 3.93 ft. R_{we} = 56 kips > 54 kips OK

It should be mentioned that those resistive forces were obtained by moment sections where reinforcement have ample development length to develop their yield stress of F_y = 60 ksi. These resistive force values will be considered valid for cast-in-place concrete barrier where the vertical reinforcement is anchored in the deck and has enough development length to develop their yield stresses at location of maximum moment, i.e., the base of the barrier. Those resistive values may not be considered valid for precast barrier since those barriers are not anchored in a similar fashion to bridge decks. The results for a bolted and a cast-in-place barrier section are presented in Table 15.

Table 15
Results for impacting and resistive forces for analyzed precast barrier

Region	Method	Resistive Force, R_w (kips)	Current F_t TL-3 / TL-4 (kips)	Proposed F_t for TL-3 / TL-4 (kips) *[2]*
Intermediate	Computed	83	54	52^2 / 76^2
	Measured	79	54	
End	Computed	56	54	52^2 / 76^2
	Measured	(n/v)[1]	54	

[1] n/v: Not Verified
[2] Proposed Update to NCHRP Report 350 (Ref. 2)

Barrier Deflection

Regarding barrier deflection, the deflection of the barrier was recorded through the LDVT that the hydraulic ram was equipped with. Deflection readings were taken as the applied load was ramped up at 1,000-lb. intervals. A maximum deflection of 2.19 in. was reached at a corresponding load of 79,000 lb. after which the barrier experienced torsional failure and stopped resisting the applied load. Table 16 shows a deflection values at different applied loads and Figure 93 shows a plot of lateral deflection vs. applied load.

Table 16
Applied loads and lateral barrier deflection

Load	Deflection	Load	Deflection	Load	Deflection	Load	Deflection
1	0.03	21	0.30	41	0.65	61	1.19
2	0.04	22	0.31	42	0.66	62	1.20
3	0.05	23	0.33	43	0.69	63	1.26
4	0.06	24	0.34	44	0.70	64	1.27
5	0.07	25	0.36	45	0.73	65	1.33
6	0.09	26	0.38	46	0.74	66	1.35
7	0.10	27	0.40	47	0.79	67	1.42
8	0.11	28	0.41	48	0.80	68	1.44
9	0.12	29	0.43	49	0.84	69	1.51
10	0.14	30	0.44	50	0.85	70	1.52
11	0.15	31	0.47	51	0.89	71	1.64
12	0.16	32	0.48	52	0.91	72	1.67
13	0.18	33	0.50	53	0.95	73	1.80
14	0.19	34	0.51	54	0.96	74	1.82
15	0.20	35	0.53	55	1.00	75	1.85
16	0.22	36	0.55	56	1.01	76	1.88
17	0.23	37	0.57	57	1.06	77	1.92
18	0.25	38	0.59	58	1.07	78	1.97
19	0.26	39	0.61	59	1.12	79	2.02
20	0.28	40	0.62	60	1.13	79	2.19
						76[1]	2.21
						48[1]	2.29
						51[1]	2.36

[1] After the barrier collapsed, its load capacity started to diminish while it continued to deflect outward. It was at this time that the loading of the barrier was terminated.

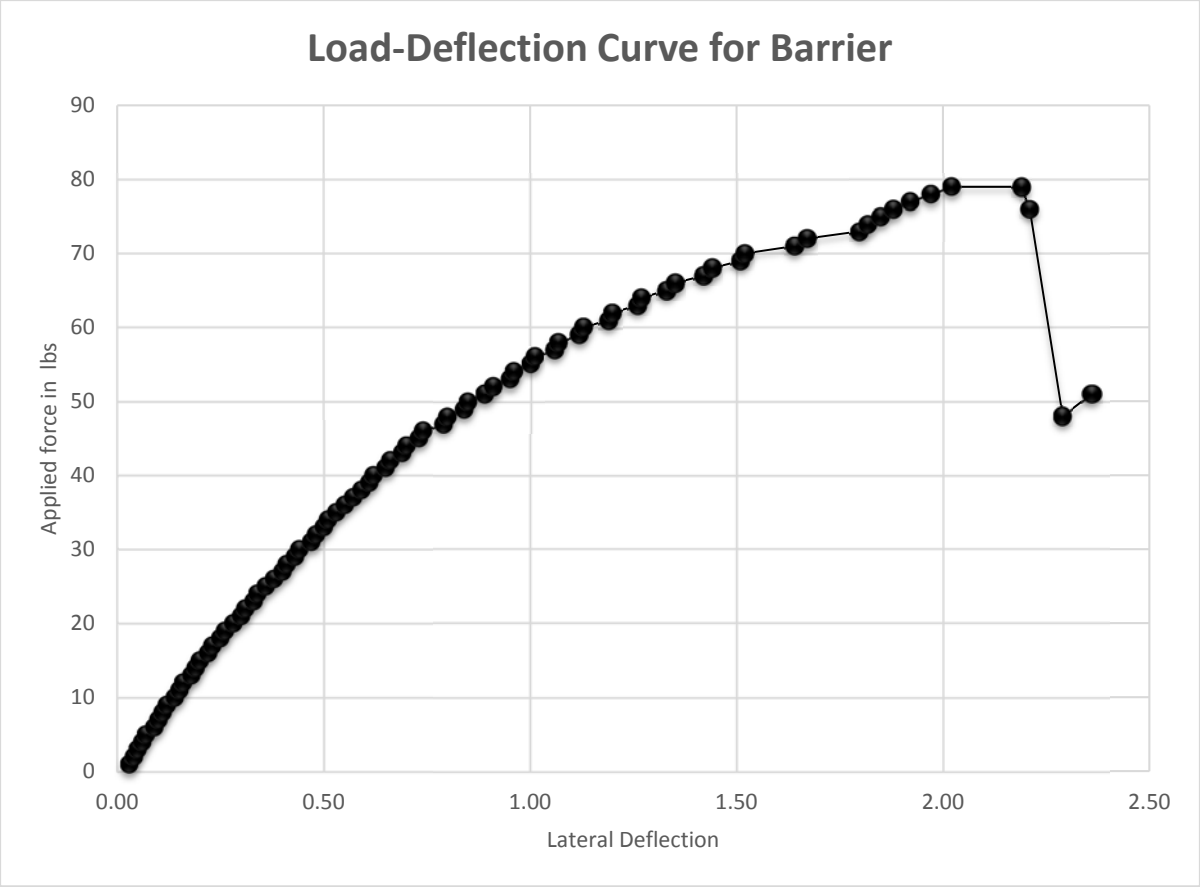

Figure 93
Lateral deflection vs. applied load

DISCUSSION OF RESULTS

Cast-in-place concrete barriers rely on the section ultimate moment capacity to withstand a vehicular impact. The capacity of the section is a function of the yield stress of reinforcements among others things.

Unlike cast-in-place barriers, precast concrete barriers are not anchored to bridge decks through the vertical reinforcement steel. The use of anchor bolts is what provide the connection. As such, at location of maximum moment, the vertical reinforcing bars may not rely on any embedment length to develop it yielding stress. Failure of such barriers, as in the study has shown, was a combination of torsion and concrete breakout at several anchor locations.

Anchorage is a major factor in the barrier strength and ought to be taken into consideration when calculating the moment strength of the wall about horizontal axis (M_c) of the bottom section of the barrier. For the top section of the barrier, the vertical reinforcement is effective in providing moment strength about the horizontal axis. However, at the bottom of the barrier, the vertical reinforcement is not anchored into the base and thus may not be able to provide the moment resistance as reported by the yield line theory. Anchorage to the base is only provided by the anchor bolts. Therefore, for the moment strength of wall about horizontal axis (Mc) of the base section, the resistance should be calculated based on the location at which the vertical bars can develop their yield stress across both sides of any horizontal section taken in the vertical wall.

By comparing the calculated results with the experimental results, it was found that the assumed yield lines provided a very close estimate of the capacity of the barrier at the middle region than the measured value (83 kips computed vs. 79 kips measured). Unlike flexural failures experienced by tested cast-in-place tested concrete members, as computed by yield line approach theory, the tested precast concrete barrier failed in torsion and anchorage pull-out.

SUMMARY AND CONCLUSIONS

Summary

This study was initiated as a result of the NHRP Report 350 recently proposed guidelines to assess the adequacy of existing roadway safety devices.

A literature review was performed before the start of the study. Though many articles, reports, and publications were found regarding the testing of cast-in-place concrete barriers, such similar publications pertaining precast concrete bridge railing were almost non-existing. Therefore testing a precast concrete barrier was the focus of this study. As such, the study of the performance of a concrete barrier with composite reinforcement was not warranted since such barriers can be replaced if they get damaged and investing in composite reinforcement would not be a good decision.

Analysis and experimental investigations were conducted in order to study the behavior and performance of a precast concrete barrier currently in use in construction zones.

Load testing was performed to assess the performance of the barrier under Test Level 2 (TL-2) as specified in NCHRP Report 350 with vehicle weights varied between 1.55 to 18 kips, travelling at 45 mph impacting a barrier at a crash angle varying between 20° and 25°, based on the vehicle characteristics (weight, width, and height of the center of gravity of the vehicle). Under the test level, the barrier would be impacted by a transverse force of 27 kips in magnitude.

Work in this study was both theoretical and experimental. The theoretical work related to the application of the yield line theory for predicated the strength of the precast barrier. Though the theory was developed for cast-in-place barriers where the lateral impact force would be transferred to the reinforcement in the deck, there was no developed equations for evaluating the strength of the precast or bolted section. The theory was tested in this study.

The experimental work related to the cast of concrete barrier, evaluating the compressive strength of the concrete used in the precast barrier, transporting it to Louisiana Tech University, connecting it to the strong floor lab. Instrumentation plan was developed and strain gauges were placed on both faces of the barrier in the intermediate and end regions. The barrier was subject to incremental static load till the barrier failed. Data were collected and analyzed. The computed ultimate strength of the barrier was obtained by using the yield line theory. The actual strength of the barrier was obtained on the static load testing that the barrier was subject to at the testing facility. It is to be noted here that in the prediction of the

ultimate strength of the concrete barrier was obtained by as computing the strength of the barrier at two locations; an intermediate region and an end region.

Computation shows that strength of the barrier at the end region is lower than that at an intermediate region. This is because the failure or the yield mechanism for each region is different for different. In the intermediate region, the failure was manifested through a yield pattern that encompassed of two negative moments on the sloping face and one positive moment on the vertical face of the barrier. At the end region, the failure region was manifested by the presence of one negative bending moment and one positive bending moment. Even though the reinforcement pattern remained unchanged along and across the faces of the barrier, the section capacity of the barrier at the end region was smaller and thus controlled the ultimate yield strength of the barrier.

Initial cracking in the intermediate region of the barrier occurred at 40 kips and progressed as testing continued to complete failure 79 kips. Testing of the barrier to failure at the intermediate region led to a secondary failure at the end region though the load was applied at the middle region. The end region failure did not allow for the opportunity of repositioning of the ram to test the end region as such testing the end section could not be performed and neither the section capacity measured.

Data from stresses at the end region could not be used since those strains were not due to direct load application in the end region.

Conclusions

The major findings are as follows:

- The test proved that the precast concrete bridge barriers in use on low-volume highway bridges, designed based on NCHRP 350 Report recommendations complied with the proposed changes.
- The measured load-to-failure of the precast barrier agreed well with the computed section capacity of the barrier obtained from the analytical analysis.
- Anchorage of the tested barrier were strong enough that cracks initiated in wall portion of the barrier and not the slab.
- The barrier test specimen failed in two different subsequent modes: torsion and breakout out of anchorage detail.

- The barrier failed at the middle region and as such testing the end region could not be performed. Based on that and until additional work is done to assessing the capacity of the section at the end region, it can be concluded that the precast concrete barriers similar to the one tested in this study are not TL3 compliant and their use should be limited to conditions that qualify for TL2. This is reserved for work zones and most local and collector roads with favorable site conditions as well as where a small number of heavy vehicles is expected and posted speeds are reduced. Speed limit in work zones is limited to 45 miles per hour.

.

RECOMMENDATIONS

One of the benefits of using precast bridge rail in lieu of cast-in-place members is the ease of connection to the bridge deck. Though all bridge railings are designed with flexure due to bending moment in mind, deflection of bridge railing is considered negligible since concrete bridge railing are classified as rigid sections (i.e., unyielding).

Replacing a cast-in-place rail is more costly, time consuming, and requires lane closure for deck rehabilitation. Compared to that, precast bridge railings are easier to replace due to the ease of re-bolting a new precast bridge rail section to the existing deck. In essence, precast bridge railings may be viewed as sacrificial flexural members when compared to cast-in-place bridge railings.

By properly increasing the section capacity of the barrier, increasing its height, and improving the anchoring connection, this type of barriers will be able withstand higher impact forces experienced under test levels 3, or higher and thus becoming a useful part of the accelerated bridge construction components. This can be done only after the redesigned railing system shows acceptable performance is demonstrated through full-scale crash tests for desired test levels in Table [A.13.7.3.1] of AASHTO (1994) *LRFD Bridge Design Specifications.*

ACRONYMS, ABBREVIATIONS, AND SYMBOLS

AASHTO	American Association of State Highway and Transportation Officials
FHWA	Federal Highway Administration
f'_c	Compressive Strength of Concrete
ft.	foot (feet)
DOTD	Louisiana Department of Transportation and Development
LTRC	Louisiana Transportation Research Center
lb.	pound(s)
m	meter(s)
in	inch(es)
ksi	1,000 pounds per square inch
Kip	1,000 lb.
L	Critical length for rail failure
LRFD	Load Resistance Factor Design
LTRC	Louisiana Transportation Research Center
Mc	Moment bending moment resistance about horizontal axis due to vertical reinforcement, ft-k/ft.
Mw	Bending moment resistance about vertical axis due to horizontal reinforcement, ft-k
NCHRP:	National Cooperative Research Program
PL	Performance Level
psi	pounds per square inch
TL	Test Level

REFERENCES

1. AASHTO (1994). *LRFD Bridge Design Specifications*, 1st ed., American Association of State Highway and Transportation Officials, Washington, DC.

2. Bligh, R. P. and Menges, W. L., "Initial Assessment of Compliance of Texas Roadside Safety Hardware with Proposed Update To NCHRP Report 350," Research Report 0-5526-1, Texas Transportation Institute, Texas A&M University, College Station, TX, September 2007.

3. Proposed Full-Scale Testing Procedures for Guardrails, *Highway Research Circular 482,* Highway Research Board, Washington, D.C., 1962.

4. Olson, R.M., Post, E.R., and McFarland W.F., "Tentative Service requirements for Bridge Rail Systems," *NCHRP Report 86*, Transportation Research Board, National Research Council, Washington, D.C., 1970.

5. Olson, R.M., Ivy, D.L., Post, E.R., Gunderson R.H., and Cetiner, A., "Bridge Rail Design- Factors, Trends, and Guidelines," *NCHRP Report 149*, Transportation Research Board, National Research Council, Washington, D.C., 1974.

6. Bronstad, M.E. and Michie, J.D., "Recommended Procedures for Vehicle Crash Testing of Highway Appurtenances," *NCHRP Report 153*, Transportation Research Board, National Research Council, Washington, D.C., 1974.

7. Recommended Procedures for Vehicle Crash Testing of Highway Appurtenances, *Transportation Research Circular 191*, Transportation Research Board, National Academy of Sciences, Washington, D.C., February, 1978.

8. Michie, J.D., "Recommended Procedures for the Safety Performance Evaluation of Highway Features," *NCHRP Report 230*, Transportation Research Board, National Research Council, Washington, D.C., March 1981.

9. Ross, Jr., H.E., Sicking, D.L., Zimmer, R.A., and Michie, J.D., "Recommended Procedures for the Safety Performance Evaluation of Highway Features," National Cooperative Highway Research Program *Report 350*, Transportation Research Board, National Research Council, Washington, D.C., 1993.

10. Bridge Railing Design and Testing - A Discussion with the AASHTO Highway Subcommittee on Bridges and Structures Technical Committee (T-7) for Guardrail and

Bridge Rail May 14, 1996.

11. Buth, C. E., Bligh, R. P., and Menges, W. L., "NCHRP Report 350 Test 3-11 of The Texas Type T411 Bridge Rail," Research Report 1804-3, Texas Transportation Institute, Texas A&M University, College Station, TX, May 1998.

12. Bligh, R. P. and Menges, W. L., "Design and Evaluation of the TxDOT F411 and T77 Aesthetic Bridge Rails," Research Report 4288-1, Texas Transportation Institute, Texas A&M University, College Station, TX, October 2002.

13. Bullard, Jr. D., L., , Buth, C. E., Williams, W. F., Mengees, W. L., and Haug, R. R. "Crash Testing and Evaluation of The Modified T77 Bridge Rail," Research Report 0-4852-1, Texas Transportation Institute, Texas A&M University, College Station, TX, September 2002.

14. Alberson, D. C., Williams F. W., Menges, W. L., and Haug, R. R., "TL-4 Crash Testing of The F411 Bridge Rail," Research Report 9-8132-P7, Texas Transportation Institute, Texas A&M University, College Station, TX, October 2004.

15. Alberson, D. C., Williams F. W., Menges, W. L., and Haug, R. R., "Testing and Evaluation of the Florida Jersey Safety Shaped Bridge Rail," Research Report 9-8132-1, Texas Transportation Institute, Texas A&M University, College Station, TX, February 2004.

16. Faller, R.K., Sicking, D.L., Larsen, J., Rohde, J.R., Bielenberg, R.W., and Polivka, K.A., "TL-5 Development of 42- and 51-In. Tall, Single-Faced, F-Shape Concrete Barriers," *Guide Specifications for Bridge Railing,* proposed, American Association of State Highway and Transportation Officials (AASHTO), Washington, D.C., April 2, 1987.

17. Polivka, K.A., Faller, R.K., Sicking, Rohde, J.R., Bielenberg, R.W., Reid, J.W., and Coon, B.A. "Performance Evaluation of the Permanent New Jersey Safety Shape Barrier-Update to NCHRP Report 350 Test No. 3-10 (2214NJ-1)," MwRSF Research Report No. TRP-03-178-06, Midwest Roadside Safety Facility (MwRSF) University of Nebraska-Lincoln, Lincoln, Nebraska, October 2006.

18. Polivka, K.A., Faller, R.K., Sicking, Rohde, J.R., Bielenberg, R.W., Reid, J.W., and Coon, B.A. "Performance Evaluation of the Permanent New Jersey Safety Shape Barrier-Update to NCHRP Report 350 Test No. 4-12 (2214NJ-2)," MwRSF Research Report No. TRP-03-178-06, Midwest Roadside Safety Facility (MwRSF) University of Nebraska-Lincoln, Lincoln, Nebraska, October 2006.

19. Alberson, D. C., Zimmer, R. A., and Menges, W. L., "NCHRP REPORT 350 Compliance Test 5-12 of the 1.07-m Vertical Wall Bridge Railing," Research Report 9-8132-1, Texas Transportation Institute, Texas A&M University, College Station, TX, February 2004.

20. *Guide Specifications for Bridge Railing,* American Association of State Highway and Transportation Officials (AASHTO), Washington, D.C., 1989.

21. Barker, R.M. and Puckett, J. A. (2007) *Design of Highway Bridges – An LRFD Approach,* 2nd ed., John Wiley & Sons, Inc., New Jersey.

22. Chu-Kia Wang, Charles G. Salmon, and José A. Pincheira (2007). *Reinforced Concrete Design.* 7th ed., John Wiley & Sons, Inc. 2007.

23. Ghali, A. and A. M. Neville (2003). *Structural Analysis—A Unified Classical and Matrix Approach*, 5th ed., Chapman & Hall, New York.

24. Hirsch, T. J., "Analytical Evaluation of Bridge Rails to Contain Buses and Trucks," Research Report 230-2, Texas Transportation Institute, Texas A&M University, College Station, TX, August 1978.

25. Calloway, B. R. (1993). Yield Line Analysis of an AASHTO New Jersey Concrete Parapet Wall, M.S. Thesis, Virginia Polytechnic Institute and State University, Blacksburg, VA.

26. Louisiana Standard Specifications for Roads and Bridges 2006 Edition, State of Louisiana, Department of Transportation and Development.

APPENDIX

1. Appendix A: Barrier Details
2. Appendix B: Concrete Strength Test Results
3. Appendix C: Instrumentation Plan
4. Appendix D: Hydraulic Actuator and Specifications
5. Appendix E: Strain Gauges, Assigned Channels, and Applied Loads

APPENDIX A BARRIER DETAILS

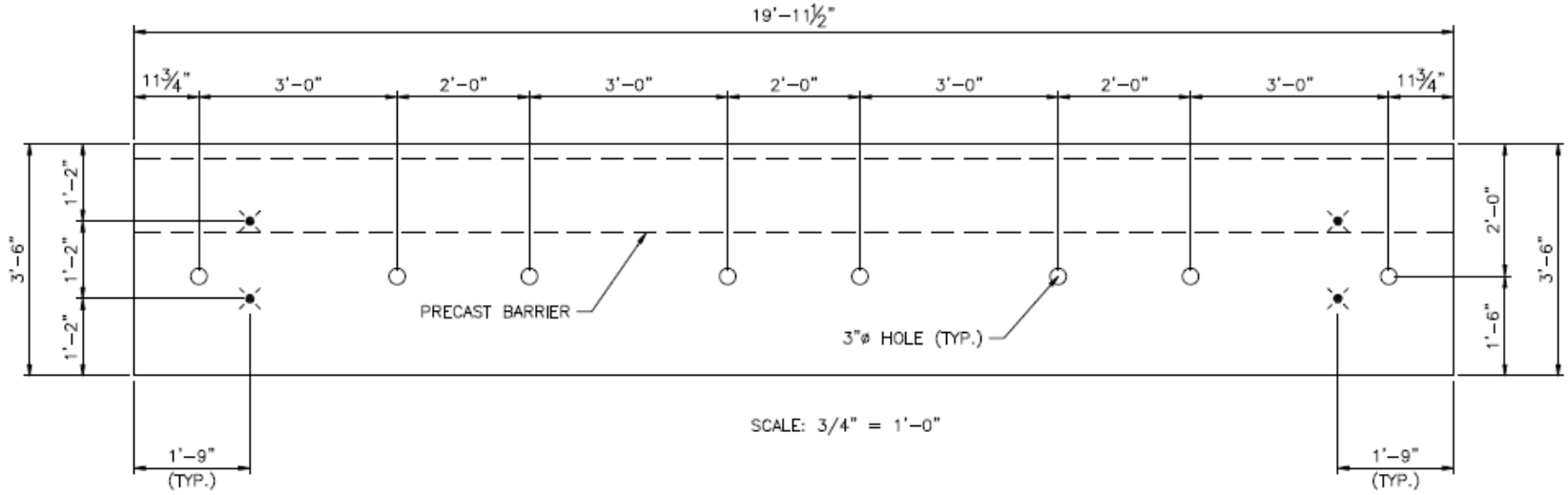

Figure 94
Plan view of the 20-ft. concrete barrier

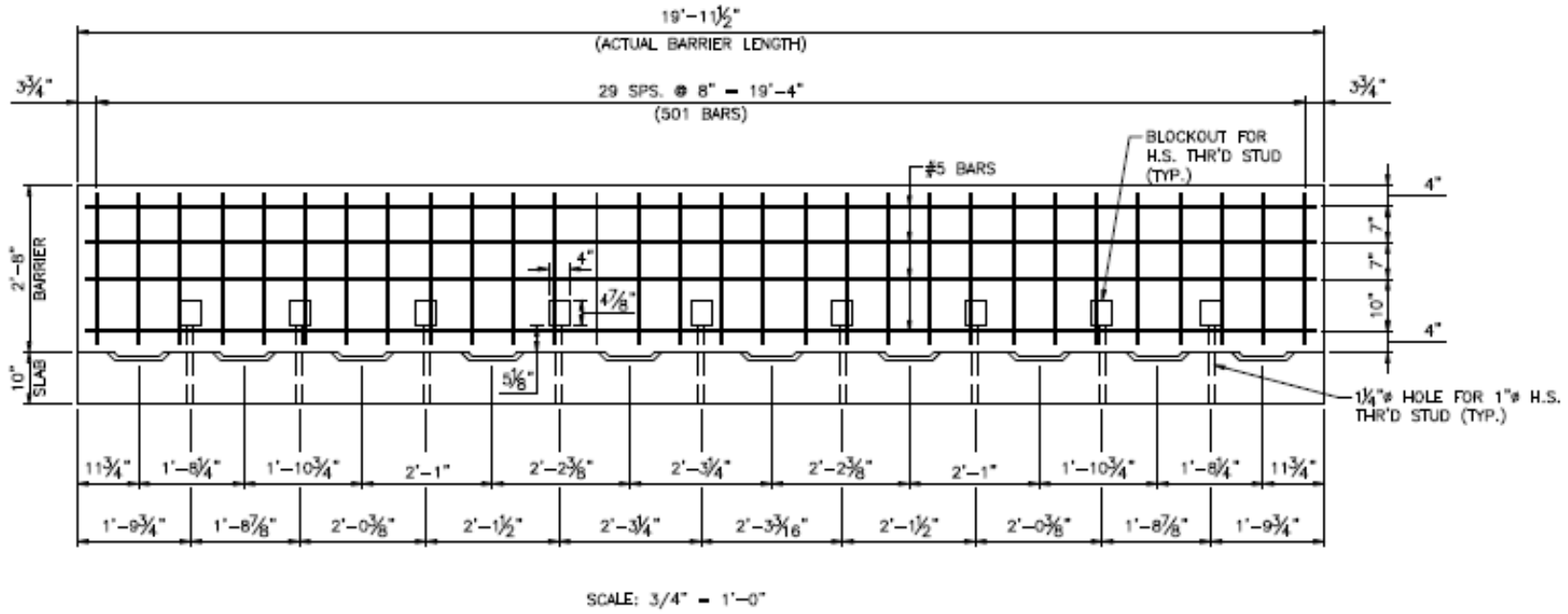

Figure 95
Elevation of the 20-ft. concrete barrier

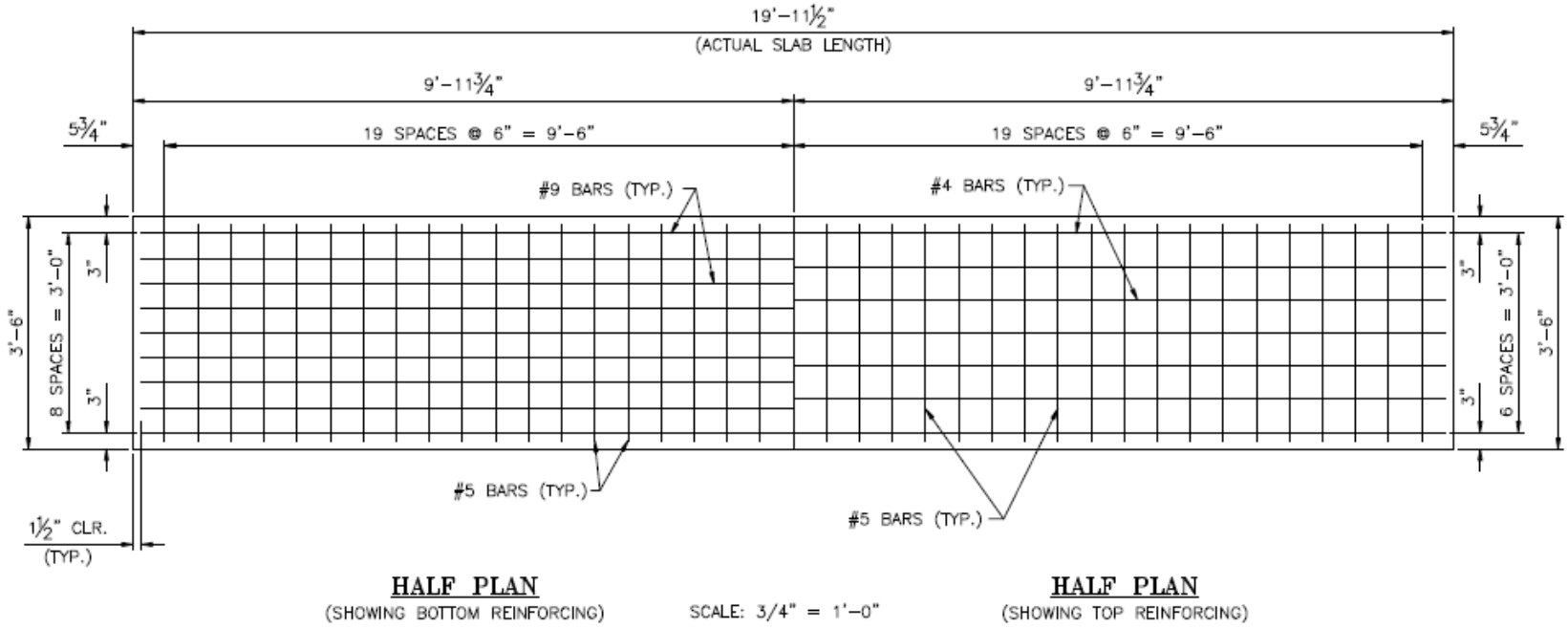

Figure 96
Reinforcing plan for the three ft. six in. barrier panel

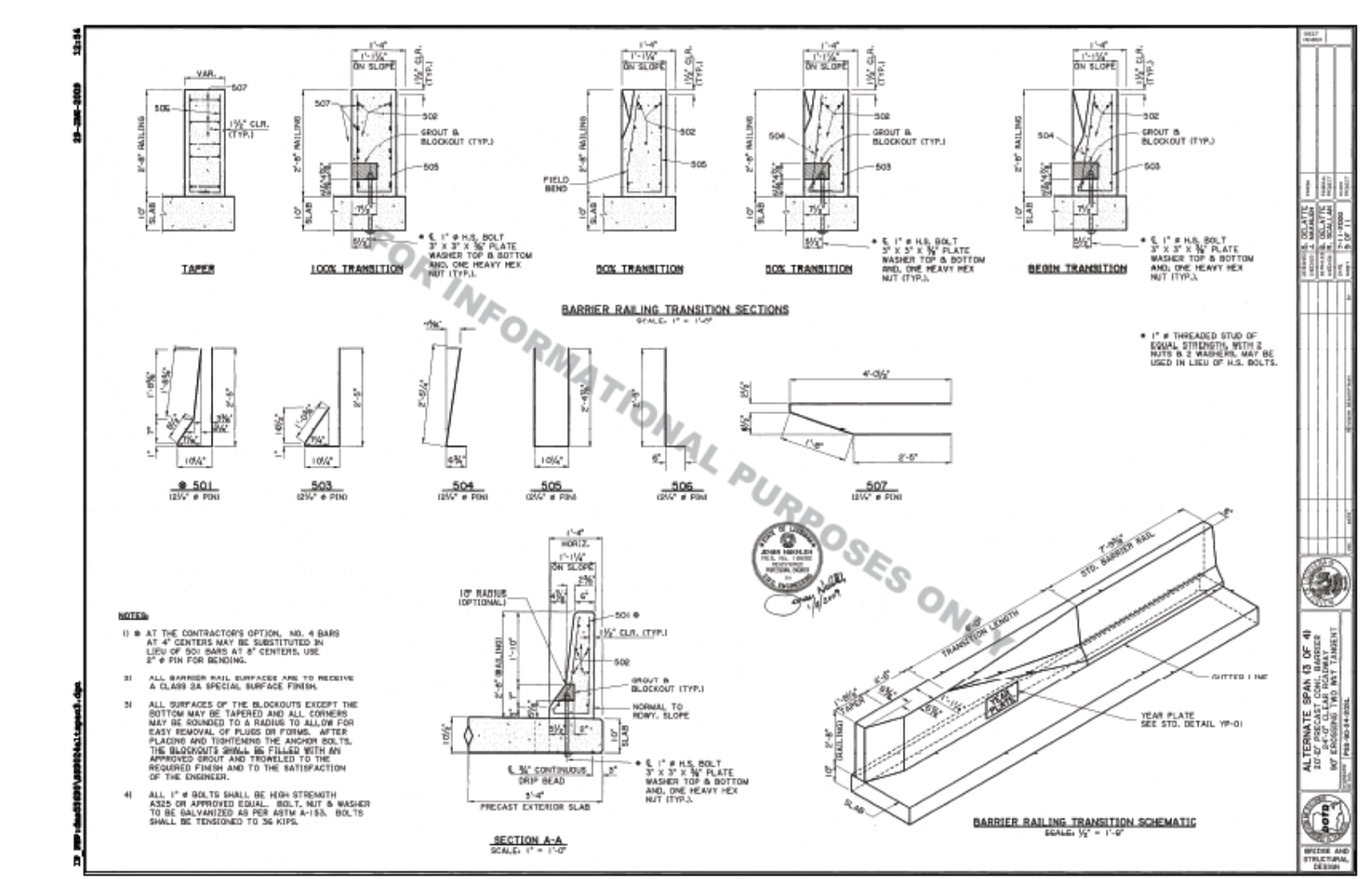

Figure 97
Cross-Section of a typical precast barrier railing used by DOTD

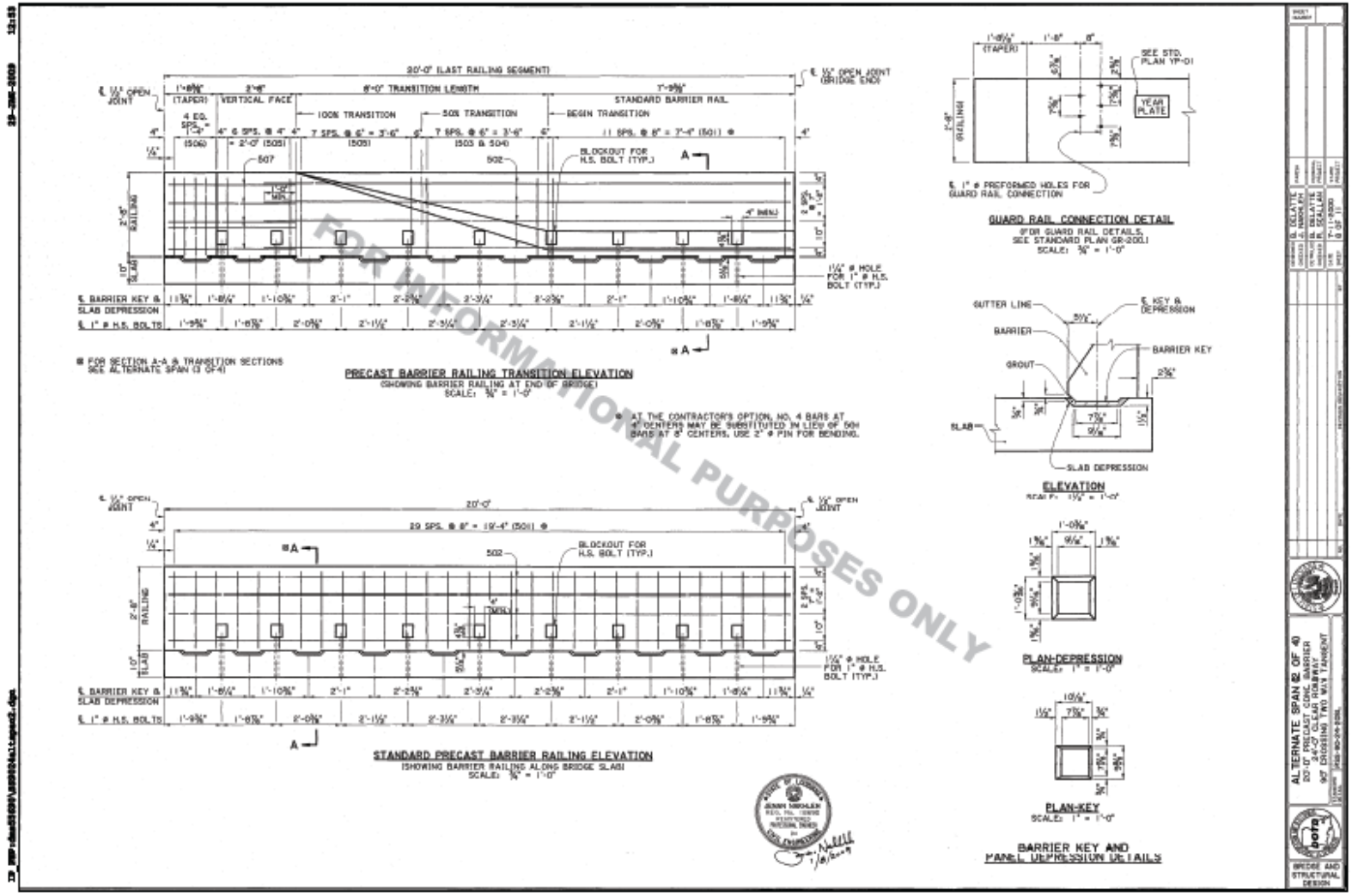

Figure 98
Standard precast barrier railing elevation

APPENDIX B CONCRETE LAB STRENGTH TEST RESULTS

SAMPLE IDENTIFICATION

Received: 6/1/2009 — Lab. No.: C-3353
Material: Class AA(P) concrete — Source: Waskey Bridge
State Project No.: — Station No.: — Address:
LTRC Project No.: (09-2ST) 09-1TA, 736-99-1560 — District No.: 03
Submitted By: Walid Alaywan (Name) — Engineer (Title) — LTRC Room 110 (Address)
Sampled from: Bridge Railing — Quantity of material represented by sample: ample for testing
Intended Use of material: 09-2ST, Bridge Railing
ASTM test samples made: 6 - 6x12 Cmp, Mod (7,28)

(ASTM C 39) COMPRESSIVE STRENGTH Of Cylindrical Concrete Specimens

Form of Specimen: 6 x 12 cylinders — Date Made: 5/28/2009

SPECIMEN OR SAMPLE NO.	DATE TESTED	Average LENGTH	Average DIAMETER	AREA ($\pi \times D^2 / 4$)	LOAD AT FAILURE LBS.	COMPRESSIVE STRENGTH PSI	AGE AT TEST DAYS	TYPE BREAK
1	06/04/09	12.050	6.130	29.513	150,618	5103	7	4
2	06/04/09	12.025	6.080	29.033	159,268	5486	7	2
3	06/04/09	12.000	6.135	29.561	157,806	5338	7	2
						5295	Avg	
						166.17	Std. Dev.	
						3.14	Coef. Var.	
4	06/25/09			0.0000			28	
5	06/25/09			0.0000			28	
6	06/25/09			0.0000			28	
							Avg	
							Std. Dev.	
							Coef. Var.	

(ASTM C 469) Static Modulas of Elasticity and Poisson's Ratio of Concrete in Compression

Avg. Peak Load (lbs): 154,943 — 40% of Load: 61,977

SPECIMEN OR SAMPLE NO.	DATE TESTED	Average LENGTH	Average WIDTH	AREA ($\pi \times D^2 / 4$)	MODULAS OF ELASTICITY	POISSON'S RATIO	AGE AT TEST DAYS	Load Rate (LBS/min)
3	06/04/09	12.000	6.135	29.561	5,750,000	0.15	7	62078
					Avg. Peak Load (lbs)	0	40% of Load	0
6	06/25/09			0.0000			28	0

Remarks: Test samples cured in accordance with ASTM C192.

Tested By: RCY — Date: 6/4/2009 — Calculations By: XLS — Checked By: GOK

Figure 99
LTRC's 7-day compressive strength test results

SAMPLE IDENTIFICATION

Received 6/1/2009 Lab. No. C-3353

Material: Class AA(P) concrete Source: Waskey Bridge

State Project No. Station No. Address:

LTRC Project No. (09-2ST) 09-1TA, 736-99-1560 District No. 03

Submitted By: Walid Alaywan (Name) Engineer (Title) LTRC Room 110 (Address)

Sampled from: Bridge Railing Quantity of material represented by sample: ample for testing

Intended Use of material: 09-2ST, Bridge Railing

ASTM test samples made: 6 - 6x12 Cmp, Mod (7,28)

Form of Specimen 6 x 12 cylinders Date Made: 5/28/2009

ASTM C 39, COMPRESSIVE STRENGTH Of Cylindrical Concrete Specimens

SAMPLE NO.	DATE TESTED	AGE AT TEST DAYS	Average LENGTH	Average DIAMETER	AREA ($\pi \times D^2 / 4$)	LOAD RATE LBS/min	LOAD AT FAILURE LBS.	COMPRESSIVE STRENGTH PSI	TYPE BREAK
1	06/04/09	7	12.050	6.130	29.513	61,977	150,618	5103	5
2	06/04/09	7	12.025	6.080	29.033	60,970	159,268	5486	5
3	06/04/09	7	12.000	6.135	29.561	62,078	157,806	5338	5
								5295	Avg
								166.17	Std. Dev.
								3.14	Coef. Var.
4	06/25/09	28	12.065	6.070	28.938	60,770	188,799	6524	2
5	06/25/09	28	12.000	6.100	29.225	61,372	189,104	6471	2
6	06/25/09	28	12.030	6.072	28.957	60,810	199,200	6879	3
								6498	Avg
								251.02	Std. Dev.
								3.86	Coef. Var.

ASTM C 469, Static Modulas of Elasticity and Poisson's Ratio of Concrete in Compression

SAMPLE NO.	DATE TESTED	AGE AT TEST DAYS	Average LENGTH	Average WIDTH	AREA ($\pi \times D^2 / 4$)	LOAD RATE LBS/min	Average Peak Load LBS	40% Peak Load LBS	MODULAS OF ELASTICITY	POISSON'S RATIO
3	06/04/09	7	12.000	6.135	29.561	62,078	154,943	61,977	5,750,000	0.15
6	06/25/09	28	12.030	6.072	28.957	60,810	188,952	75,581	6,000,000	0.15

Remarks: Test samples cured in accordance with ASTM C192.

Tested By SS Date 6/25/2009 Calculations By RCY Checked By RCY

Figure 100
LTRC's 28-day compressive strength test results

APPENDIX C INSTRUMENTATION PLAN

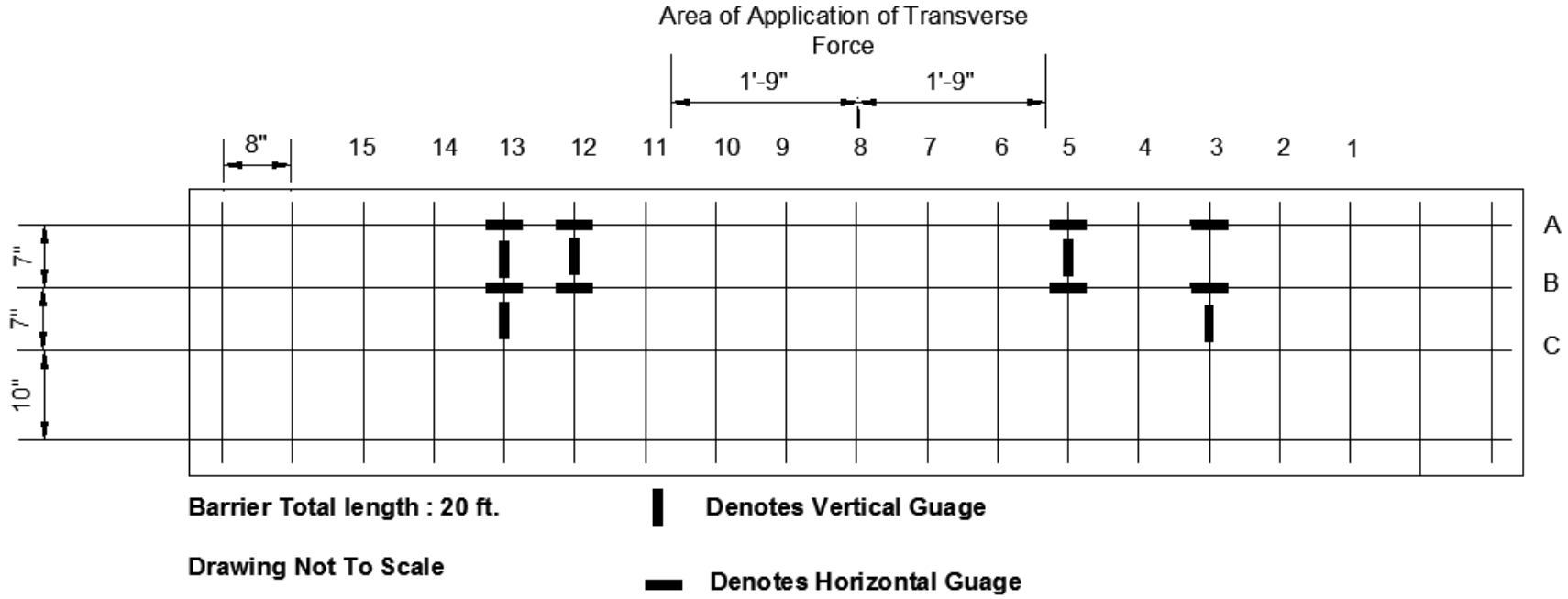

Figure 101
Instrumentation plan of sloping face of barrier

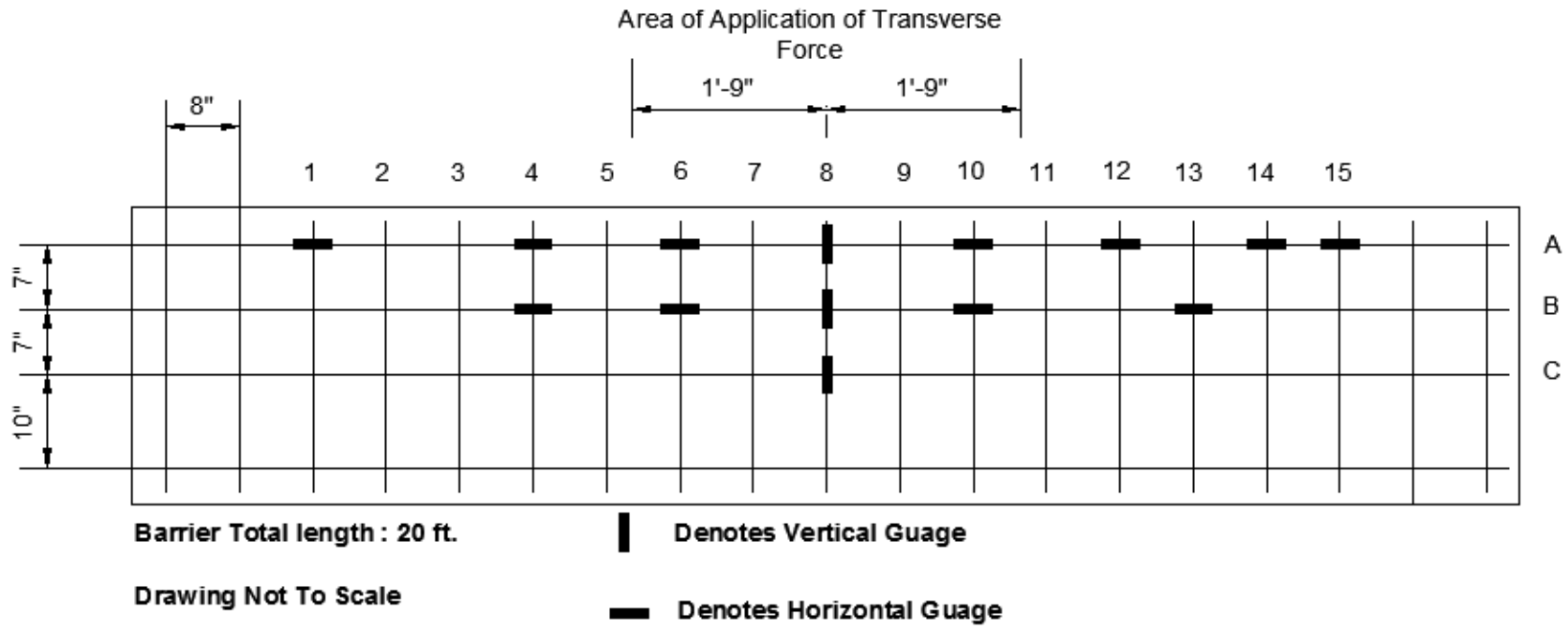

Figure 102
Instrumentation plan of vertical face of barrier

APPENDIX D
HYDRAULIC ACTUATOR AND SPECIFICATIONS

Series 201 Hydraulic Actuator

Benefits

Large Selection
- Available in tension force ratings from 7 to 400 kip with proportionally higher compressive force ratings.

Range of Application
- Targeted for low frequency applications that require accurate servo-controlled performance.

Economical Design
- Closed-loop servo-hydraulic actuator features in a streamlined design.

Non-metallic Bearings
- High quality non-metallic bearings provide long life and resist galling failures.

Precise Control
- Designed for use with MTS' closed looped servohydraulic accessories.

Ease of Service
- A special housing design permits piston rod bearings and seals to be replaced without dismantling the cylinder/end cap assembly.

MTS Series 201 hydraulic actuators are heavy duty, fatigue rated force generators designed for long stroke and/or low dynamic applications. Compatible with MTS' feedback and control components, these actuators provide precise performance ideal for low frequency test and simulation applications.

Flexible enough to meet all your force and motion control needs, this actuator is available in 11 force ratings, 4 standard lengths and make to order custom lengths.

MTS 201 Actuators are designed for superior responsiveness and reliability. Our actuator design incorporates high and low pressure seals and a drain arrangement rarely found on competing products. These features provide lower friction and control oil leaks. Non-metallic bearings provide side load tolerance and greater resistance to galling therefore extend operational life.

Options

Force Rating
- With a wide variety to select from, you can match a 201 Actuator to your application for the best performance and spatial fit. Tension force ratings to 400 kip and compressive to 580 Kip.

Stroke Length
- 201 Actuators are available in standard stroke lengths of 10, 20, 30, and 40 inches and in custom stroke lengths providing the flexibility to meet a wide variety of requirements.

Transducers
- High quality MTS transducers are available for the 201 Actuator series. These actuators are compatible with MTS load cells, LVDTs, and magnetorestrictive transducers.

Mountings
- A variety of mounting methods are available including pedestal, clevis, and swivel designs. For applications with load transitions that cross from tension to compression, MTS' 249 Swivel with anti-backlash adjustment is the perfect solution.

Servovalve
- The MTS 252 Servovalve, rated from 1 to 16.5 gpm, mounts directly to the actuator. If more flow is required, a manifold for adding a second servovalve is a standard option. When greater flows are required, custom actuators are available.

Lift Kit
- Provides secure balanced lift equipment for handling actuators.

Specifications

201 Series Actuator Force Rating, Piston Area

Model	Piston Area				Force			
	Tension Area		Compression Area		Tension		Compression	
	in²	cm²	in²	cm²	kip	kN	kip	kN
201.17	2.5	16.2	4.9	31.7	7	32	14	63
201.20	5.2	33.3	8.3	53.5	15	66	24	107
201.25	7.7	49.4	12.6	81.1	22	99	36	162
201.30	12.6	81.1	19.6	126.7	36	162	57	253
201.35	18.7	120.3	28.3	182.4	55	240	80	365
201.40	22.6	145.7	38.5	248.3	65	290	110	495
201.45	34.4	221.7	50.3	324.3	100	445	145	650
201.60	50.3	324.3	78.5	506.7	145	650	230	1015
201.70	74.6	481.4	113.1	729.7	215	965	330	1460
201.80	103.7	668.9	153.9	993.2	300	1340	445	1985
201.90	137.4	886.7	201.1	1297.2	400	1775	590	2595

201 Series Basic Cylinder Dimensions

Model	Rod Dia.		A		B		C		D		E		F		G	
	in	mm	in	mm	in	mm	in	mm	US cust.	SI metric	in	mm	in	mm	in	mm
201.17	1.75	44.5	4.9	124	7.9	199.9	2.1	53.8	1"-14	M27 x 2	1.8	44.5	2.00	50.8	2.0	51
201.20	2.0	50.8	5.1	129	8.4	212.6	2.1	53.8	1"-14	M27 x 2	1.8	44.5	2.00	50.8	2.0	51
201.25	2.5	63.5	5.1	129	8.4	212.6	2.1	53.8	1"-14	M27 x 2	1.8	44.5	2.00	50.8	2.0	51
201.30	3.0	76.2	5.6	141	9.3	235.5	2.6	66.5	1 1/2"-12	M36 x 2	2.3	57.2	2.00	50.8	2.0	51
201.35	3.5	88.9	5.8	148	10.0	254.8	2.9	73.2	1 1/2"-12	M36 x 2	2.3	57.2	2.00	50.8	2.0	51
201.40	4.5	114.3	7.3	185	11.0	279.4	3.8	95.3	2"-12	M52 x 2	2.3	57.2	2.00	50.8	2.3	57
201.45	4.5	114.3	7.3	185	11.9	302.3	3.8	95.3	2"-12	M52 x 2	2.3	57.2	2.00	50.8	2.3	57
201.60	6.0	152.4	9.08	231	13.65	346.7	5.0	127.0	3"-12	M76 x 2	3.0	76.2	2.0	50.8	2.5	64
201.70	7.0	177.8	10.2	259	16.0	405.6	5.6	142.7	3 1/2"-12	M90 x 2	3.5	88.9	2.00	50.8	2.8	70
201.80	8.0	203.2	10.5	265	16.9	429.3	5.6	142.7	3 1/2"-12	M90 x 2	3.5	88.9	2.00	50.8	2.8	70
201.90	9.0	228.6	11.0	278	18.4	467.9	5.6	142.7	4 1/2"-8	M125 x 4	4.5	114.3	2.00	50.8	2.8	70

Series 201 Actuator Dimensions

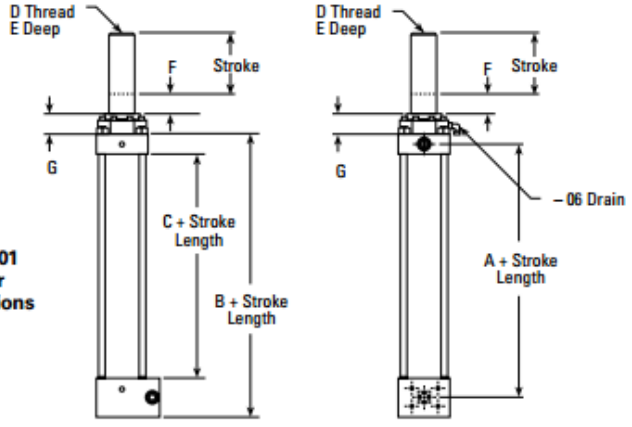

MTS Systems Corporation
14000 Technology Drive
Eden Prairie, Minnesota 55344-2290 USA
Toll Free: 800-328-2255
Fax: 952-937-4515
E-mail: info@mts.com
www.mts.com

ISO 9001 CERTIFIED QMS

100-155-284a HydraulicActuator201 Printed in U.S.A. 5/06

APPENDIX E
STRAIN GAUGES, ASSIGNED CHANNELS, AND APPLIED LOADS

Table 17
Applied loads and strains in channels 101-105

Load (lb.)	Channel Strains				
	101	102	103	104	105
2000	2.18E-07	4.76E-06	4.87E-06	2.66E-06	1.98E-06
4000	2.41E-07	6.17E-06	1.02E-05	4.28E-06	9.18E-06
6000	5.27E-07	4.69E-06	1.46E-05	4.87E-06	1.09E-05
8000	1.04E-06	9.76E-06	1.92E-05	5.29E-06	1.50E-05
10000	2.67E-08	9.87E-06	2.27E-05	7.97E-06	1.69E-05
12000	1.44E-07	4.38E-05	2.76E-05	9.28E-06	1.74E-05
14000	2.57E-06	6.70E-05	3.05E-05	1.15E-05	1.85E-05
16000	3.22E-06	8.10E-05	3.38E-05	1.40E-05	2.00E-05
18000	6.80E-06	7.44E-05	3.51E-05	1.87E-05	2.03E-05
20000	5.51E-06	7.20E-05	3.78E-05	2.08E-05	2.26E-05
22000	6.69E-06	7.24E-05	4.20E-05	2.17E-05	2.38E-05
24000	8.97E-06	8.23E-05	4.50E-05	2.46E-05	2.50E-05
26000	1.11E-05	7.58E-05	4.51E-05	2.83E-05	2.35E-05
28000	1.65E-05	7.20E-05	4.83E-05	3.12E-05	2.38E-05
30000	1.90E-05	1.10E-04	5.32E-05	3.29E-05	2.27E-05
32000	2.15E-05	1.90E-04	5.72E-05	3.05E-05	2.53E-05
34000	2.65E-05	2.40E-04	5.65E-05	4.12E-05	2.44E-05
36000	3.24E-05	2.50E-04	2.28E-05	3.86E-05	1.59E-05
38000	3.42E-05	2.50E-04	1.13E-05	4.21E-05	9.54E-06
40000	3.36E-05	2.60E-04	4.02E-06	4.45E-05	6.64E-06
42000	3.77E-05	2.70E-04	1.03E-06	4.45E-05	5.54E-06
44000	4.27E-05	3.10E-04	3.53E-06	2.57E-05	4.91E-06
46000	4.64E-05	3.50E-04	8.90E-06	5.94E-06	8.36E-06
48000	4.78E-05	3.70E-04	1.87E-05	1.30E-04	2.65E-05
50000	4.91E-05	4.50E-04	2.16E-05	2.70E-04	4.00E-04
52000	5.00E-05	3.20E-04	2.05E-05	4.20E-04	9.70E-04
54000	4.96E-05	2.10E-04	2.28E-05	4.90E-04	1.20E-03
56000	4.94E-05	1.80E-04	2.40E-05	5.50E-04	1.42E-03
58000	4.86E-05	2.60E-04	2.93E-05	5.90E-04	1.65E-03
60000	4.75E-05	3.10E-04	3.08E-05	6.20E-04	1.88E-03
62000	2.17E-06	3.00E-04	3.18E-05	6.50E-04	2.05E-03
64000	1.26E-04	4.30E-04	3.67E-05	7.50E-04	2.17E-03
66000	1.35E-04	5.90E-04	4.28E-05	9.40E-04	2.17E-03
68000	1.32E-04	5.10E-04	4.54E-05	1.08E-03	2.09E-03
70000	1.26E-04	3.62E+34	6.42E-05	1.23E-03	2.05E-03
72000	1.22E-04	1.33E+35	7.91E-05	1.68E-03	1.98E-03
79500	1.24E-04	1.33E+35	8.56E-05	1.62E+33	1.98E-03

Table 18
Applied loads and strains in channels 106-110

Loads (lb.)	Channel Strains				
	106	107	108	109	110
2000	7.98E-07	4.59E-06	4.85E-06	3.24E-06	5.56E-06
4000	4.35E-06	4.72E-06	8.84E-06	6.05E-07	1.08E-05
6000	8.44E-06	4.10E-06	1.28E-05	2.17E-06	1.62E-05
8000	1.80E-05	5.21E-06	1.74E-05	6.90E-06	2.31E-05
10000	2.55E-05	6.42E-06	1.97E-05	8.99E-06	2.74E-05
12000	2.85E-05	8.05E-06	2.33E-05	1.24E-05	3.28E-05
14000	3.28E-05	1.04E-05	2.60E-05	1.37E-05	3.89E-05
16000	3.80E-05	6.51E-06	2.76E-05	1.56E-05	4.38E-05
18000	4.28E-05	7.37E-06	2.68E-05	9.65E-06	4.88E-05
20000	4.57E-05	4.65E-06	2.87E-05	1.03E-05	5.53E-05
22000	4.70E-05	3.85E-06	3.10E-05	1.03E-05	6.12E-05
24000	5.03E-05	4.13E-07	3.65E-05	1.16E-05	6.80E-05
26000	5.51E-05	7.75E-06	5.38E-05	3.39E-06	6.99E-05
28000	5.85E-05	1.46E-05	7.36E-05	2.69E-07	7.20E-05
30000	6.29E-05	1.65E-05	9.03E-05	2.20E-05	7.45E-05
32000	7.06E-05	1.87E-05	0.000113	2.76E-05	7.79E-05
34000	8.28E-05	2.13E-05	0.000132	2.82E-05	7.54E-05
36000	1.45E-04	2.94E-05	1.66E-04	2.82E-05	7.06E-05
38000	1.64E-04	3.78E-05	2.01E-04	2.67E-05	6.76E-05
40000	1.74E-04	4.57E-05	2.54E-04	2.64E-05	6.55E-05
42000	1.88E-04	4.78E-05	2.99E-04	2.32E-05	6.79E-05
44000	1.92E-04	5.28E-05	3.52E-04	6.63E-06	6.59E-05
46000	1.99E-04	5.66E-05	3.97E-04	1.06E-05	6.22E-05
48000	1.78E-04	4.96E-05	4.49E-04	3.73E-05	4.97E-05
50000	1.83E-04	8.66E-05	5.02E-04	5.36E-05	4.55E-05
52000	1.89E-04	1.28E-04	6.05E-04	6.06E-05	4.10E-05
54000	1.81E-04	1.41E-04	7.10E-04	6.97E-05	3.44E-05
56000	1.61E-04	1.58E-04	8.05E-04	8.81E-05	3.06E-05
58000	1.62E-04	1.71E-04	9.05E-04	1.03E-04	2.65E-05
60000	1.76E-04	1.33E-04	1.03E-03	1.19E-04	2.85E-05
62000	1.67E-04	1.25E-04	1.16E-03	1.49E-04	8.57E-05
64000	1.28E-04	1.28E-04	1.33E-03	2.02E-04	1.16E-04
66000	1.05E-04	1.35E-04	1.52E-03	2.45E-04	1.89E-04
68000	2.85E-05	1.48E-04	1.71E-03	2.84E-04	2.62E-04
70000	1.61E-05	1.58E-04	1.91E-03	3.63E-04	8.77E-04
72000	1.53E-04	2.11E-04	2.31E-03	9.48E-04	1.62E-03
79500	1.62E+33	2.54E-04	2.54E-03	1.32E-03	1.96E-03

Table 19
Applied loads and strains in channels 111-115

Load (lb.)	Channel Strains				
	111	112	113	114	115
2000	1.20E-05	4.60E-06	4.85E-06	2.63E-07	2.47E-06
4000	2.04E-05	7.57E-06	3.29E-06	1.75E-07	4.56E-06
6000	2.46E-05	9.05E-06	9.91E-06	4.71E-07	7.24E-06
8000	2.94E-05	9.67E-06	1.12E-05	6.73E-07	7.59E-06
10000	3.41E-05	1.06E-05	5.63E-06	2.56E-07	7.72E-06
12000	3.81E-05	1.25E-05	7.27E-06	3.70E-06	9.30E-06
14000	4.12E-05	1.48E-05	7.28E-06	5.97E-06	1.24E-05
16000	4.37E-05	1.66E-05	1.24E-05	6.42E-06	1.28E-05
18000	4.97E-05	1.83E-05	1.26E-05	6.27E-06	1.40E-05
20000	5.29E-05	1.95E-05	2.57E-05	8.73E-06	1.39E-05
22000	5.45E-05	2.01E-05	1.83E-05	9.53E-06	1.42E-05
24000	5.68E-05	2.16E-05	2.15E-05	1.33E-05	1.68E-05
26000	6.08E-05	2.53E-05	2.17E-05	1.52E-05	1.74E-05
28000	6.51E-05	2.69E-05	2.13E-05	1.65E-05	1.86E-05
30000	7.01E-05	2.81E-05	1.48E-05	2.51E-05	2.21E-05
32000	6.99E-05	2.85E-05	2.22E-05	3.46E-05	2.62E-05
34000	8.50E-05	2.87E-05	2.77E-05	2.91E-05	4.77E-05
36000	8.61E-05	2.56E-05	6.06E-06	5.20E-05	5.78E-05
38000	9.17E-05	2.77E-05	5.17E-06	5.91E-05	6.40E-05
40000	9.70E-05	2.99E-05	1.07E-05	6.42E-05	6.84E-05
42000	1.07E-04	3.05E-05	3.58E-05	7.05E-05	6.96E-05
44000	1.06E-04	3.34E-05	6.83E-05	8.29E-05	6.83E-05
46000	1.07E-04	3.49E-05	7.29E-05	1.00E-04	7.58E-05
48000	1.10E-04	3.53E-05	7.29E-05	1.42E-04	8.94E-05
50000	1.18E-04	3.64E-05	7.60E-05	1.60E-04	9.50E-05
52000	1.37E-04	3.15E-05	6.88E-05	1.77E-04	1.13E-04
54000	1.55E-04	3.33E-05	6.64E-05	1.93E-04	1.33E-04
56000	1.70E-04	3.46E-05	7.20E-05	2.07E-04	1.47E-04
58000	1.87E-04	3.95E-05	1.02E-04	2.19E-04	1.68E-04
60000	1.67E-04	4.25E-05	1.62E-04	2.30E-04	1.94E-04
62000	1.57E-04	4.31E-05	2.28E-04	2.39E-04	2.22E-04
64000	1.51E-04	4.39E-05	3.10E-04	2.60E-04	2.35E-04
66000	1.34E-04	4.88E-05	4.05E-04	2.70E-04	1.09E-04
68000	1.89E-05	5.40E-05	5.72E-04	2.80E-04	2.81E-05
70000	1.77E-04	5.75E-05	6.87E-04	2.80E-04	4.49E-05
72000	4.94E-04	6.37E-05	5.42E-04	7.38E-05	1.03E-04
79500	6.88E-04	7.45E-05	3.31E-04	2.37E-04	1.02E-04

Table 20
Applied loads and strains in channels 116-120

Load (lb.)	Channel Strains				
	116	117	118	119	120
2000	5.33E-05	5.96E-07	1.92E-04	6.75E-06	3.38E-06
4000	5.83E-05	3.36E-06	2.36E-04	7.27E-06	4.11E-06
6000	2.17E-04	5.16E-06	2.33E-04	8.83E-06	6.29E-06
8000	2.26E-04	4.04E-06	2.39E-04	9.50E-06	7.77E-06
10000	2.75E-04	4.79E-06	2.46E-04	9.89E-06	9.24E-06
12000	2.50E-04	5.09E-06	2.38E-04	1.04E-05	1.05E-05
14000	1.90E-04	6.11E-06	2.30E-04	9.97E-06	1.09E-05
16000	2.16E-04	5.57E-06	2.43E-04	1.05E-05	1.20E-05
18000	3.59E-04	5.53E-06	2.80E-04	1.05E-05	1.38E-05
20000	2.24E-04	5.11E-06	2.89E-04	1.08E-05	1.53E-05
22000	2.67E-04	5.36E-06	3.05E-04	1.10E-05	1.84E-05
24000	2.90E-04	5.27E-06	3.19E-04	1.36E-05	2.11E-05
26000	3.06E-04	3.32E-06	3.28E-04	1.15E-05	2.22E-05
28000	3.63E-04	1.67E-06	3.32E-04	1.01E-05	2.36E-05
30000	4.61E-04	8.85E-07	3.44E-04	8.85E-06	2.34E-05
32000	4.09E-04	2.06E-06	3.70E-04	8.88E-06	2.28E-05
34000	3.56E-04	1.37E-06	3.03E-04	9.49E-06	2.08E-05
36000	2.25E-04	2.22E-06	2.58E-04	1.05E-05	1.92E-05
38000	1.04E-04	4.59E-07	2.68E-04	1.09E-05	1.84E-05
40000	6.25E-05	4.68E-08	2.98E-04	1.13E-05	1.62E-05
42000	3.75E-05	1.75E-07	2.94E-04	1.03E-05	1.37E-05
44000	6.13E-06	1.38E-06	2.54E-04	8.77E-06	1.13E-05
46000	7.53E-05	2.72E-06	2.76E-04	9.94E-06	8.62E-06
48000	1.36E-04	2.40E-05	2.79E-04	9.38E-06	2.21E-05
50000	1.62E-04	9.06E-05	3.39E-04	1.73E-05	2.47E-05
52000	1.54E-04	1.33E-04	3.89E-04	2.43E-05	2.02E-05
54000	1.55E-04	1.51E-04	3.93E-04	2.34E-05	3.70E-05
56000	2.08E-04	1.70E-04	3.93E-04	2.57E-05	4.12E-05
58000	2.65E-04	1.87E-04	4.07E-04	2.82E-05	5.44E-05
60000	3.03E-04	2.01E-04	4.37E-04	2.64E-05	6.92E-05
62000	3.80E-04	2.13E-04	4.41E-04	2.50E-05	6.76E-05
64000	3.58E-04	2.22E-04	4.55E-04	2.67E-05	7.36E-05
66000	3.72E-04	2.25E-04	4.48E-04	3.31E-05	6.41E-05
68000	3.94E-04	2.22E-04	4.47E-04	3.54E-05	5.96E-05
70000	1.80E-04	2.20E-04	4.62E-04	3.45E-05	5.65E-05
72000	6.26E-04	2.14E-04	4.71E-04	2.81E-05	6.52E-05
79500	1.64E+33	2.24E-04	1.64E+33	3.59E-05	6.18E-05